Son Of X-Shooter

SOXS

Commissioning Report

Issue: 3.0

Date: 2026-05-14

	NAME	SIGNATURE
PREPARED	P. D'Avanzo	
APPROVED	P. Schipani S. Campana	
RELEASED	S. Campana	

CHANGE RECORD

ISSUE	DATE	SECTION/PARAGRAPH AFFECTED	REASON/INITIATION DOCUMENTS/REMARKS
1.0	10/09/2025	All	First issue
2.0	29/10/2025	All	Second issue
2.1	26/01/2026	3.5, 3.6, 3.7, 4.1, 4.2, 4.3, 4.4, 4.5, 4.6, 4.7, 4.8, 4.9, 4.10, 4.11, 4.12, 4.13, 4.14, 5	Second issue, update 1
3.0	14/05/2026	All	First issue for PAC

TABLE OF CONTENTS

1 INTRODUCTION

1.1 Overview and Scope

SOXS (Son Of X-Shooter) is a spectroscopic facility for the ESO-NTT telescope in La Silla (Chile) for the follow-up of transient sources. Its design foresees two high-efficiency spectrographs with a resolution slit product of about 4500 (1" slit), covering the UV-VIS (350–850 nm) and NIR band (800–2000 nm). A light imaging capability in the visible band will be provided. The instrument will be located at the Nasmyth A interface of the telescope.
The purpose of this document is to report on the status of the commissioning of SOXS at the NTT. Eventually, when the commissioning is completed, this document will serve as the final report on the SOXS commissioning at La Silla.

1.2 Applicable Documents

Ref.	Document title	Document ID
[AD1]	Memorandum of Understanding No. 11378/LET/CP/AMA *for the SOXS Instrument on the NTT Telescope*	N/A

1.3 Reference Documents

Ref.	Document title	Document ID
[RD1]	Assembly, Integration and Test Plan	SOXS-PLA-0003
[RD2]	AIV Status	SOXS-TRE-0078
[RD3]	Calibration Plan	SOXS-PLA-0006
[RD4]	SOXS Scheduler Design	SOXS-TRE-0045

1.4 Abbreviations and Acronyms

AC	Acquisition Camera
ADC	Atmospheric Dispersion Corrector
CU	Calibration Unit
ETC	Exposure Time Calculator
INS	Instrument Software
NISE	Near Infrared Slit Exchanger
NTT	New Technology Telescope
OB	Observing Block
PAC	Preliminary Acceptance in Chile
PAE	Preliminary Acceptance in Europe
SNR	Signal to Noise Ratio
SOXS	Son Of X-Shooter
TIO	Telescope and Instrument Operator

1.5 Commissioning tasks summary

Task	Status	To Do
UV-VIS Detector characterization	Done	No more activity needed
NIR Detector characterization	Done	Keep monitored detector stability
AC Detector characterization	Done	No more activity needed
AC Image Quality & Sensitivity	Done	No more activity needed
AC Focus Position	Done	Monitoring and check for possible temperature effects
Slit Focus Position (UV-VIS)	Done	No more activity needed
Slit Focus Position (NIR)	Done	No more activity needed
Slit Alignment (UV-VIS)	Done	No more activity needed
Slit Alignment (NIR)	Done	No more activity needed
Flexure Effects (UV-VIS)	Done	Keep monitored
Flexure Effects (NIR)	Done	Keep monitored
Spectrograph Image Quality (spatial resolution and resolving power; UV-VIS)	Done	Keep monitored
Spectrograph Image Quality (spatial resolution and resolving power; NIR)	Done	Keep monitored
Spectral Format Stability (UV-VIS)	Done	Keep monitored. Check 2nd order dispersion solution using sky lines.
Spectral Format Stability (NIR)	Done	Keep monitored. Check 2nd order dispersion solution using sky lines.
Calibration Lamp Exposure Times	Done	No more activity needed
Flat Field Accuracy and stability (UV-VIS)	Done	Keep monitored
Flat Field Accuracy and stability (NIR)	Done	Keep monitored
Wavelength Coverage (UV-VIS)	Done	No more activity needed
Wavelength Coverage (NIR)	Done	No more activity needed
Acquisition Sequences	Done	No more activity needed
ADC Check	Done	No more activity needed
Scale Along Slit (UV-VIS)	Done	No more activity needed
Scale Along Slit (NIR)	Done	No more activity needed

Overall Sensitivity (UV-VIS & AC)	Done	Keep monitored. Cross-check the uniformity of ETC and pipeline procedures for the determination of efficiency,
Overall Sensitivity (NIR)	Done	Keep monitored. Cross-check the uniformity of ETC and pipeline procedures for the determination of efficiency,
Observing Templates Verification	Done	No more activity needed
Parasitic Light & Ghosts	To be done	Parasitic light test pending
ETC Verification (UV-VIS & NIIR)	Done	Keep monitoring. Cross-check the uniformity of ETC and pipeline procedures for the determination of efficiency, photo-electrons from target, SNR.
Pipeline Verification	Done (Systematic re-analysis with v0.17.1)	Cross-check the uniformity of ETC and pipeline procedures for the determination of efficiency, photo-electrons from target, SNR. Check compliance of the pipeline reduced data with ESO Phase 3 format.
Data Flow Compatibility	Done / In Progress	Some FITS keyword compliance to be fixed. Check compliance of the pipeline reduced data with ESO Phase 3 format.
Quality Control Procedures	Done / In Progress	A first (static) QC web page is available. Convert QC data to ESO format and create dynamic web page for QC monitoring.
Scheduler Verification	Done / In Progress	Scheduler functionalities fully tested with success. Extensive testing simulating routine science operations is recommended.

2 Introduction

The SOXS arrived at La Silla on January 31, 2025. The SOXS team made seven visits to La Silla for the AIV and commissioning of the SOXS instrument. Details about the AIV plan and current status can be found in [RD1] and [RD2], respectively. In the following sections, we report a preliminary report of the current status of commissioning activities.

3 Missions to La Silla

In this Section, we provide a summary of the main commissioning activities carried out during the SOXS team's missions to La Silla. Detailed information about the status of the commissioning activities is reported in Section 4.
A night log is available here:
https://docs.google.com/spreadsheets/d/1AsI1TT19whIaFnG2KOR9JKU7HyNnRJhjxJXAGONHhM4/edit?usp=sharing

3.1 Mission 1

This first mission (February 22 - March 25, 2025) has been planned as fully dedicated to AIV activities. However, it included some pre-commissioning activities as well. Indeed, during this mission, it was possible to achieve the milestones of the first light of both the acquisition camera (on March 7) and of the UV-VIS spectrograph (on March 14). Therefore, some pre-commissioning activities were carried out. Among those:

- UV-VIS detector characterisation (Sect. 4.1)
- check of the UV-VIS spectral resolution (Sect. 4.5)
- implementation of the acquisition procedure (Sect. 4.8)

3.2 Mission 2

This run, from May 2 to 16, 2025, was a mix of AIV and commissioning. During the run, the milestone of the NIR first light has been achieved (May 8). Among the main commissioning activities we highlight:

- full alignment of the instrument (Sect. 4.3)
- preliminary NIR detector characterisation (Sect 4.1)
- check of the NIR spectral resolution (Sect. 4.5)
- setting of the p2ls and archive (Sect. 4.16)
- Check of the stability of NTT guiding, deriving the conclusion that SOXS does not need secondary guiding

Unfortunately, due to an issue with the compressor-cold head cryo-vacuum system first and then with the near-infrared slit exchanger (NISE), the NIR has not been available in the May - October period.

3.3 Mission 3

This run, from June 1 to 14, 2025, was mainly devoted to the commissioning (with minor AIV activities) of the UV-VIS and AC. Among the main commissioning activities we highlight:

- soxspipe installed and running @ La Silla (Sect. 4.15)
- UV-VIS throughput measure (Sect. 4.11, 4.14)

3.4 Mission 4

This run, from August 30 to September 12, 2025, was a mix of AIV and commissioning. The five days preceding this run (Aug 25-30) were dedicated to AIV activities, aimed at changing and testing the new NIR compressor (see [RD 2]). The main commissioning activities have been devoted to the testing and debugging of the SOXS scheduler.

3.5 Mission 5

This run, from October 7 to 28, 2025, was mainly devoted to the UV-VIS and AC commissioning. A 2-week AIV run (Oct 28 - Nov 10) has been attached to carry out the NISE fix and the full recovery of the NIR arm.

3.6 Mission 6

This run, from November 22 to December 1 2025 and from December 7 to 17, 2025 (11 + 10 nights), was mainly devoted to commissioning activities, with a particular focus on ADC fix, final UV-VIS tests and extensive NISE tests (checking for repeatability of movements in open loop), with some minor activity dedicated to the scheduler testing.

3.7 Mission 7

This run, from January 7 to 28, 2026 (21 nights) has been dedicated to extensive scheduler testing and further NIR characterisation (together with AIV activities dedicated to the investigation of possible NISE electrical issues). Other activities included the instrument software fine tuning and the pipeline @ La Silla debugging (at that time version 0.14.1). The training of TiOs training started, with dedicated seminars and with a side-by-side hands-on tutorial during the main day and nighttime activities related to SOXS operations. ESO people had the opportunity to carry out independent tests on the instrument performances.

4 Status of commissioning activities

In this Section, we list all the commissioning activities included in the SOXS Calibration Plan [RD3], providing for each of them a short description, the status, and the activities still to be done.

The fits/PDF files used to produce the plots of this report are retrievable from the ESO Special Access Science Archive Facility:
(https://archive.eso.org/wdb/forms/cas/eso_archive_main.html; see also Sect. 4.16) or from dedicated repositories linked in the given sections/captions.

Important note on the Acquisition Camera (AC). According to the MoU between the SOXS consortium and ESO, the AC is included in SOXS with the main goal of serving (and being offered) for acquisition purposes only. Therefore, following the Xshooter experience, only a simple imaging mode with limited functionalities which uses the AC camera and its set of filters is planned to be offered. Acquisition images can be used to flux calibrate spectra in addition to the usual spectrophotometric observations and to determine the magnitudes of transient objects. Consequently, a minimal calibration plan is provided [RD3] and no pipeline support is currently planned to be provided for the imaging data.
Nonetheless, the AC has been extensively tested during the commissioning run, also in light of a possible future offer as a full science imager (not currently planned). The results are

reported in the following dedicated sections for the sake of completeness and should be taken into account in light of the above considerations. The data collected so far indicate that the AC has good scientific imaging capabilities (see Tables 2 and 5), as expected from tests performed during the PAE. Larger-scale image defects (e.g. coma) are present in some of the images. The cause is still under investigation.

4.1 Spectrograph detectors' full characterization

UV-VIS

Description. A series of frames with the shutter closed (dark & bias) and a series of lamp flat-fields. Frames to be taken with different integration times and different binning.
Parameters to be measured:

- Gain (e-/ADU)
- RON (e-)
- Linearity peak-to-peak (%)
- Dark Current (e-/pix/hr)
- Bias Level (ADU)
- QE
- Bad pixel fraction
- Fixed pattern search

Status. Enough data taken. All values measured, confirming those obtained at PAE. In Table 1, the values obtained during the detector characterisation are reported. No significant fraction of bad pixels is present so far, nor fixed patterns (Fig. 1). A linearity plot is shown in Fig. 2.

To do. Done (no more activities planned during commissioning). Update the User Manual with the measured values.

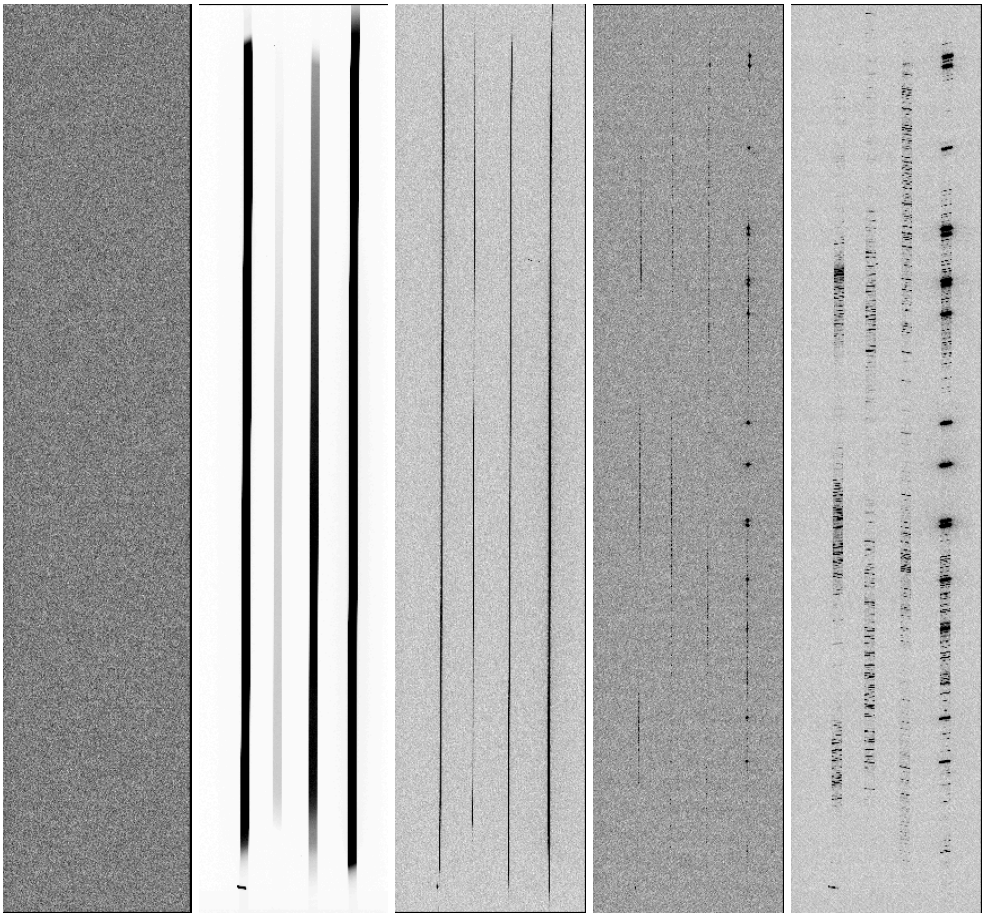

Figure 1: Example of UV-VIS calibration frames (from top left): Bias (SOXS.2025-10-21T09:10:55.538.fits), QTH 1" flat (SOXS.2025-10-21T09:31:33.902.fits), QTH pinhole flat (SOXS.2025-10-21T09:40:41.754.fits), ThAr pinhole spectrum (SOXS.2025-10-21T10:03:23.147.fits), ThAr multipinhole spectrum (SOXS.2025-10-11T10:10:11.553.fits).

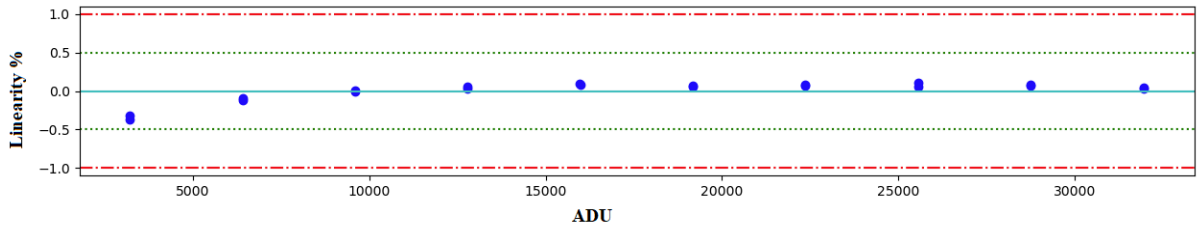

Figure 2: SOXS UV-VIS CCD linearity measured during AIV.

NIR

Description. A series of frames with the shutter closed (dark) and a series of lamp flat-fields. Frames to be taken with different integration times.
Parameters to be measured:

- Gain (e-/ADU)
- RON (e-)
- Linearity peak-to-peak (%)
- Dark Current (e-/pix/hr)
- QE
- Bad pixel map
- Fixed pattern search
- Persistence

Status. Enough data taken, mainly after the NIR recovery during the 2025 Oct-Nov AIV run. All values measured, confirming those obtained at PAE. In Table 1, the values obtained during the detector characterisation are reported. An example of a full set of NIR calibration frames is reported in Fig. 3. A linearity plot is shown in Fig. 4. The median dark value is stable over sequences of frames obtained over timescales of hours and is consistent with the value measured at PAE (Fig. 5 - 8). A higher level of thermal background seems to be present when taking frames with the NISE in slit position different from “BLANK” (Fig. 9 - 11), which may need the acquisition of more sequence of data for a more careful characterisation. A bad pixel map is reported in Fig. 12. Some pattern is apparent, with a partial overlap with the detector area occupied by the spectral orders (Fig. 13). The result of a persistence test is reported in Fig. 14.

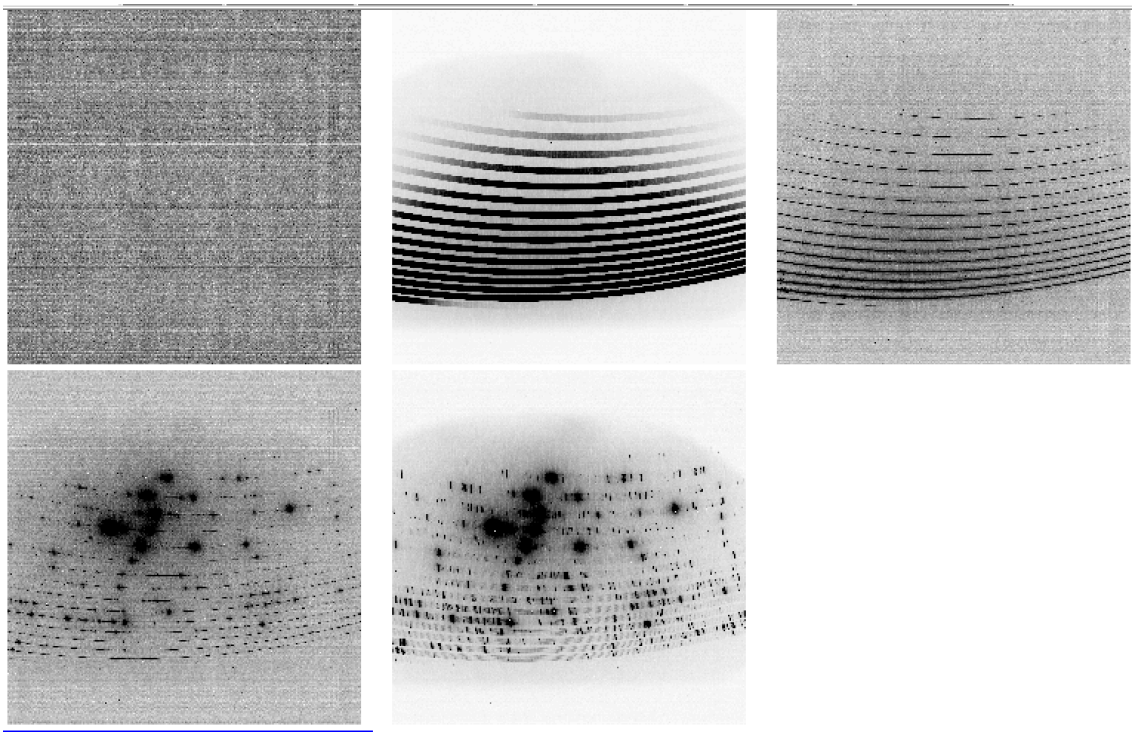

Figure 3: Example of NIR calibration frames (from top left, clockwise): Dark (SOXS.2025-05-17T11:47:47.376.fits), QTH 1” flat (SOXS.2025-05-17T11:07:56.525.fits), QTH pinhole flat (SOXS.2025-05-17T11:19:33.929.fits, arc lamps pinhole spectrum (SOXS.2025-05-17T11:53:16.311.fits), arc lamps multipinhole spectrum (SOXS.2025-05-17T11:53:47.686.fits).

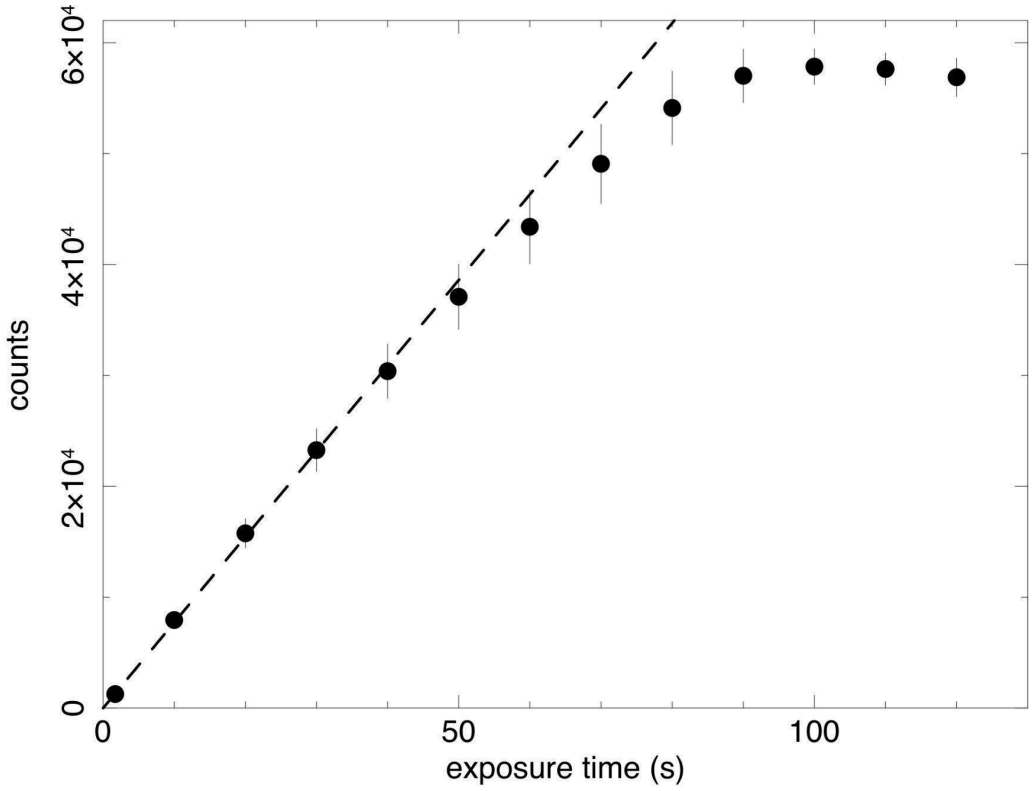

Figure 4: Linearity plot for the NIR detector, obtained from a series of QTH flats with increasing exposure times in Dec 2025. Data are available here:
https://drive.google.com/drive/folders/1e7xB1LlwnUlSLOKea_2eiBpbwZxWvl8e?usp=sharing

Dark. The results of the tests aimed at measuring the NIR dark current level (T_bench = 140 K) are shown in the Fig. from 5 to 8. The median dark is at a level of 0.004 counts/pixel/s, which is equivalent to 0.009 e-/pixel/s (given the detector gain of 2.3 e-/DN). This value is fully consistent with the one measured at PAE.

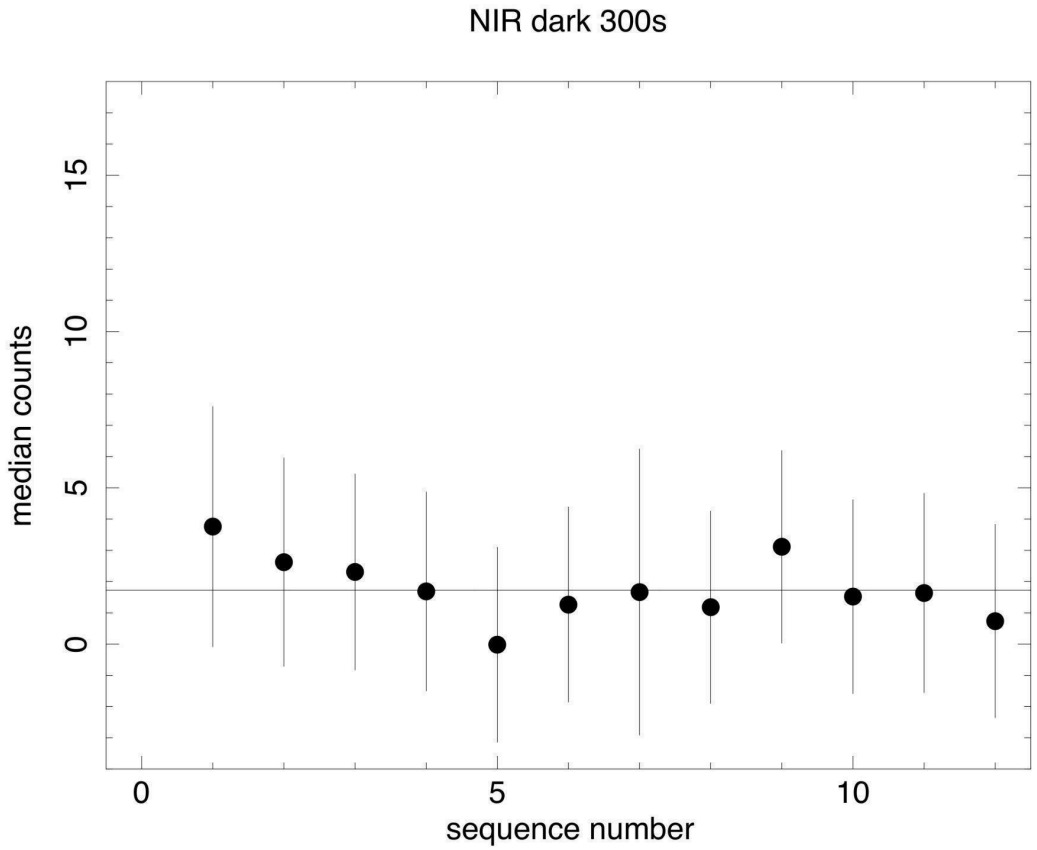

Figure 5: NIR dark level measured in a series of 300s exposures (NISE position: BLANK). Data has been taken on 2026 Jan 13, from 18:05:54 UT (SOXS.2026-01-13T18:05:54.640.fits) to 19:07:43 UT (SOXS.2026-01-13T19:02:43.402.fits). The solid line marks the average dark level (1.7 +/- 0.9 counts/pixel, which correspond to 4.0 +/- 2.2 e-/pixel).

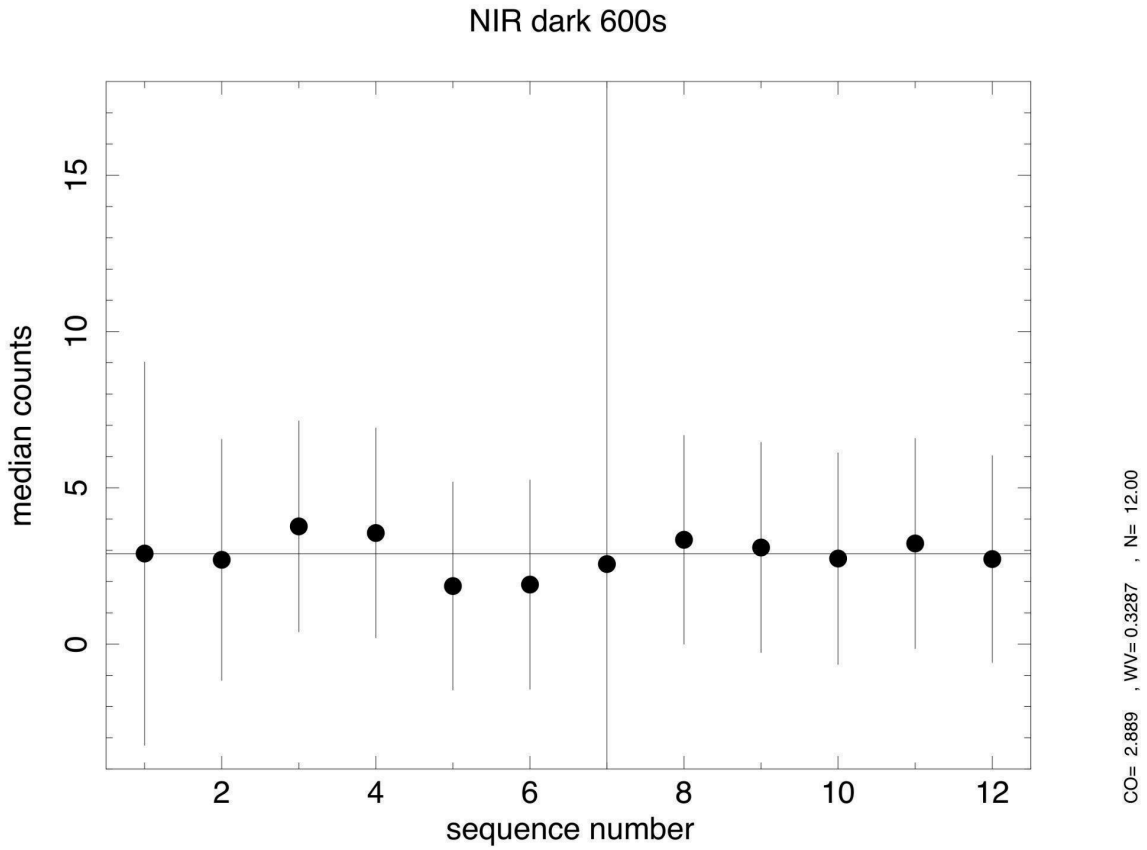

Figure 6: NIR dark level measured in a series of 600s exposures (NISE position: BLANK). Data has been taken on 2026 Jan 13, from 13:31:56 UT (SOXS.2026-01-13T13:31:56.266.fits) to 15:33:43 UT (SOXS.2026-01-13T15:23:43.413.fits). The solid line marks the average dark level (2.9 +/- 1.1 counts/pixel, which correspond to 6.7 +/- 2.5 e-/pixel). The dark #7 has a large error due to a bright spot (of unknown origin) in the image.

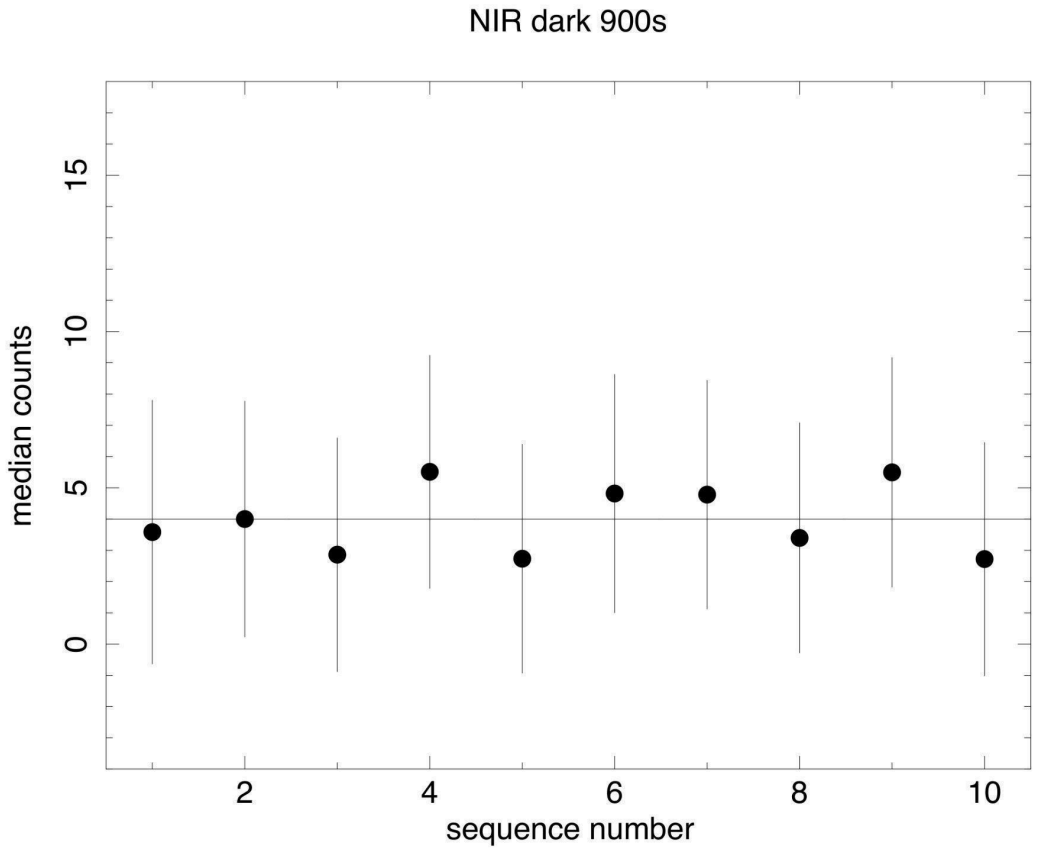

Figure 7: NIR dark level measured in a series of 900s exposures (NISE position: BLANK). Data has been taken on 2026 Jan 13, from 15:34:04 UT (SOXS.2026-01-13T15:34:04.500.fits) to 18:05:33 UT (SOXS.2026-01-13T17:50:33.405.fits). The solid line marks the average dark level (4.0 +/- 1.2 counts/pixel, which correspond to 9.2 +/- 2.8 e-/pixel).

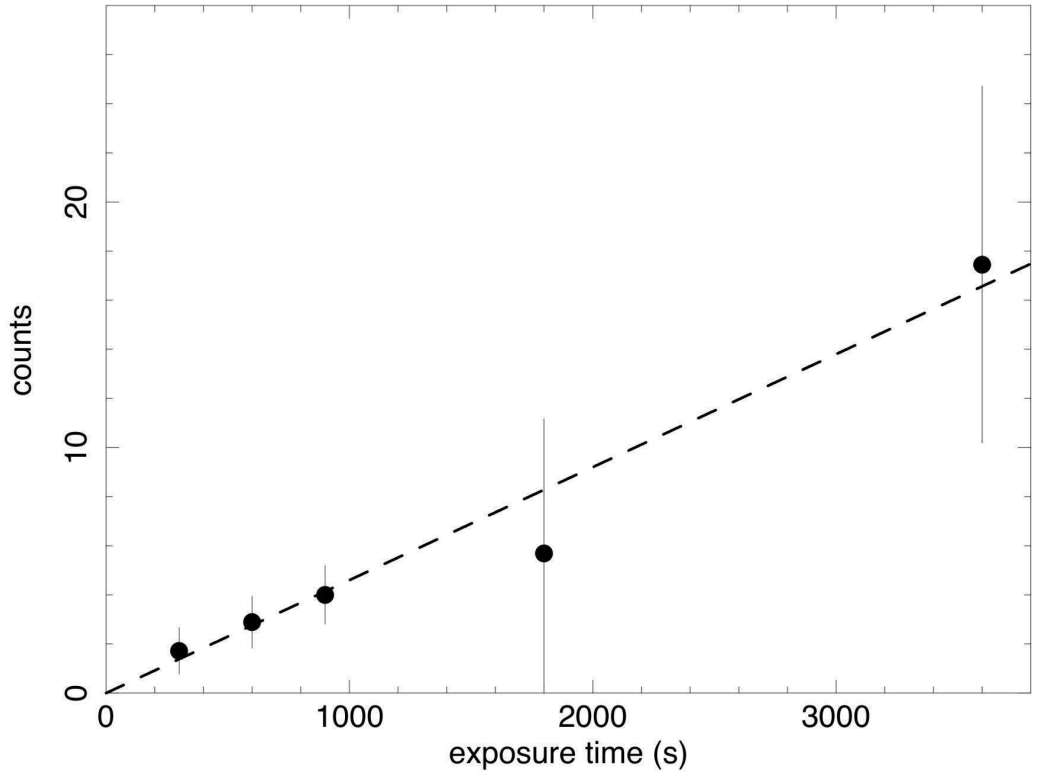

Figure 8: NIR dark level measured at different exposure time (NISE position: BLANK). The values for the exposure times of 300, 600 and 900 seconds are those from Figures 5-7. The last two data points have been obtained from the analysis of single images (explaining the worst statistics; SOXS.2026-01-12T19:09:04.513.fits, SOXS.2026-01-12T19:39:24.537.fits). The slope of the linear fit (dashed line) is of 4.0e-3 counts/pixels, which is equivalent to 1e-2 e-/pixel/s.

Thermal background. To estimate the thermal background inside the NIR spectrograph, we carried out a series of daytime observations with the 1.0" slit (on 2025-11-27 and on 2026-01-13), instrument shutter closed, lamps off and Nasmyth room dark. The exposures reveal the presence of thermal background affecting the reddest orders of the NIR spectrograph (Fig. 9 - 11).

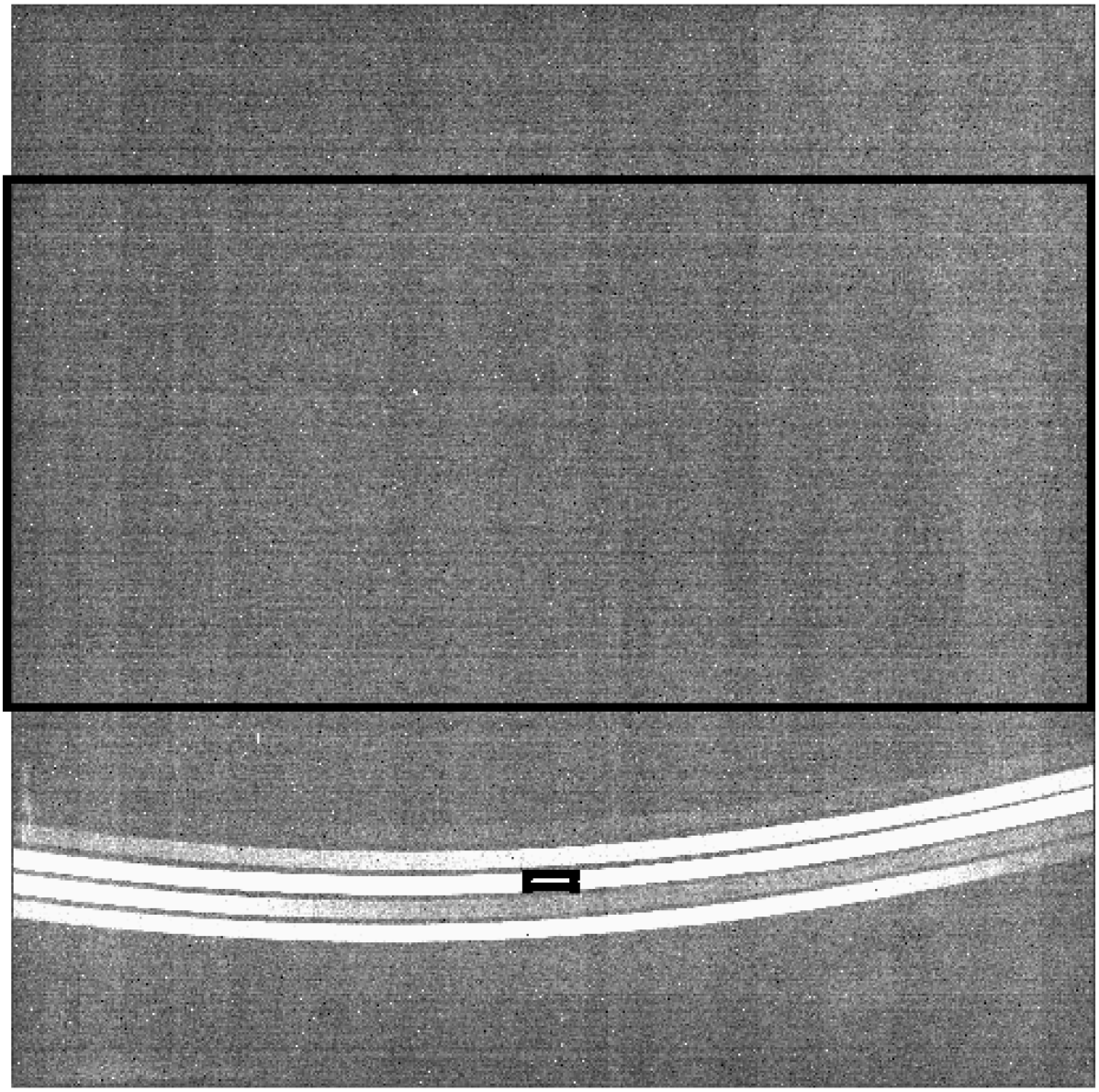

Figure 9: NIR thermal background frame obtained on 2025-11-27 with the 1.0" slit (SOXS.2025-11-27T11:55:36.284.fits). The 2048x1000 pix box marks the "no leakage area" where the NIR bluer spectral orders are expected to fall. The 90x25pix box marks the area ("leakage area") where the contribution of the NIR light leakage to the thermal noise is measured (see plots below).

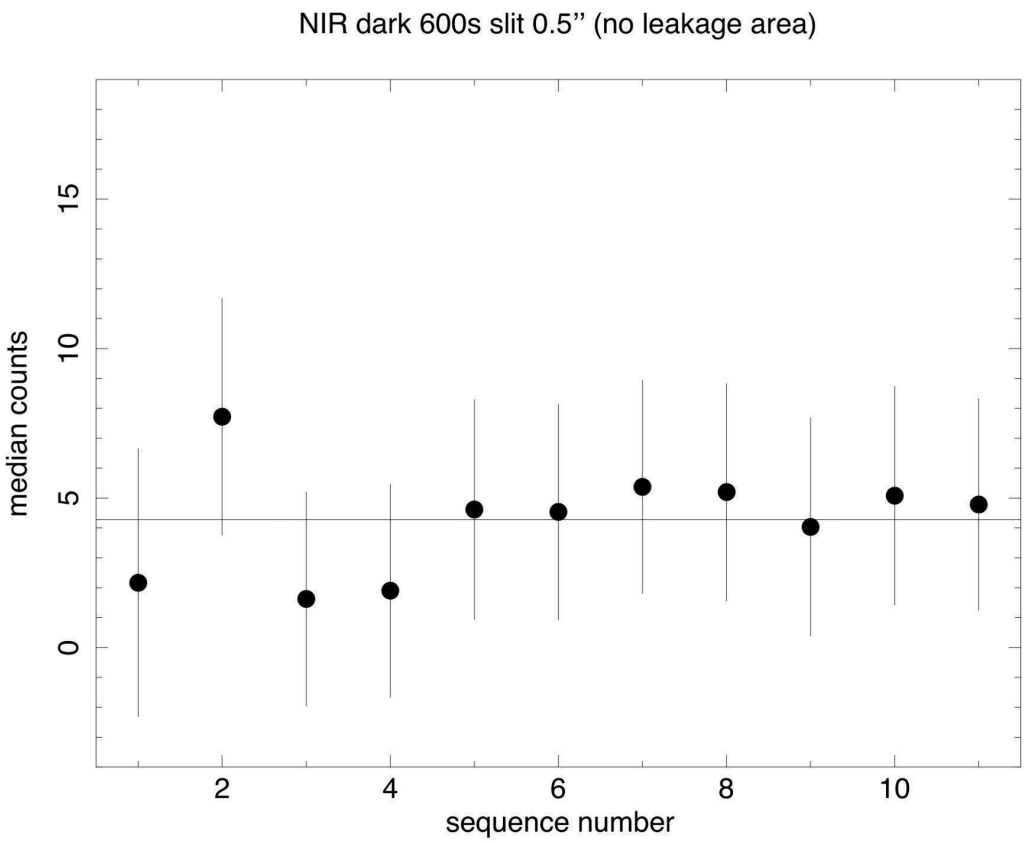

Figure 10: NIR dark level measured in a series of 600s exposures (NISE position: 1.0") over a 2048x1000 pix "no leakage area" shown in Fig. 9. Data has been taken on 2025 Nov 27, from 11:55:36 UT (SOXS.2025-11-27T11:55:36.284.fits) to 14:01:26 UT (SOXS.2025-11-27T13:51:26.219.fits). The solid line marks the average dark level (4.3 +/- 1.1 counts/pixel, which correspond to 9.9 +/- 2.5 e-/pixel). This Figure has to be compared with Fig. 6 (same exposure time).
NOTE: in spite of the plot title, the NISE position was 1.0" and not 0.5". This will be fixed in the next release.

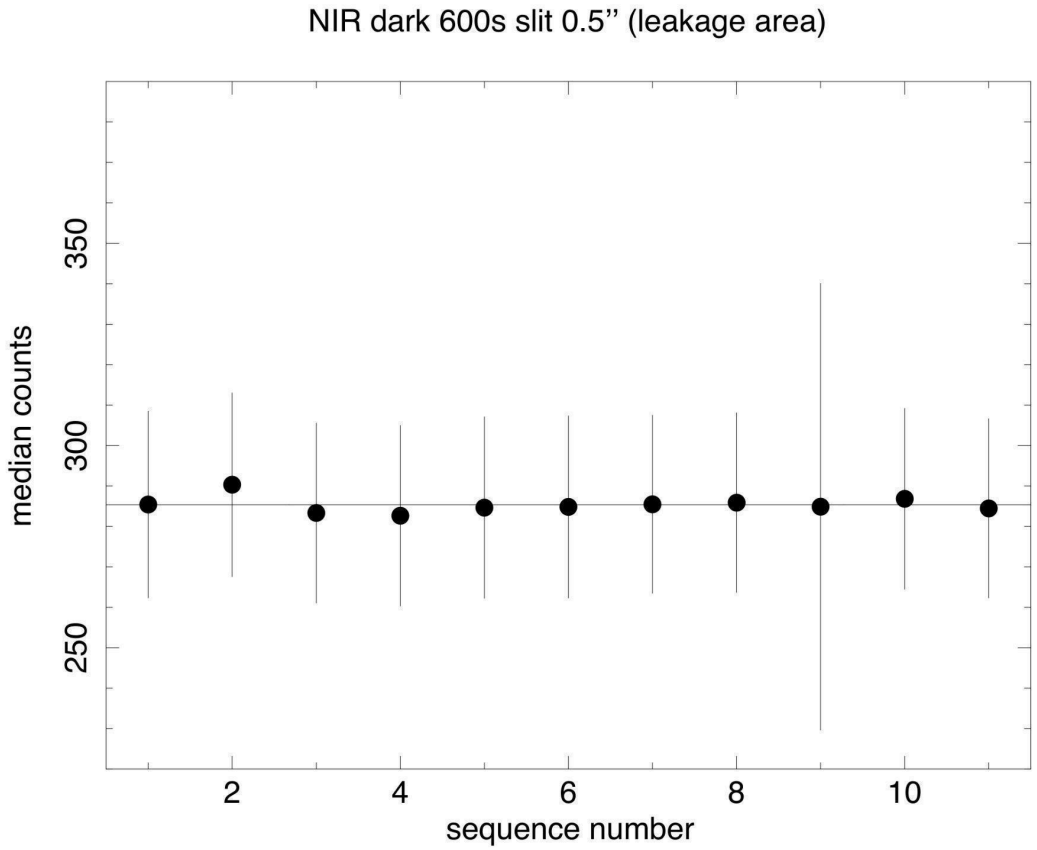

Figure 11: NIR dark level measured in a series of 600s exposures (NISE position: 1.0") over a 90x25 pix "leakage area" shown in Fig. 9. Data has been taken on 2025 Nov 27, from 11:55:36 UT (SOXS.2025-11-27T11:55:36.284.fits) to 14:01:26 UT (SOXS.2025-11-27T13:51:26.219.fits). The solid line marks the average dark level (285 +/- 7 counts/pixel, which correspond to 656 +/- 216 e-/pixel).
NOTE: in spite of the plot title, the NISE position was 1.0" and not 0.5". This will be fixed in the next release.

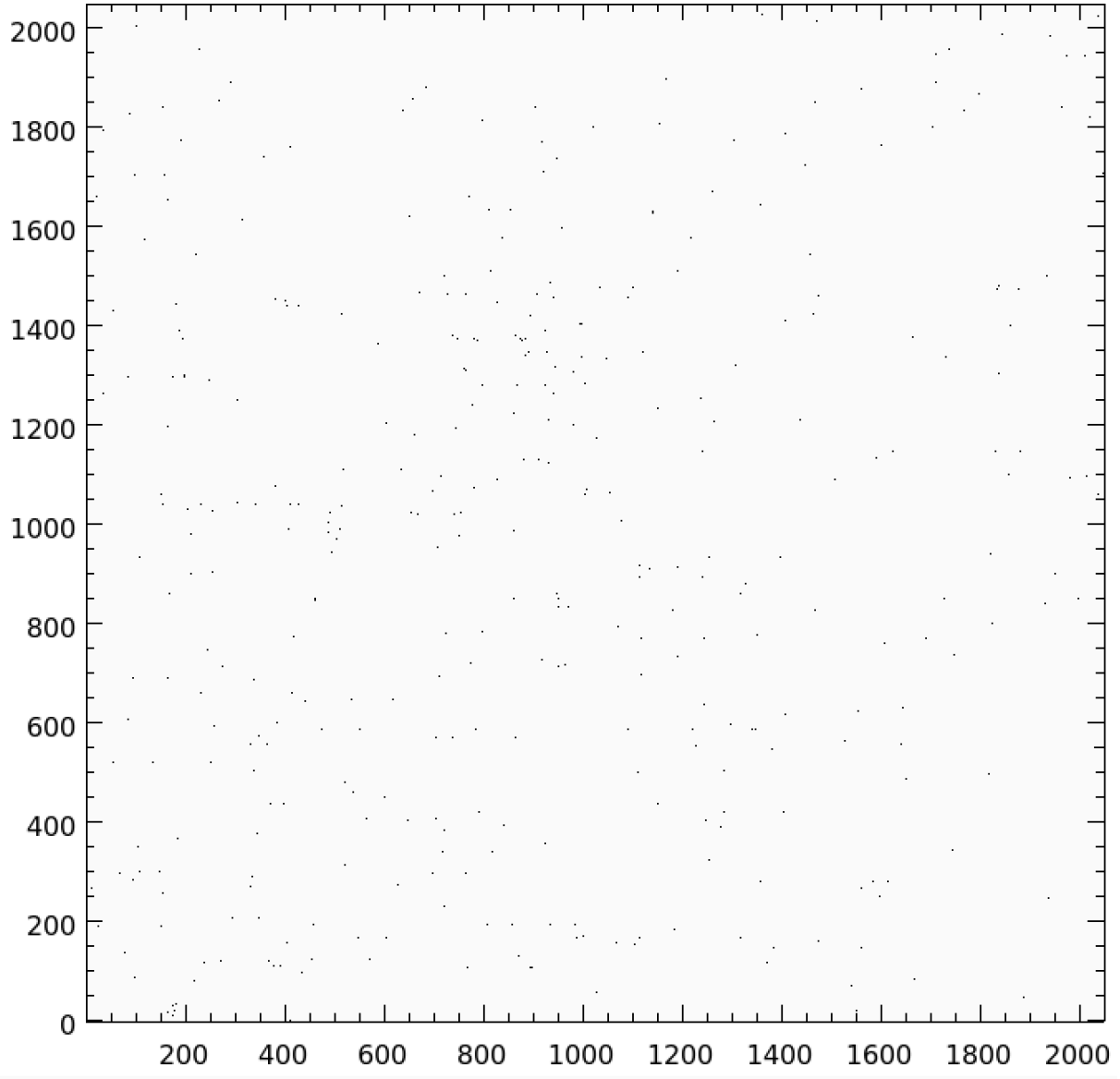

Figure 12: NIR bad pixel map (threshold = 10 sigma). Less than 1% of hot / bad pixels. Data available here: https://drive.google.com/drive/folders/1uOcOHHgWXS6t5MNjGk3ToOvU5lu2150A?usp=sharing

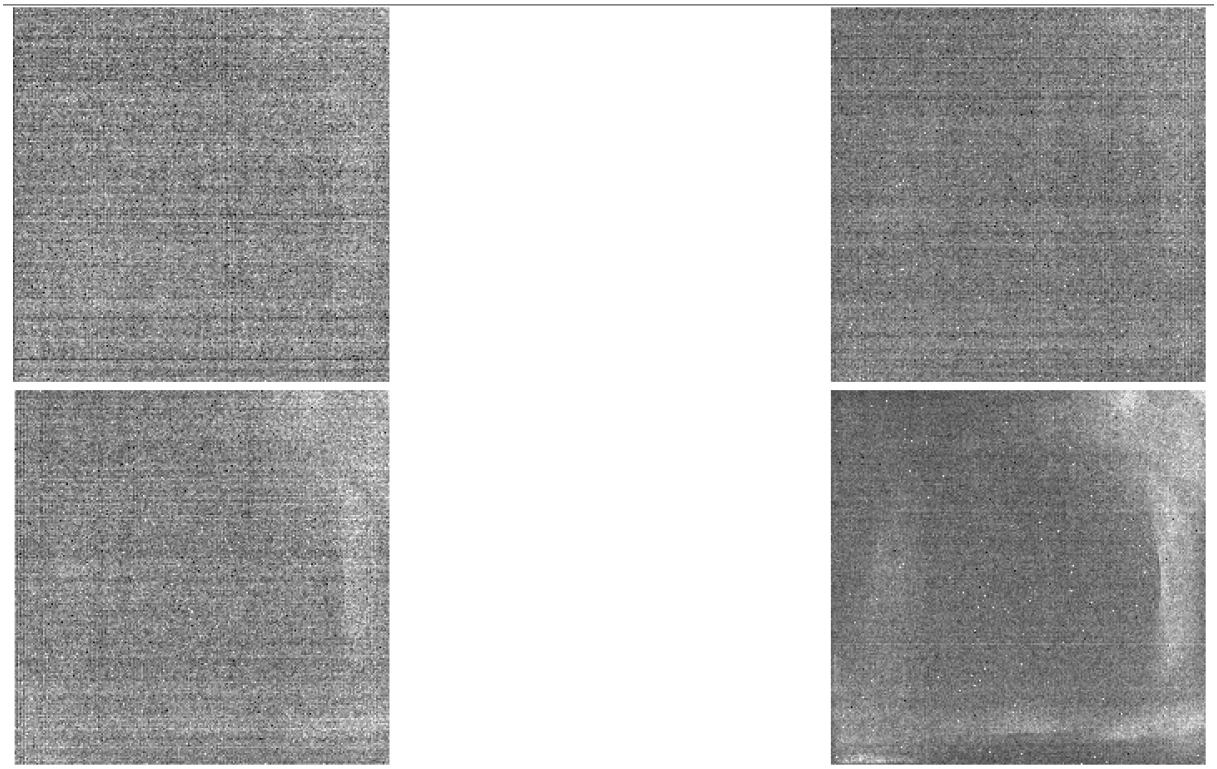

Figure 13: NIR darks (NISE position: blank) with texp = 300s, 600s, 900s, 3600s. A clear pattern is evident on the right side and at the bottom of the detector.

Persistence. A persistence test has been carried out on 2025, Dec 10. The NIR detector has been illuminated by the DEUT lamp (NISE: 5"). Then, after shutting off the lamp, a series of 60s frames was obtained (NISE: 5"). The median count per pixel level has then been measured over the same area in all the frames. As can be seen in Fig. 14, the persistence effect for a source with a brightness of ~ 25k counts/pixel is reduced by a factor > 1000 already after 120 seconds, becoming negligible after ~300 seconds.

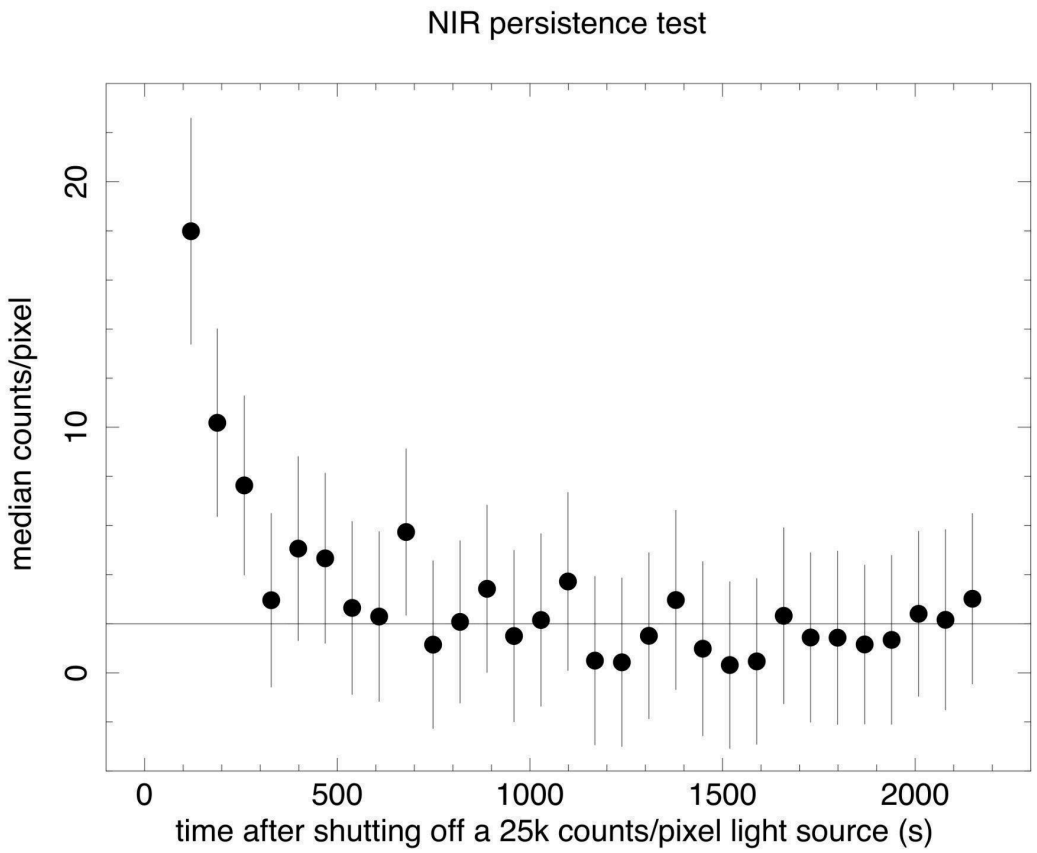

Figure 14: Results of the NIR persistence test carried out on 2025, Dec 10. Data available here: https://drive.google.com/drive/folders/1IcNpnAE-h7PgJRwFSCaAFvKf6a7kXm5n?usp=sharing

To do. Done. No major activity planned, apart from the thermal background monitoring (also in light of carrying out extensive pipeline testing to properly handle it). Repeat the persistency test with brighter sources (closer to saturation limit, i.e. 40k counts). Eventually share the set of data obtained between November and January with ESO NIR detector experts (e.g. Derek Ives). Update the User Manual with the measured values and persistency test results. In Table 1, the values obtained during the detector characterisation are reported.

Table 1: Measured properties of the SOXS detectors.

	UV-VIS	**NIR**	**AC**
Detector type	e2V CCD44-82	H2RG	BEX2-DD: Back Illuminated, Deep Depletion with fringe suppression, extended range dual AR coating
Operating temperature	155 K	45 K	183 K
QE	37.4 % at 350 nm 79.3 % at 400 nm 75.3 % at 500 nm 78.4 % at 650 nm 54.4 % at 900 nm 4.0 % at 1000 nm	70.0 % at 800 nm 82.0 % at 1000 nm 77.0 % at 1200 nm 78.0 % at 1400 nm 78.0 % at 1600 nm 83.0 % at 2000 nm	50.0 % at 350 nm 90.0 % at 450 nm 88.0 % at 550 nm 92.0 % at 650 nm 94.0 % at 750 nm 60.0 % at 950 nm
Number of pixels	2048 x 4096	2048 x 2048	1024 x 1024
Pixel size	15.0 µm	18.0 µm	13.0 µm
Gain (e-/ADU)	Slow High Gain: 1.1 Fast Low Gain: 2.0 Slow Low Gain: 2.1 Fast High Gain: 1.0	2.3	1.0
Readout noise (e- rms)	Slow High Gain: 3.6 Fast Low Gain: 5.7 Slow Low Gain: 4.0 Fast High Gain: 4.9	16.3	3.1
Dark current level	< 2 e-/pix/h	< 30 e-/pix/h	< 7 e-/pix/h
Non-linearity (deviation)	< 1% (mode 1)	< 5% @ ~ 40k counts	< 1%

4.2 Acquisition Camera performances

CCD characterization

Description. A series of frames with the shutter closed (dark & bias) and a series of sky and dome flat-fields. Frames to be taken with different integration times and different binning.
Parameters to be measured:

- Gain (e-/ADU)
- RON (e-)
- Linearity peak-to-peak (%)
- Dark Current (e-/pix/hr)
- Bias Level (ADU)
- QE
- Bad pixel map
- Fringing (if any, in the redder filters)

Status. All the needed data has been taken. In Table 1, the preliminary values obtained during the detector characterisation are reported.
We found no evidence for fringing and managed to obtain good sky-flats at twilight (Fig. 15). Some pattern is present in flats obtained with the SDSS-u filter, as typically observed with this filter.
Sky-flats will be the main source for flat-field calibration; however, a combination of lamps has been found for dome flats, if needed (Fig. 16), enabling us to obtain ~20k counts in 1 sec exposure (SDSS-r filter). However, AC dome flats are not currently implemented in the calibration plan.

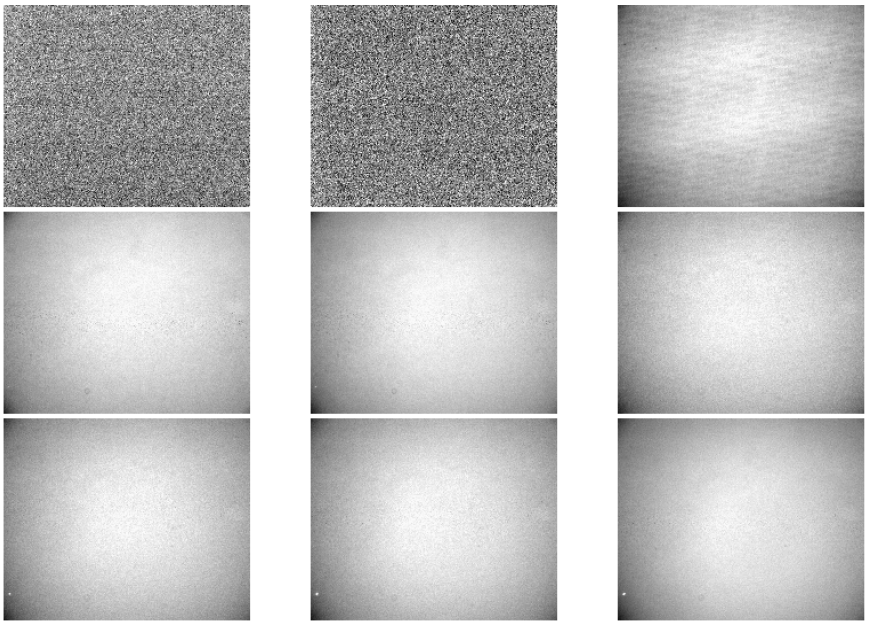

Figure 15: Example of AC calibration frames (from top left, clockwise): Bias (SOXS.2025-10-20T23:34:04.668.fits), Dark (SOXS.2025-10-21T12:08:56.563.fits), sky-flats in SDSS-u, VIMOS-Y, SDSS-z, SDSS-g, VIMOS-V, SDSS-r, SDSS-i (SOXS.2025-10-20T23:10:56.392.fits, SOXS.2025-10-20T23:14:37.097.fits, SOXS.2025-10-20T23:17:35.726.fits, SOXS.2025-10-20T23:20:26.680.fits SOXS.2025-10-20T23:23:42.874.fits, SOXS.2025-10-20T23:27:06.930.fits, SOXS.2025-10-20T23:30:41.896.fits).

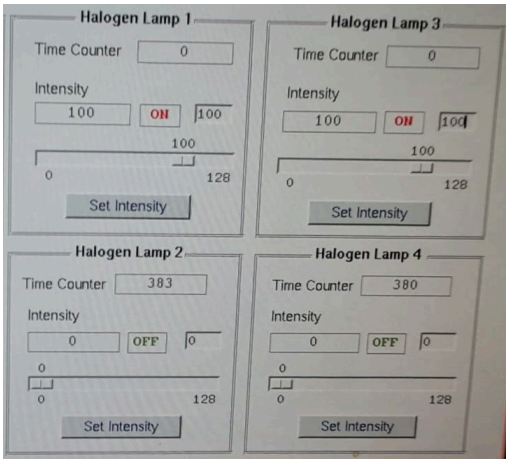

Figure 16: Configuration of NTT dome lamps for the AC imaging dome flats.

Bias statistics. We analyzed all the bias series (usually between 9 and 11 frames) that were taken between March and November 2025. As it is visible from the histogram in the left side of Fig. 17 the bias stability is on average within ~4 counts (less than 2% of the median bias value), but the median bias value can change up to 7 ADU within a series. As it is visible in the right side of the figure for the histogram the most common average value of the master bias is around 234 counts.

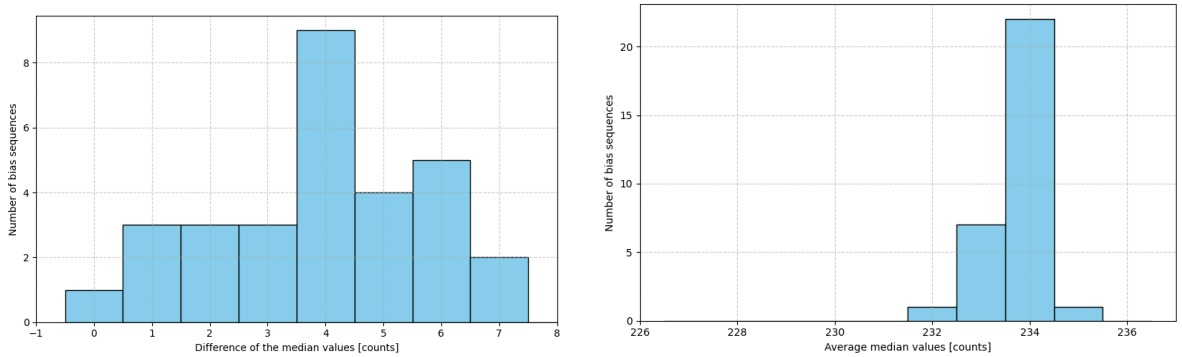

Figure 17: (left side) Difference between the maximum and minimum median values of a bias sequence. (Right side) Distribution of the average of bias median values in a sequence.

Dark Current. Taking into account the variations in the bias level, which in some cases are larger than the dark current signal, we measured the dark current by acquiring a set of 14 dark frames at the operating temperature of the ANDOR camera (−90 °C), with exposure times ranging from 2 to 15 minutes. We then computed the median value of each full-frame image and fitted these values as a function of exposure time with a straight line (see Fig. 18). The slope of the fitted line provides the dark current, while the intercept represents the average bias level of the 14 dark frames. The measured dark current is 0.002 ± 0.002 e^{-} s^{-1}, which lies between the values reported in the ANDOR datasheet: 0.017 e^{-} s^{-1} at −80 °C and 0.00012 e^{-} s^{-1} at −100 °C. The relatively large uncertainty is mainly due to variations in the bias level.

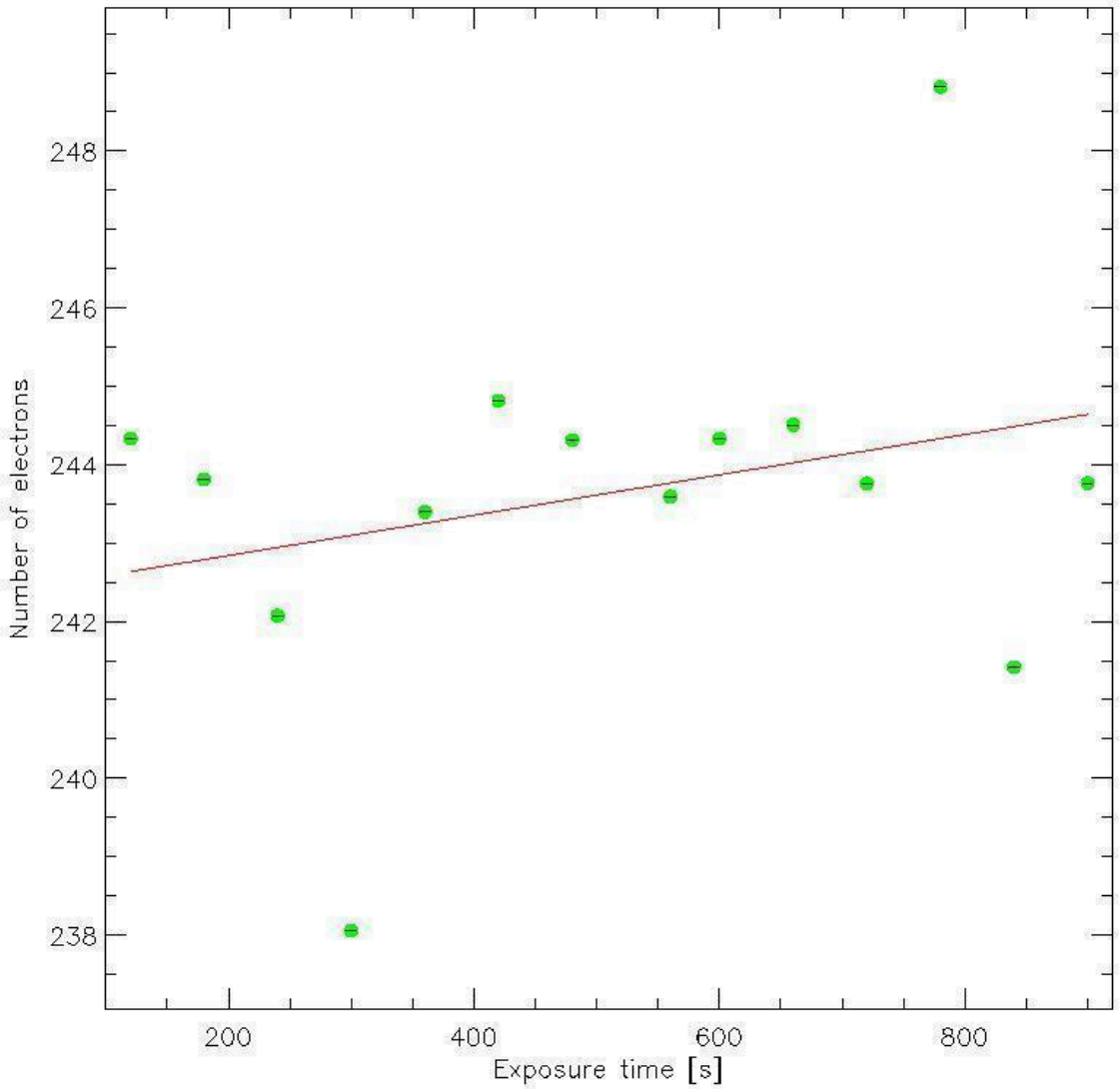

Figure 18: Measure of the AC dark current.

Linearity. Linearity was assessed by acquiring a series of dome flats with exposure time ranging from 4 to 26 s (From SOXS_ACQ_2025-11-27T19_51_07.345.fits to SOXS_ACQ_2025-11-27T20_12_50.610.fits). A total of 23 images were taken, each of those were corrected for dark current. The resulting frames were then divided by their respective exposure times, producing a signal normalized to exposure time for each pixel. For each pixel, the values in this normalized signal vector were divided by their mean, and a standard deviation was calculated. The distribution of these standard deviations is presented on the left side of Fig. 19. On the right side of the same figure we show the median normalized residuals in bin of 1000 ADU in function of the signal. The plot revealed a clear trend which is different from what was found in the same test taken at Padova observatory. The minimum maximum difference is within 1.3%. The clear drop register by the last point is

due to saturation which occurs around 61000 ADU. It is worth mentioning that the light distribution is not constant, therefore the pixel in the center of the frame reaches saturation at exposure times shorter than those on the corners. The latter causes the initial drop register by the penultimate bin.

Summarizing the CCD shows linearity with on for most of the pixels; however, measurements confirm the presence of a 'non-linear' column that was detected with the same test carried out at Padova Observatory (see Fig. 20).

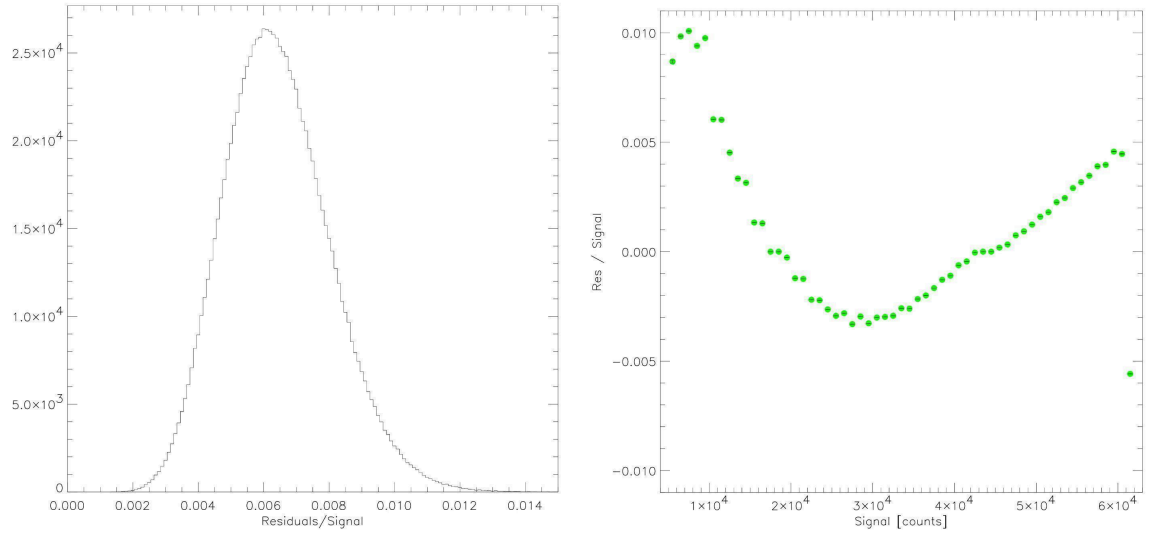

Figure 19: (left side) Distribution of the standard deviation relative to each pixel of the AC frames. (Right side) Median residuals in bin of 1000 ADU in function of the signal. Error bars are usually smaller than the points

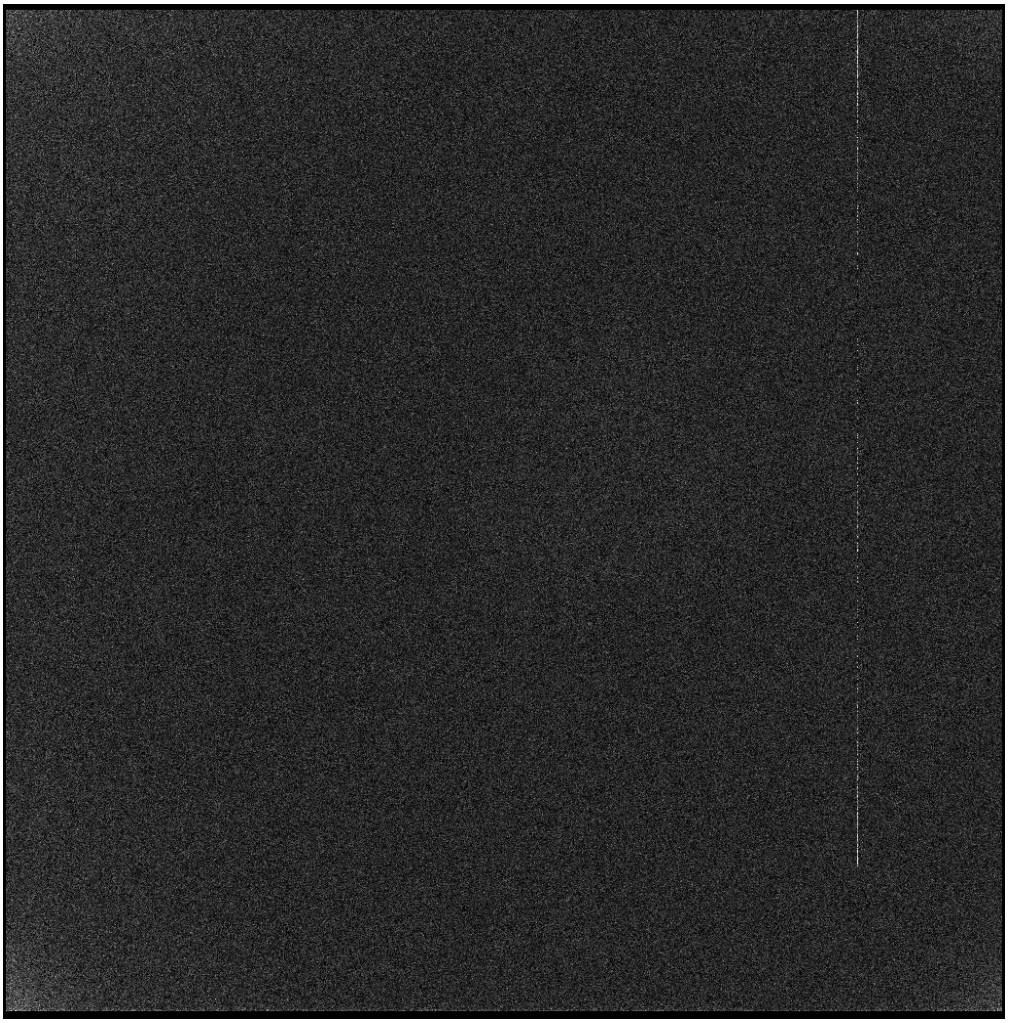

Figure 20: Bad column in the AC camera.

To do. Done (no more activities planned).

Image quality and sensitivity

Description. Observe a set of stellar fields (e.g. open clusters) to measure the FWHM of the stars in all filters (to be compared with the values of the DIMM), to check the plate scale and to check for image distortions at the edges of the CCD. Observe a set of photometric standards in all filters to determine the zero points. Use short-time exposure observations of bright standard stars (and/or of sky flats) to check for shutter delay effects and for the illumination function.

Status. Enough data taken (photometric standard fields and crowded stellar fields). In detail:

Plate scale. The plate scale has been measured by computing the astrometric solution on the acquisition images obtained during Mission 1. It resulted in 0.207”/pixel, value confirmed through the various missions.

We carried out a systematic analysis of a total of more than 1000 acquisition images taken between March and September. We divided each FITS file into an 8x8 grid and estimated the median FWHM along X and Y in the central region (2x2 cells) and in each of the edge quadrants, always using the same detection algorithm and the same detection threshold.

FWHM vs. DIMM. From a systematic analysis of the AC images obtained during the October run (during which we typically had excellent seeing conditions), the FWHM measured from the stars is on average slightly higher w.r.t. the seeing value reported by the DIMM (Fig. 21). On one hand, this can be generally expected, given that the DIMM observes at the best conditions (at the zenith). On the other hand, this trend may indicate that, in some cases, the whole system (telescope + AC) was not perfectly in focus.

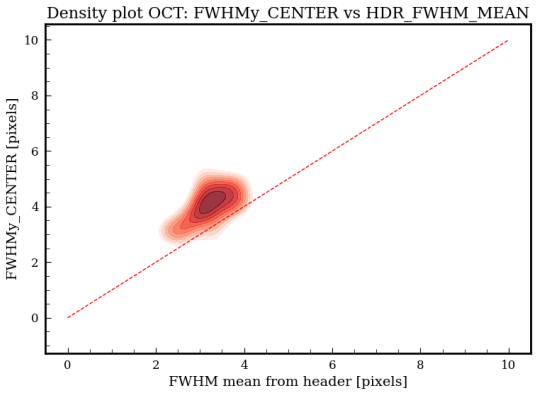

Figure 21: Comparison of the FWHM for stars in the central quadrant (128x128 pixels) measured on the images obtained with the AC camera during the October run w.r.t. the FWHM value reported by the DIMM (header). The plate scale is 0.207”/pixel.

Distortions. There are no significant differences between the x and y FWHM for the stars at the center of the images (no distortions; Fig. 22), while some asymmetry (distortion) is clear for the stars in the edge quadrants (Fig. 23).

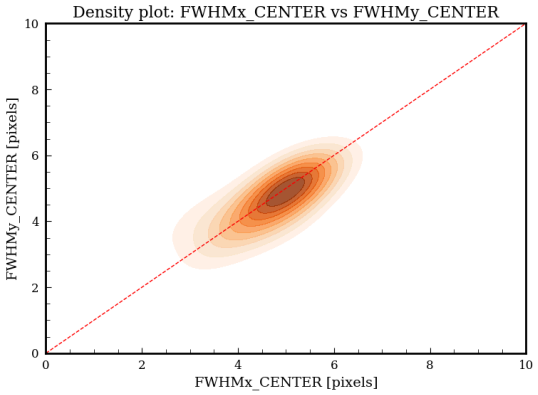

Figure 22: Comparison of the FWHM x and y for stars in the central quadrant (128x128 pixels) of images obtained with the AC camera. The analysis has been carried out over 1053 images collected during the commissioning runs. The plate scale is 0.207”/pixel.

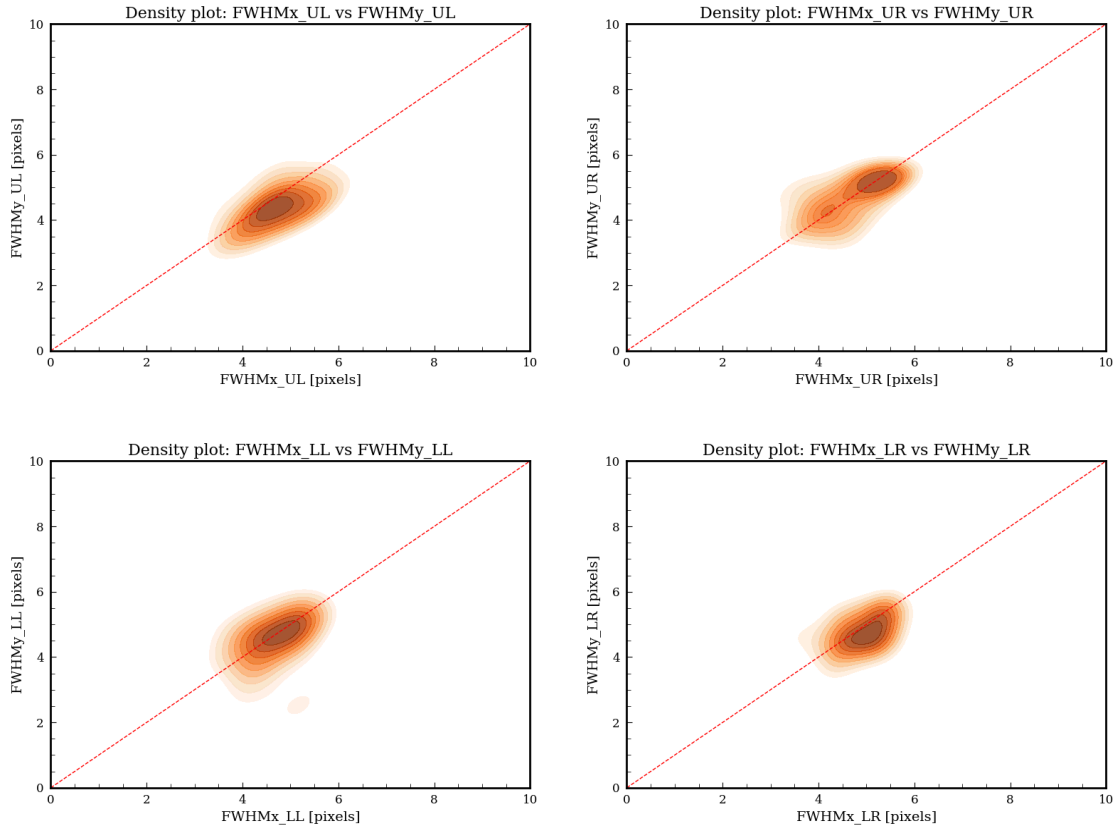

Figure 23: Comparison of the FWHM x and y for stars in the Upper Left (UL), Upper Right (UR), Lower Left (LL) and Lower Right (LR) corners (128x128 pixels each) of images obtained with the AC camera. The analysis has been carried out over 1053 images collected during the commissioning runs. The plate scale is 0.207”/pixel.

Zero-point determination. Zero-points have been measured against photometric STD stars observed during the June run (Fig. 24, Table 2).

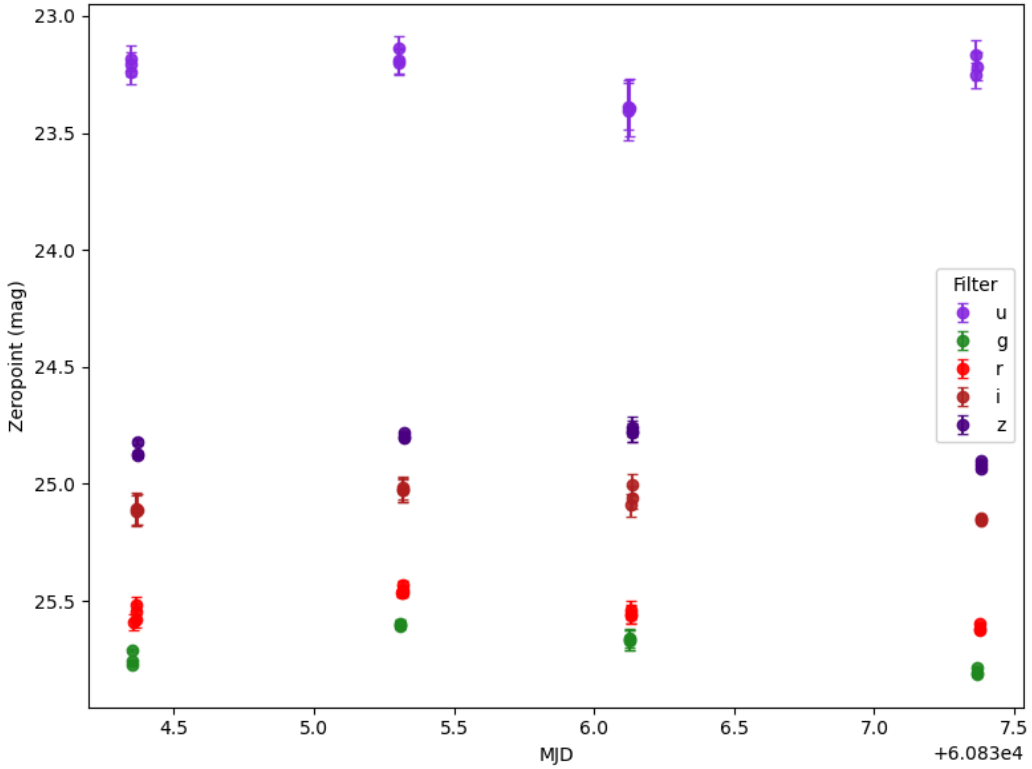

Figure 24: AC photometric zeropoints. Measurements made against the photometric STD Stetson fields E5 and E8 observed during the June run (see night log link in Sect. 3).

Table 2: Average photometric zeropoints, derived from the measurements shown in Fig. 9.

Filter	Mean Zeropoint (AB mag)
u	23.25 +/- 0.09
g	25.70 +/- 0.08
r	25.54 +/- 0.06
i	25.08 +/- 0.06
z	24.83 +/- 0.06

Shutter delay characterisation. Test carried out during the November run. A set of dome flats were taken starting with an exposure time of 0.1 s until 5.0 s. All dome flats were bias subtracted and the ratio of median values computed on the pixels inside the red circle and between the red and yellow circles visible in Fig. 25 (left side) were estimated. These are plotted against the integration time in Fig. 25 (right side) The effect of the shutter is negligible starting at ~1.5 s (< 0.5%). To visualise the foot print of the shutter in Fig. 26 we show the ratios of the dome flats of 0.1s and 5.0 s (left side) and 1.5s and 5.0s (right side).
Data available here:
https://drive.google.com/drive/folders/11c2ug-iKeOIZeYmWDpZiJzsFyz_cKgaa?usp=sharing

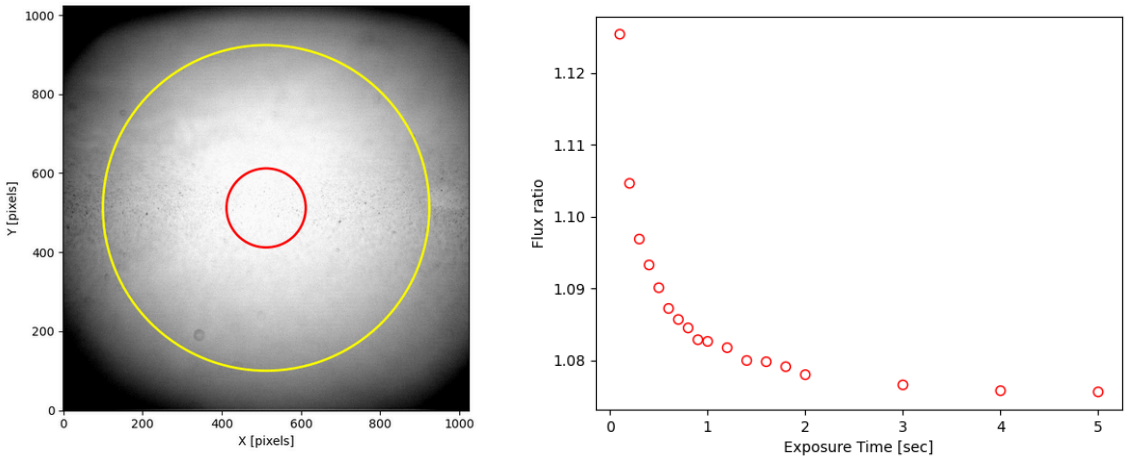

Figure 25: Left side: 5.0 s dome flat with overplotted the regions where the median value was computed. Right side: Ratio between the median values of the counts of the pixel inside the red circle and between the red and yellow circles, respectively as a function of the exposure time.

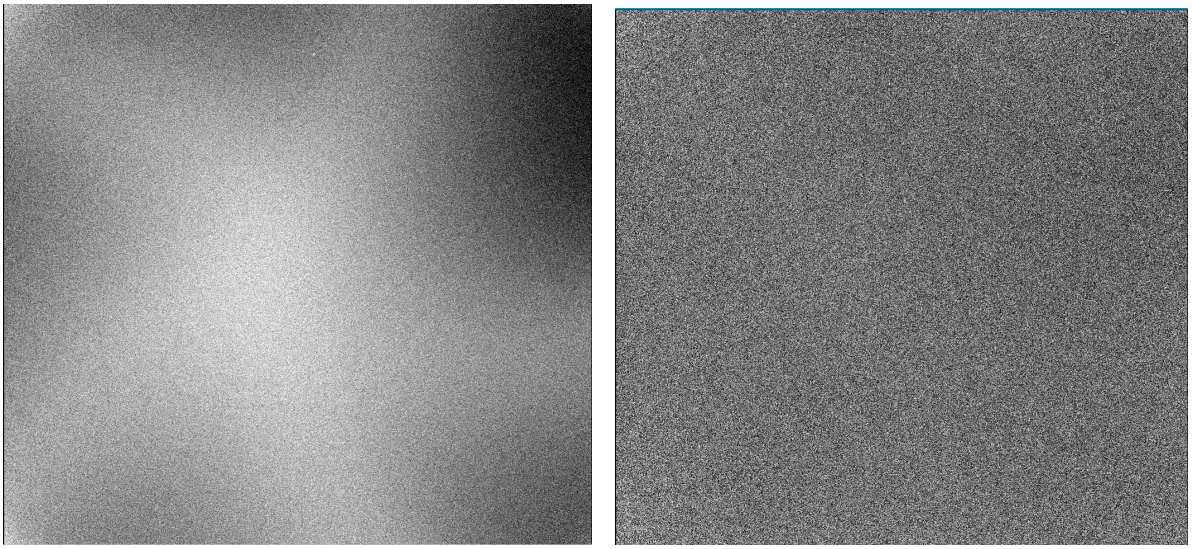

Figure 26: Left side: ratio between the 0.1 sec and 2.0 sec dome flats. Right side ratio between the 1.0 sec and 5.0 sec dome flats. In the 0.1 sec image the footprint of the shutter is clearly visible

To do. Done. No major tests are planned. It may be useful to keep observing photometric STD fields (when the nights are photometric) to monitor the magnitude zero-points. The investigation of the causes of the distortions observed (including a possible tilt of the detector) is currently under investigation.

4.3 Focus and alignment

Acquisition camera focus position

Description. Set manually the focus position by optimising the image quality (e.g. obtained from diffuse light through the pinhole). Obtain the focus curve and find the best focus. Perform a check also on the sky, possibly during stable seeing conditions.

Status. Done. We have the absolute and relative (to the SDSS-r filter) best focus position for the AFOC (AC focusser) optical element (Table 3). Being an operation not too time-consuming (~30 min to obtain the focus curves in all filters), we prefer to repeat it in every future commissioning run to increase statistics (also about different/seasonal ambient / temperature conditions).

Table 3: AFOC (AC focusser) positions for the best focus of the AC filters.

Filter	Value of the AFOC focusser (mm)
SDSS-u	15.0[1]
SDSS-g	11.3
VIMOS-V	9.8
SDSS-r	8.7
SDSS-i	7.5
SDSS-z	6.4
VIMOS-Y	6.1

To do. Done. Keep monitoring the AC focus values during the next runs, and check for temperature effects.

[1] End of the AFOC range.

Slit focus position

Description. Set the focus position manually by optimising the image quality. Obtain the focus curve and find the best focus. Perform a check also on the sky, possibly during stable seeing conditions.

Status. Done. We measured that the UV-VIS is in focus after setting the NTT M2 at the position determined from the NTT image analysis procedure, with no need for further focus change. If the ONECAL procedure is carried out, then an offset of +0.2 mm has to be applied to M2 to have the UV-VIS in focus (Fig. 27). Once the UV-VIS focus is set (as described above), the focus position for the NFOC (NIR focusser) optical element has been found to be stable at the position of 2.8 mm.

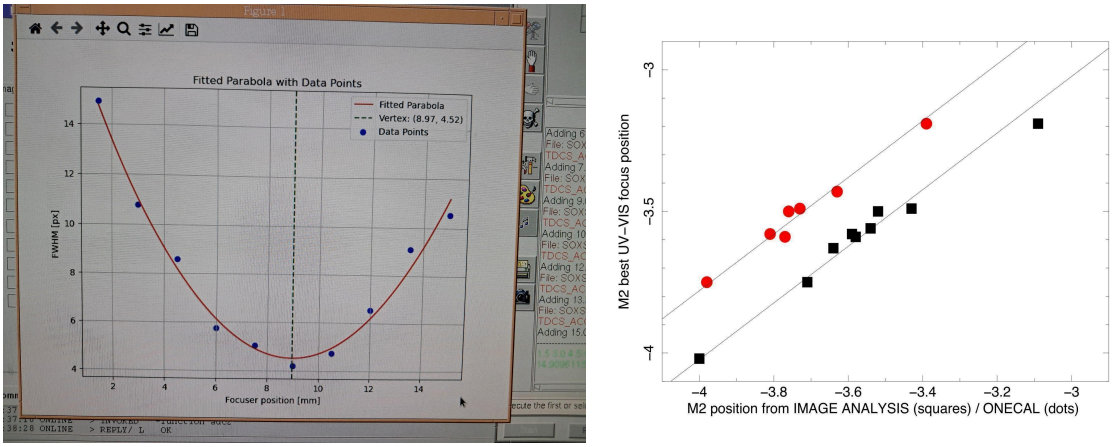

Figure 27: *Left*: Screenshot showing the output of the UV-VIS focus procedure. *Right:* The measured offsets between the NTT M2 position obtained with the IMAGE ANALYSIS procedure (dots) / ONECAL procedure (squares) and the M2 position computed through the UV-VIS focus procedure. No significant offset is found w.r.t. to the IMAGE ANALYSIS M2 position, while a +0.2 mm offset is found w.r.t. the ONECAL M2 position.

To do. Done (no more activities planned, monitoring excluded).

Alignment of the slits

Description. Illuminate each slit position for each arm using the calibration box as a light source to obtain the projected image of the different slits on the acquisition camera (through the pellicle) and to measure the position on the detector.

Status. Done during AIV for both the UV-VIS and NIR spectrographs. Regularly verified during commissioning.

To do. Done. A technical template to quickly monitor (through back-reflection illumination of the slits) the alignment has been developed and successfully tested during the Jan 2026 run).

4.4 Flexure effects check

Description. Starting from the look-up table acquired in Europe, we run a series of tests on both spectrographs (UV-VIS and NIR) to check the flexure compensation system and to improve it at the telescope. For each arm, take a series of arc spectra for a set of telescope elevations and instrument position angles (possibly sampling positions for which extreme flexures are expected), measure any mismatch in the spectral line position and the needed correction to be applied to the tip-tilt mirror on the common path. To be repeated also on-sky observing bright targets (e.g. spectrophotometric standard stars, narrow emission line Hii regions of star-forming galaxies). On-sky data can also be used to determine the center of rotation for the spectrograph and the acquisition camera.

Status. The lookup table has been obtained during the AIV and implemented in the instrument software. The goodness of the flexure correction has been checked with the dispersion solution obtained by the pipeline from the observations of arc lamps through the pinhole in the daily calibrations. For the UV-VIS, the difference between the measured and expected position of the arc lamp spectral lines along the dispersion direction (Y axis) can be up to 12 pixels (Fig. 28**;** ~ 2.4 Angstrom). For the NIR, where the dispersion direction is along the X axis, the difference can be up to 4 pixels (Fig. 29**;** ~2.4 Angstrom). Along the spatial direction, such a difference can be up to 6 pixels (Fig. 30; ~ 1.2 Angstrom) and 3 pixels (Fig. 31; ~1.8 Angstrom), for the UV-VIS and NIR, respectively.

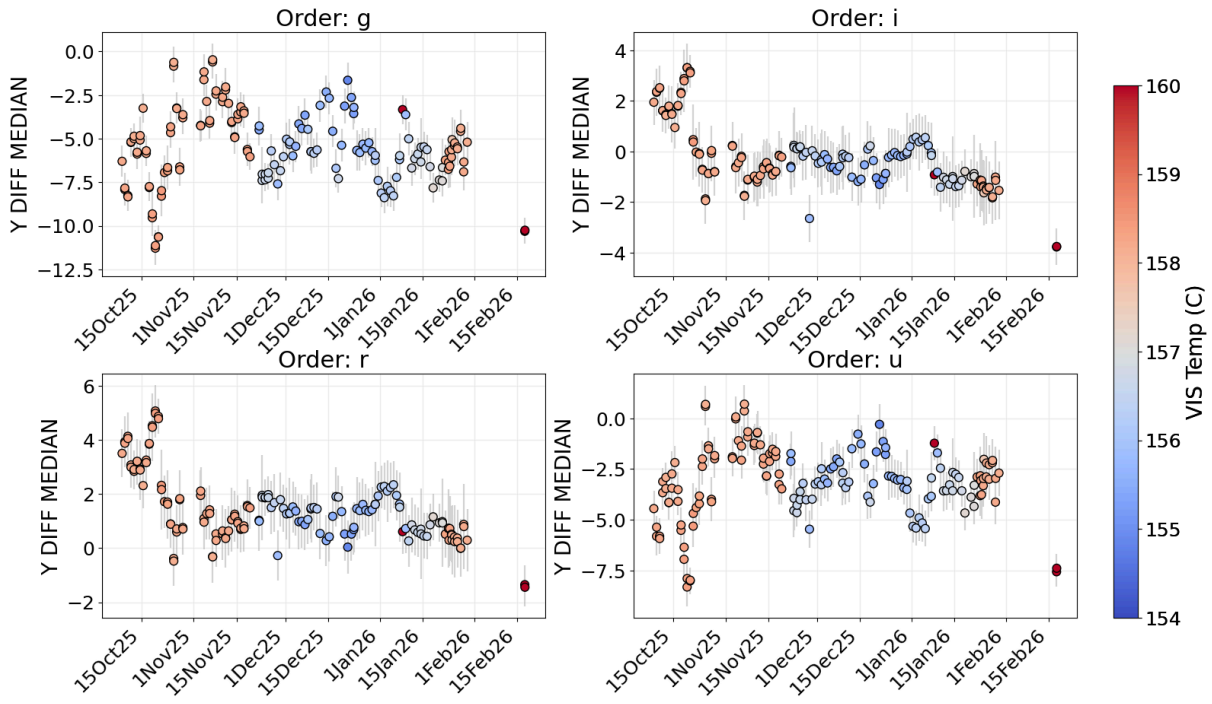

Figure 28: Difference between the measured and expected position of the arc lamp spectral lines (single pinhole) along the UV-VIS dispersion direction (Y axis).

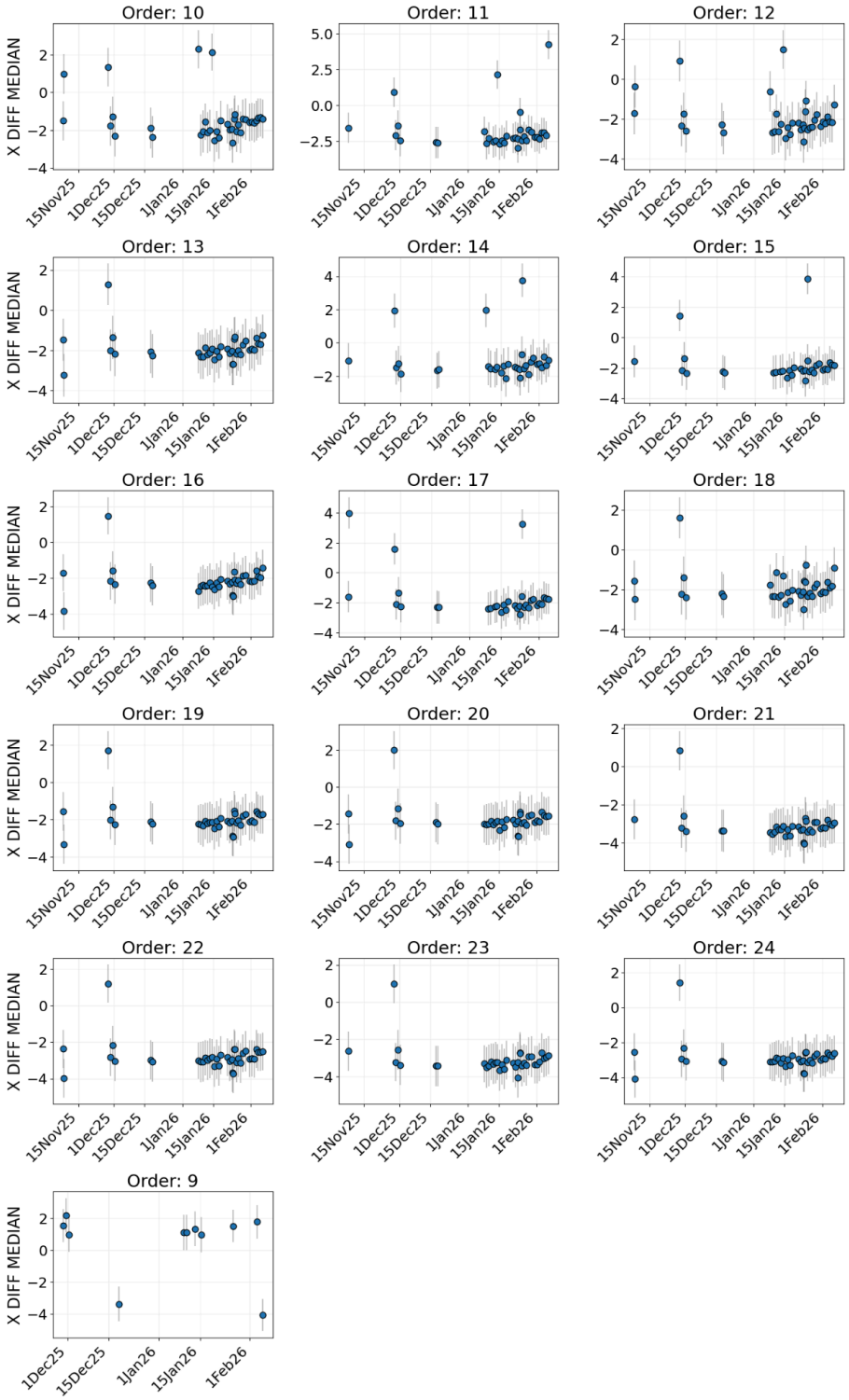

Figure 29: Difference between the measured and expected position of the arc lamp spectral lines (single pinhole) along the NIR dispersion direction (X axis).

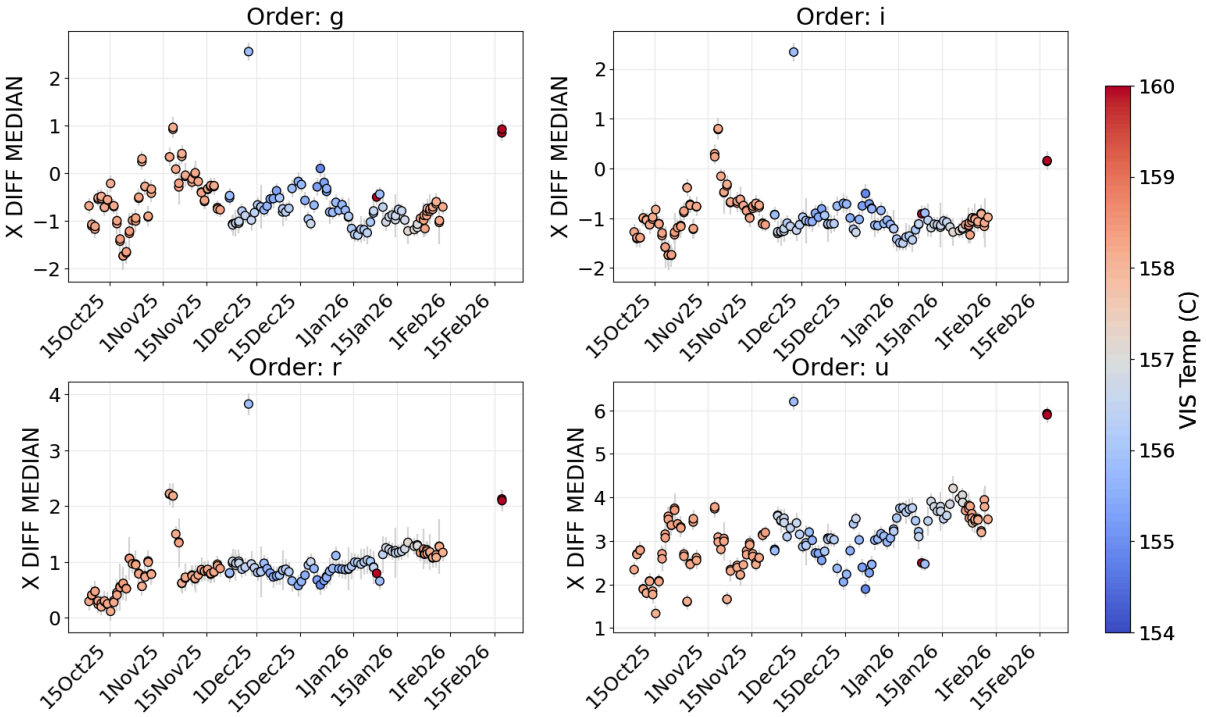

Figure 30: Difference between the measured and expected position of the arc lamp spectral lines (single pinhole) along the UV-VIS spatial direction (X axis).

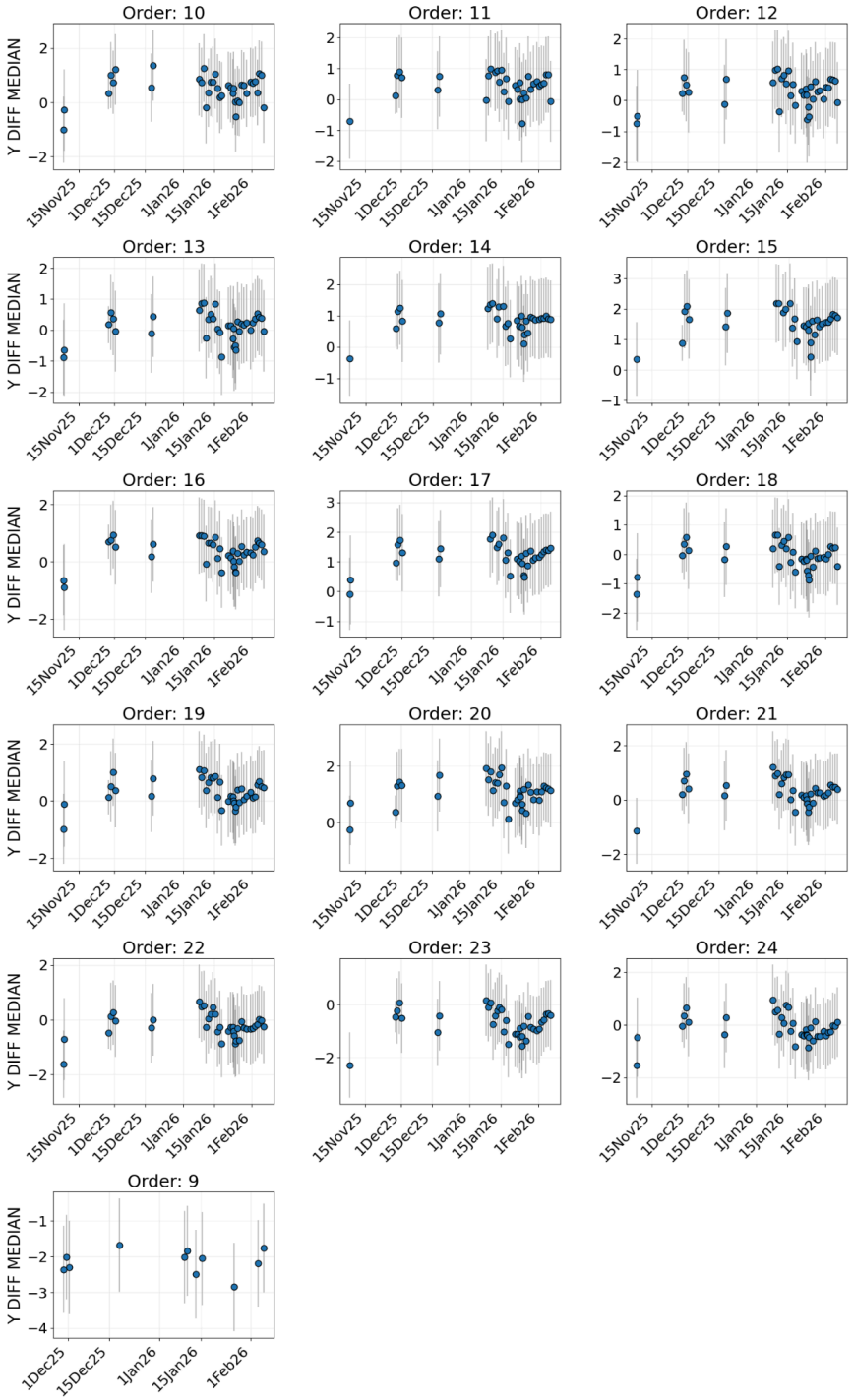

Figure 31: Difference between the measured and expected position of the arc lamp spectral lines (single pinhole) along the NIR spatial direction (Y axis).

To do. Done. A second-order correction of the dispersion solution is ready to be implemented in the next pipeline release. A re-analysis of the calibration data will be carried out to check the improvement of the dispersion solution stability.

4.5 Spectrographs Image Quality

Spatial resolution along the slit

Description. For both arms, measure the FWHM of the spectral trace at the centre and at the edges of each order from flat field QTH lamp spectra. Check for possible temperature effects.

Status. Enough data has been taken. The pipeline computes the FWHM (in pixels) of the spectral traces for the single pinhole spectroscopic flat field. Plots are stored in files named *OLOC_PINHOLE_10.0S_SOXS_residuals*pdf. (see an example in Fig. 32). Analysis of the data collected reveals no issues (Fig. 33-34, showing the UV-VIS orders FWHM from single pinhole spectra of the QTH flat field lamp).

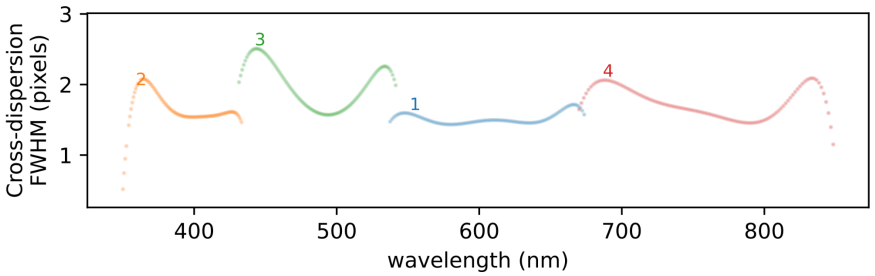

Figure 32: Example of the pipeline automatic product showing the measure of the UV-VIS orders FWHM.

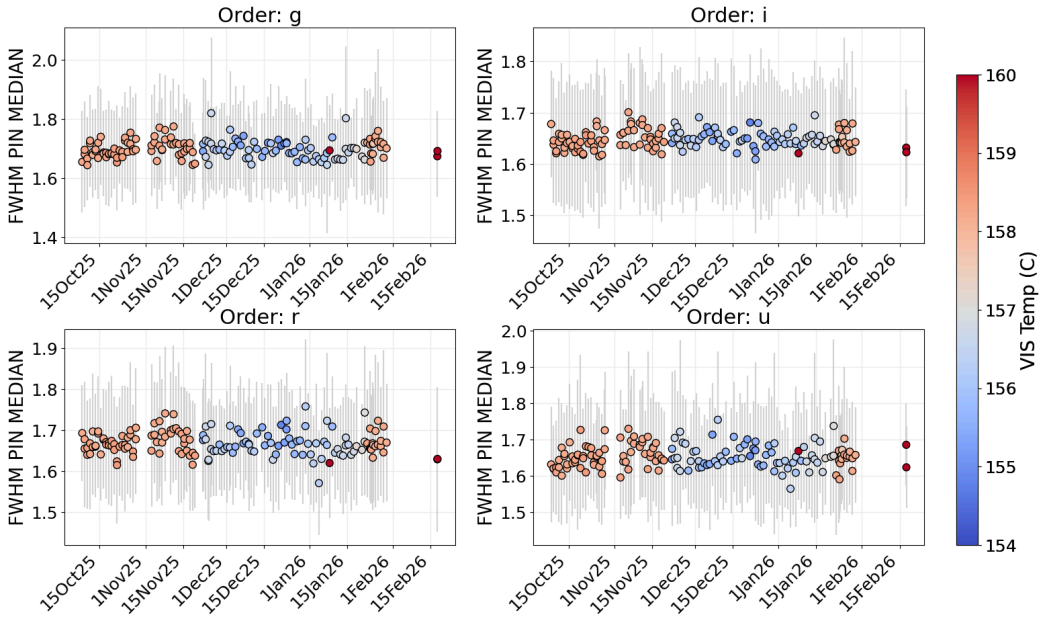

Figure 33: Measure of the UV-VIS orders median FWHM from data obtained during the 2025 Oct- 2026 Jan run.

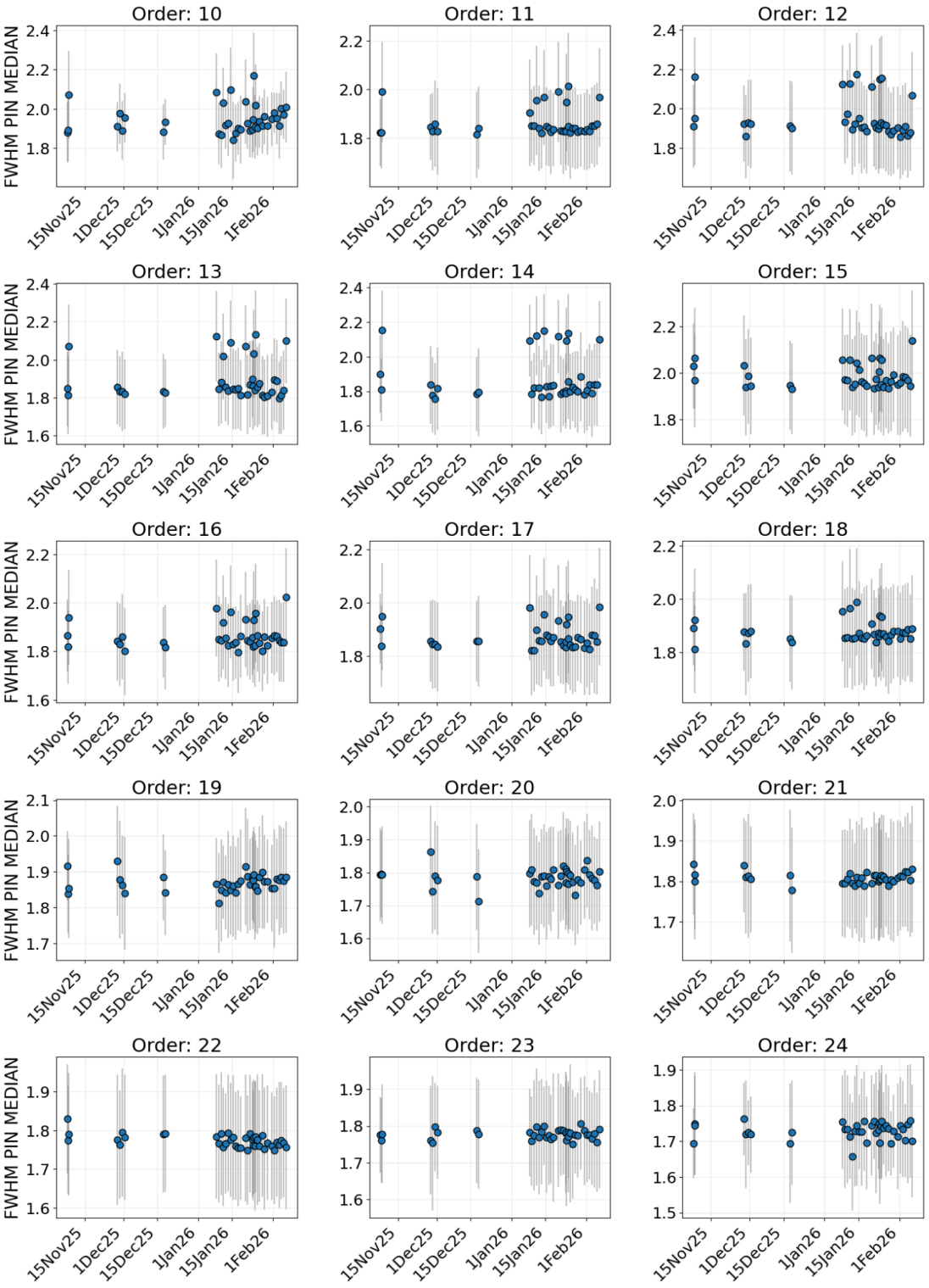

Figure 34: **Median FWHM of the NIR orders from the data obtained during the 2025 Nov - Jan run.**

To do. Done. No more activities planned.

Resolving power

Description. Measure the spectral resolving power for all slits in each arm by taking arc spectra. Consider both the FWHM of the lines at various wavelengths and the possibility of resolving adjacent lines. Repeat this test for all the slits.

Status. Done. The spectral resolving power from arc lines is measured by the pipeline. The spectral resolving power from arc lines is measured by the pipeline. The results for a 0.5" pinhole are stored in the FITS tables named *DSOL_PINHOLE_*_SOXS_FITTED_LINES.fits (where you can find wavelength, fwhm_pin_px, R_pin) with the corresponding plot stored in the files named *DSOL_PINHOLE_*_SOXS_RESIDUALS*.pdf (directory: qc/soxs-disp-solution).
The results for the 1" slit are stored in the FITS tables named *SSOL_MULTPIN_*_SOXS_FITTED_LINES.fits and the corresponding plots in the PDF files named SSOL_MULTPIN_*_SOXS_RESIDUALS_*.pdf (directory: qc/soxs-spatial-solution)

All measurements confirm that the spectral resolution is above requirements for both the UV-VIS and NIR (Fig. 35 and Fig. 36). The UV-VIS and NIR data collected so far indicate that the resolution is also stable over time (Fig. 37-38).

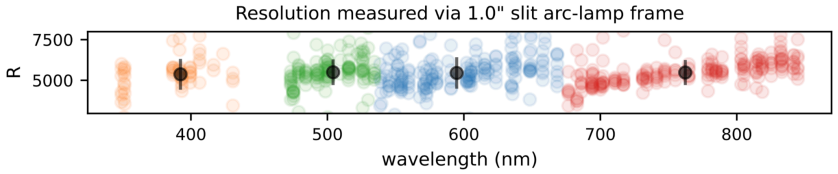

Figure 35: UV-VIS spectral resolution (1" slit; pipeline output).

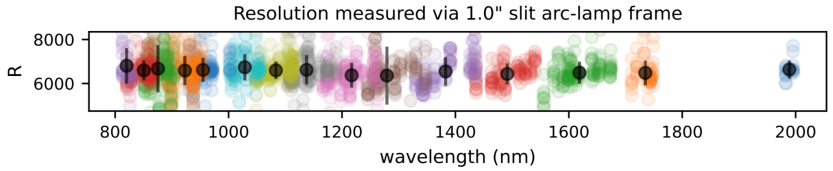

Figure 36: NIR spectral resolution (1" slit; pipeline output).

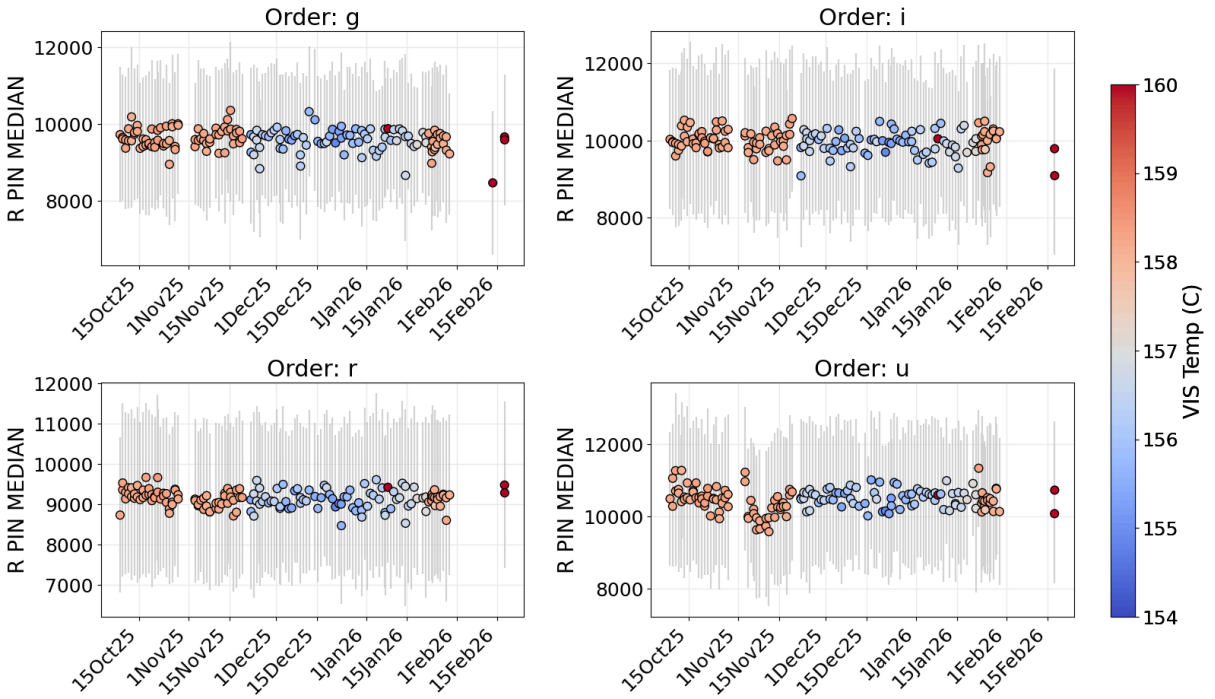

Figure 37 : Median resolution of the UV-VIS spectrograph (0.5" pinhole; pipeline output) over the 2025 Oct - 2026 Feb period.

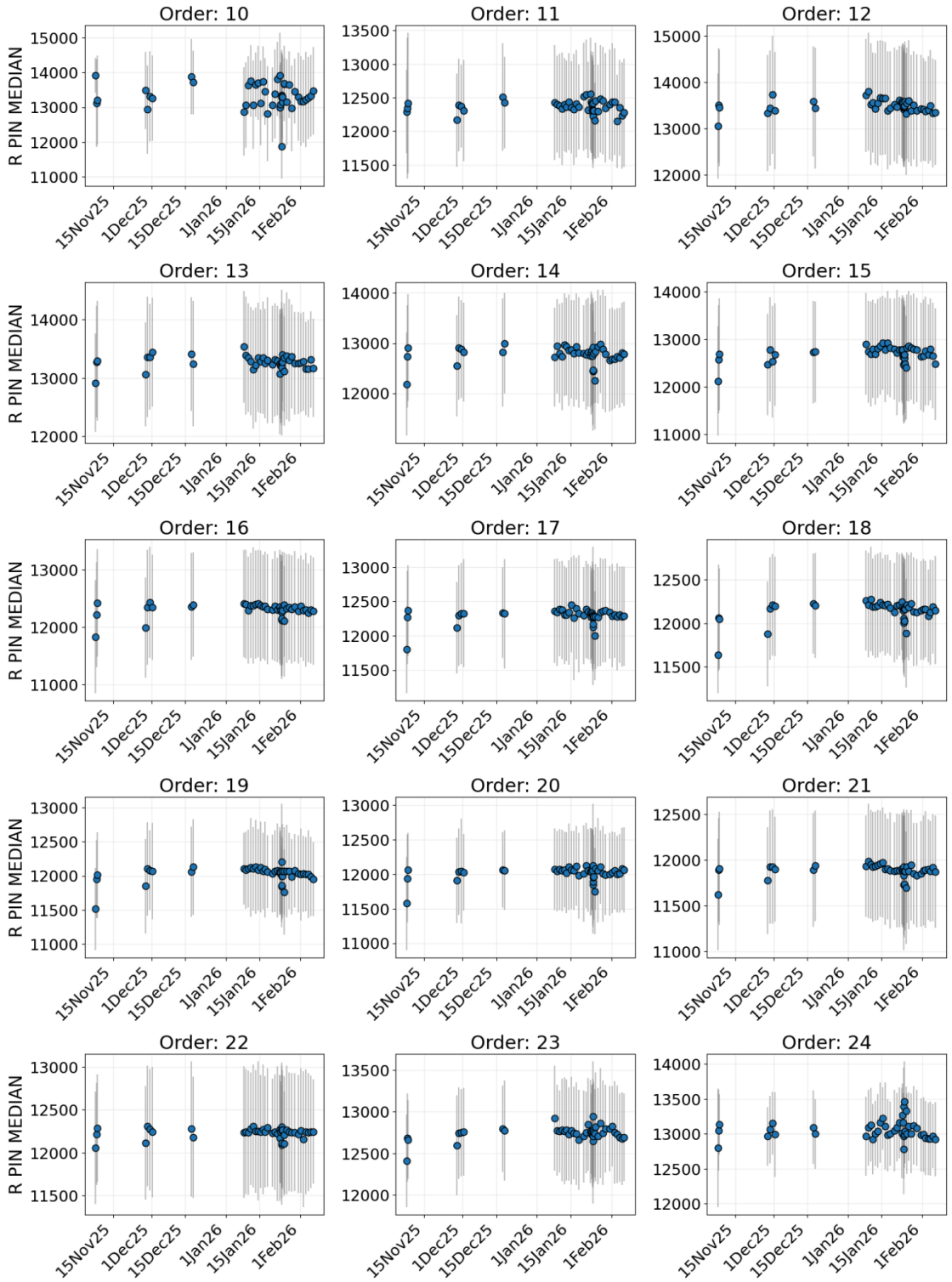

Figure 38: Median resolution of the NIR spectrograph (0.5” pinhole; pipeline output) over the 2025 Nov - 2026 Feb run.

To do. Done. No more activities planned.

4.6 Spectral format stability

Description. Compare the recorded spectral format of the UV-VIS arm with different slits with the expected shape for a proper light illumination from the CU, checking the position on the detector and the separation among the four quasi-orders.
Compare the recorded echellogram of the NIR arm with different slits with the expected shape for a proper illumination from the CU, checking the position on the detector, and the separation among orders.
Take a series of arc spectra in each arm with all slits and check for any variation in the line positions (in both X and Y direction) at different temperatures (check for temperature effects) and at different telescope elevations (check for effects of flexures).

Status. The pipeline produces a FITS table named *_OLOC.fits (under reduced/soxs-mflat) where the order edges for spectroscopic flats are stored. The results obtained so far indicate a stable spectral format (Fig. 39 - 40).

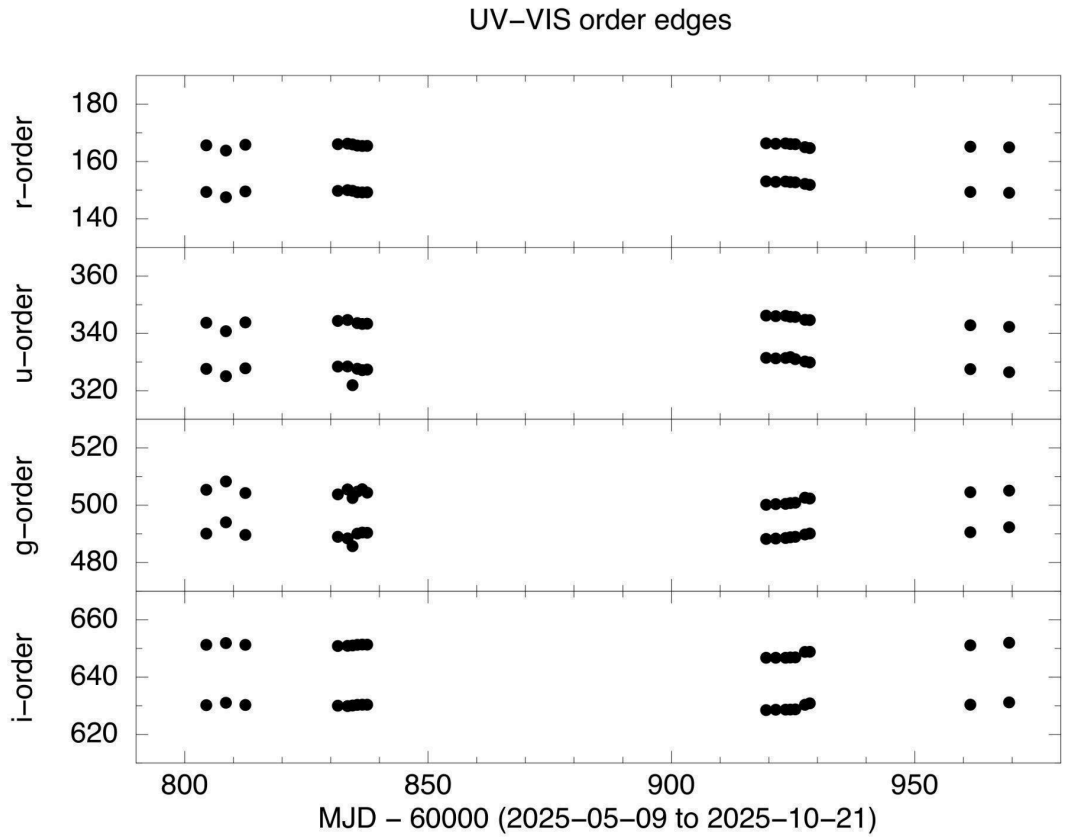

Figure 39: UV-VIS order edges measured over the 2025 May - October period.

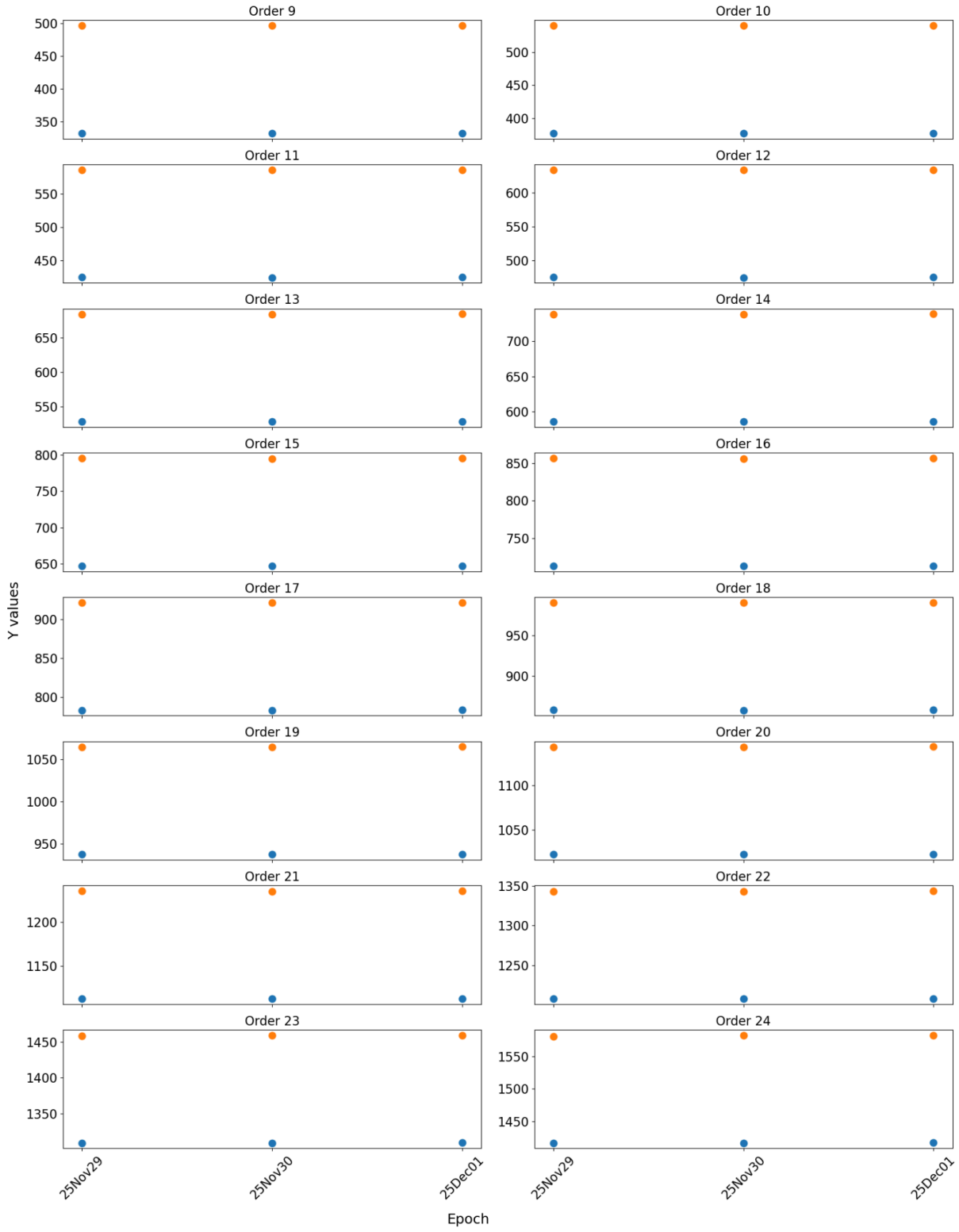

Figure 40: NIR order edges measured over the 2025 Nov - Dec run.

To do. Done. No more activities planned.

4.7 Verification of the calibration procedures

Calibration lamps exposure times determination

Description. Take different arc and flat-field halogen lamp spectra with all the slits for each arm. Check arc line intensities and flat field illumination in order to optimise the exposure times for each slit width, for each arm of the spectrograph.

Status. Exposure times and lamp intensities for the UV-VIS are set and tested (Table 4). A calibration OB has been put in place with a simple “END-OF-NIGHT” procedure that is currently started at the end of each night by the Telescope Operator (TIO). The whole CALOB lasts a bit less than 3 hours.
In addition to what was planned, UV-VIS dome flats have been tested (Fig. 41) with the determination of the lamp's configuration and exposure times. This is because analysis of the UV-VIS spectra revealed problems with the flat field correction of the u-order. Concerning this issue, we noted that:

- The use of the Deuterium flat field lamp in the reduction cascade introduces too much noise (it has emission lines in the g, r and i orders)
- The use of the QTH flat field lamp only works very well for the reduction of the g, r, and i orders, but provides a noisy reduction for the u-order, having too few counts in that band.
- Increasing the exposure times of the QTH lamp is not a feasible solution: to have enough counts in the u-band, we saturate the i-band.

We are currently carrying out tests with QTH and dome flats to achieve the best possible improvement of the u-order flat-field correction in the reduced spectra. A first conclusion is that the use of a “weekly” QTH flat (obtained from the co-add of ~ 30 - 40 QTH flats, 5 per day over 7 days) provides the best tradeoff between quality of the reduced spectra and calibration exposure time budget. In light of this:

- The Deuterium flats have been removed from the calibration plan
- The UV-VIS dome flat have been removed from the calibration plan

Exposure times and lamp intensities for the NIR are set, too, and tested.

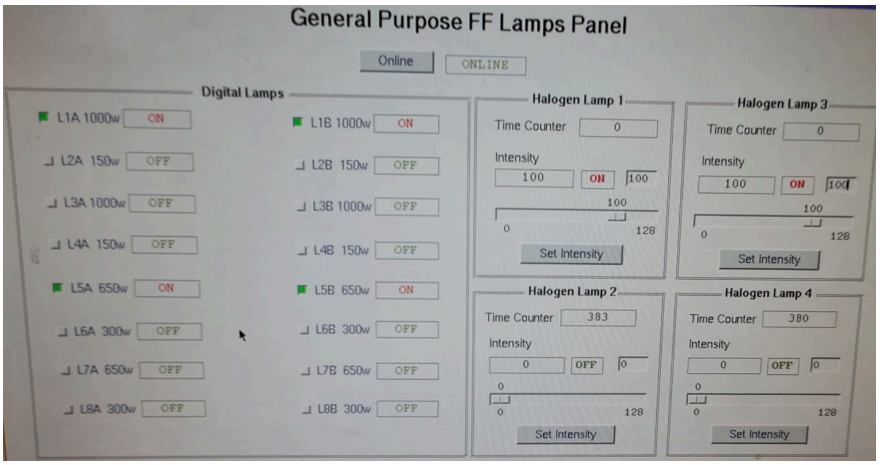

Figure 41: Configuration of NTT dome lamps for the UV-VIS spectroscopic dome flats.

Table 4: optimal exposure times for the calibration lamps (UV-VIS and NIR).

CALIBRATION	LAMP	SLIT	Texp (s)
LAMP, FLAT	QTH	0.5”	20.0
LAMP, FLAT	QTH	1.0”	10.0
LAMP, FLAT	QTH	1.5”	7.0
LAMP, FLAT	QTH	5.0”	2.0
LAMP, FLAT	QTH	PINHOLE	10.0
DOME, FLAT	Halogen	0.5”	12.0
DOME, FLAT	Halogen	1.0”	6.0
DOME, FLAT	Halogen	1.5”	4.0
DOME, FLAT	Halogen	5.0”	1.0
LAMP, WAVE	ThAr	0.5”	20.0
LAMP, WAVE	ThAr	1.0”	10.0
LAMP, WAVE	ThAr	1.5”	10.0
LAMP, WAVE	ThAr	5.0”	5.0
LAMP, WAVE	ThAr	PINHOLE	30.0
LAMP, WAVE	ThAr	MULTIPINHOLE	30.0

To do. Done. Lamp exposure times have been determined and implemented in the END-OF-NIGHT CALOB that is currently run every day. These exposure times demonstrated to be optimal for the NIR arm too.

Flat field accuracy and stability

Description. Once the optimal exposure times are found, repeat the flat field halogen lamp spectra over the different commissioning runs and check flat field stability.

Status. The obtained results indicate that both the UV-VIS and NIR flats are stable over time. (Fig. 42 and Fig. 43).

To do. Done (no more activities planned rather than QC monitor).

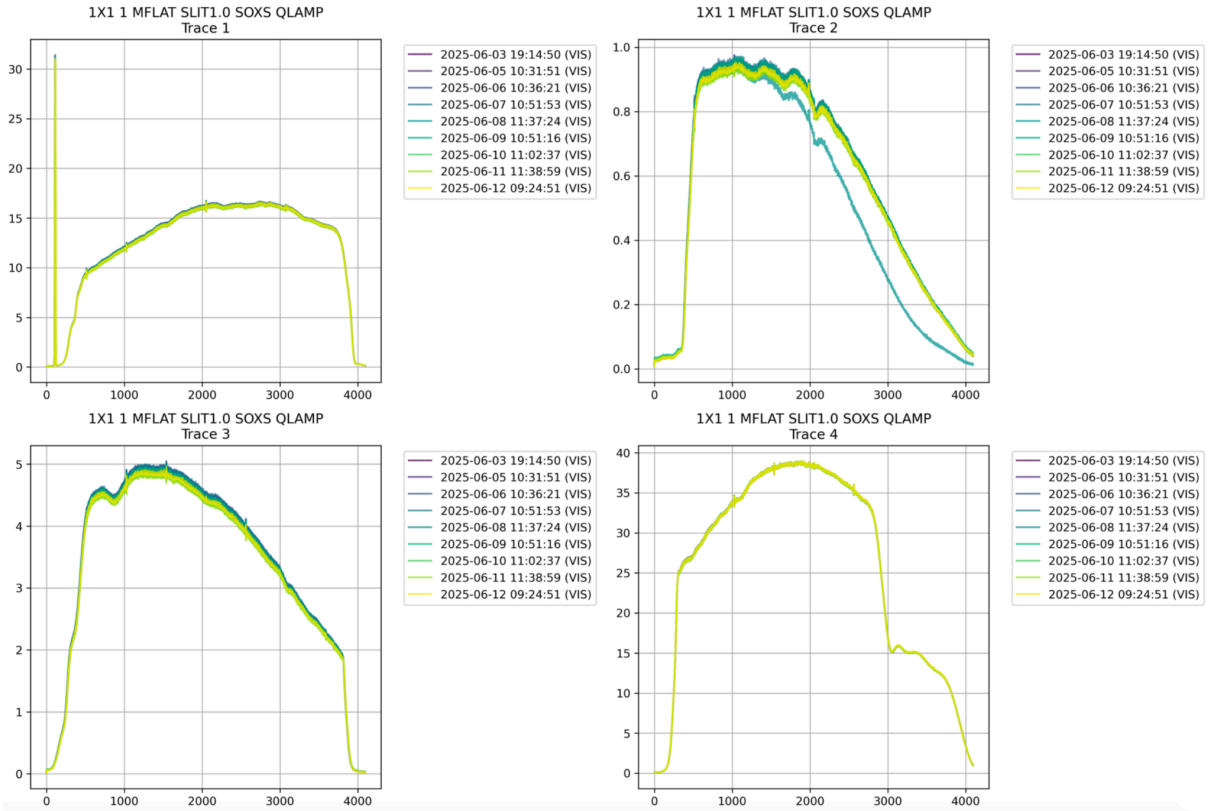

Figure 42: Comparison of the spectroscopic flat-fields for each of the four UV-VIS quasi-orders obtained during the June run. The flat-field shape is constant over time, with in some cases a simple scaling.

The same analysis has also been carried out for the flats collected in the May and September runs. Results are available at the following links:
UV-VIS flat analysis (May), available at
https://drive.google.com/file/d/1S7_H2XImsw0XKDOStKkvYgZXKi9GlbTm/view?usp=drive_link
UV-VIS flat analysis (June), available at
https://drive.google.com/file/d/17g1xPN73uzc5YBbcSpZQSUCPRgBo67Rz/view?usp=drive_link
UV-VIS flat analysis (September), available at
https://drive.google.com/file/d/11i0lIRa3CL8m88L_4L2SwDJcvLgJVlOe/view?usp=drive_link

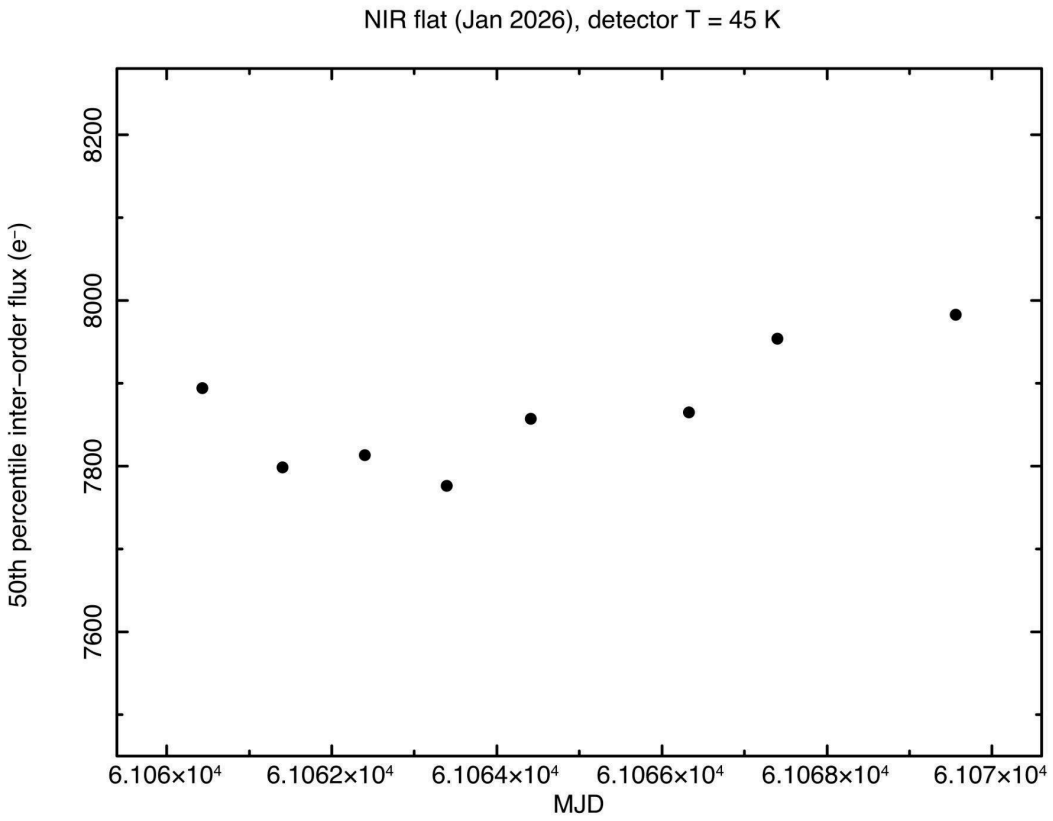

Figure 43: Measure of the 50th percentile inter-order flux for the NIR master flat over the period 2026 Jan 20 - 29, with the detector temperature set at 45 K.

Wavelength coverage and calibration

Description. For each arm, illuminate the system with the CU proper light, and check the wavelength coverage.

Status. Enough data taken for both the UV-VIS and the NIR. The obtained results indicate that the UV-VIS and NIR wavelength coverage is as expected (see plots in Section 6). The wavelength solution zero point is stable across the whole spectral range within +/- 0.6 Angstrom over a timescale of 4 months for the UV-VIS (Fig. 44) and within +/- 0.9 Angstrom over a timescale of 1.5 months for the NIR (Fig. 45). The data are available here: https://drive.google.com/drive/folders/19H6x1AOj-LNO_kTKhZDfeBrreV-nuAOL?usp=sharing

To do. Done. A second-order correction of the dispersion solution is ready to be implemented in the next pipeline release. A re-analysis of the calibration data will be carried out to check the improvement of the dispersion solution stability.

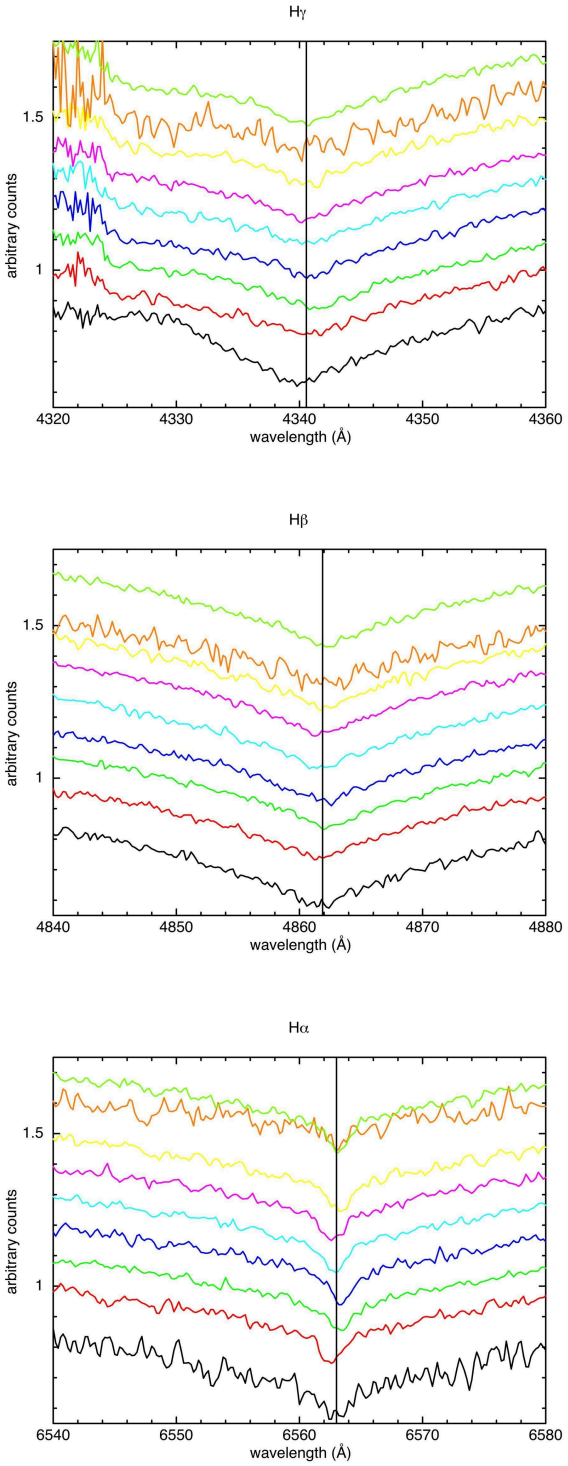

Figure 44: Check for the wavelength solution stability by comparing the Hgamma (at the joint between the u and g order), Hbeta (g order), Halpha (r order) absorption lines centroids (in the spectra of the spectrophotometric standard GD71 observed with the 1" slit between October 2025 and January 2026 (each plot shows from bottom to top the earlier to latest spectrum).

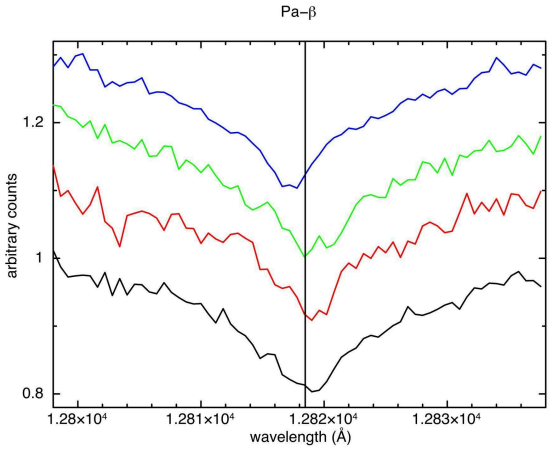

Figure 45: Check for the wavelength solution stability by comparing the Paschen Beta line centroid in the spectra of the spectrophotometric standard LTT3218 observed with the 1" slit between November and January 2025 (the plot shows from bottom to top the earlier to latest spectrum).

4.8 Verification of the acquisition sequences

Description. Execute the observing templates SOXS_slt_obs_Stare, SOXS_slt_obs_StareSyncro, SOXS_slt_obs_AutoNodOnSlit in order to check the:

- centering algorithm
- time required to acquire a target and start the exposure
- position angle of the slit
- faint targets acquisition through blind offset

Status. Done (no more activities planned). The acquisition sequence has been developed and established for all the acquisition templates (Fig. 46), and the position angle in the SOXS reference frame has been determined (Fig. 47).

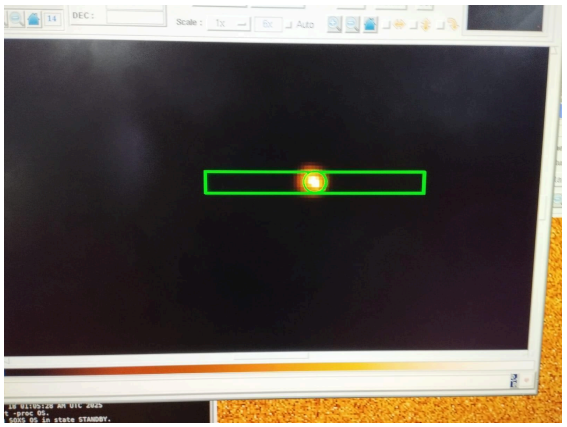

Figure 46: Screenshot from the ACQ procedure.

Acquisition procedure description. The acquisition procedure is done through the Real Time Display (RTD) of the AC available at the SOXS terminal in the La Silla control room. Once the acquisition image has been obtained and displayed over the RTD, a “pick object” window pops up asking the user (the TiO, in normal SOXS operations) to identify the target through the “pick object” tool of the RTD. Once the object is picked and confirmed, the script computes the offsets w.r.t. the acquisition pixel and sends them to the telescope. A further acquisition image is then obtained. Once displayed over the RTD, a confirmation request appears as a pop-up window. Then, the user can confirm the position or choose to retry picking the object. If confirmed, the OB automatically proceeds to the acquisition of the first spectrum. Before confirming, a warning message appears to remind the user to check that the telescope is guiding.

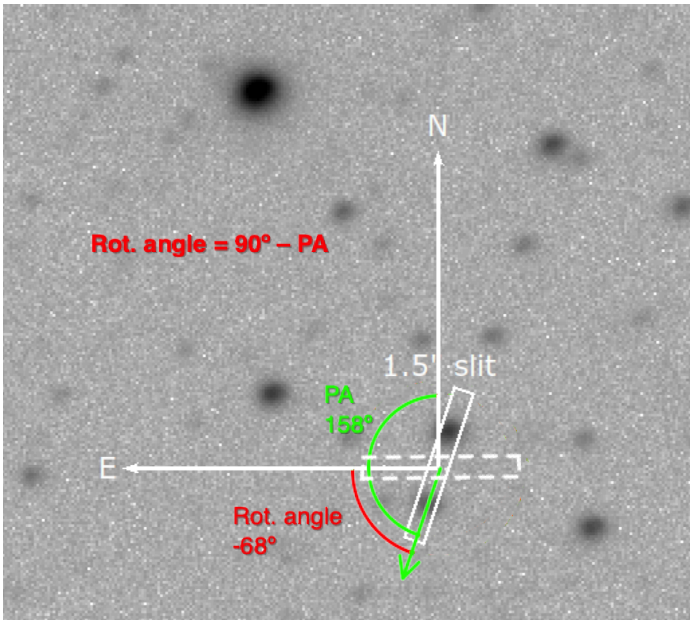

Figure 47: Figure showing the position angle computation method in the SOXS reference frame.

To do. Done (no more activities planned).

4.9 ADC check

Description. Take spectra with and without the ADC and check the differences in the 2D rectified spectra.

Status. ADC is now properly working since the November - December 2025 run, without failures. To test the ADC performances the following test has been carried out on the night of 2025, Nov 24. During such a test, the spectrophotometric standard star LTT3218 has been observed with the 5” slit at different airmasses (ranging from 1.9 to 1.3). Four spectra have been obtained. Two with the ADC turned OFF and the slit position angle (PA) put at 90 deg w.r.t. the parallactic angle (worst possible case) and with the PA as the parallactic angle. Then two more spectra have been obtained with the ADC turned ON, again with the slit position angle (PA) put at 90 deg w.r.t. the parallactic angle (worst possible case) and with

the PA as the parallactic angle. With the ADC turned OFF and the slit PA oriented 90 deg w.r.t the parallactic angle, a clear drop of flux in the bluest part of the spectrum is observed. Such a flux drop is not present in the spectra obtained with the same slit orientation and the ADC turned ON (Fig. 48).

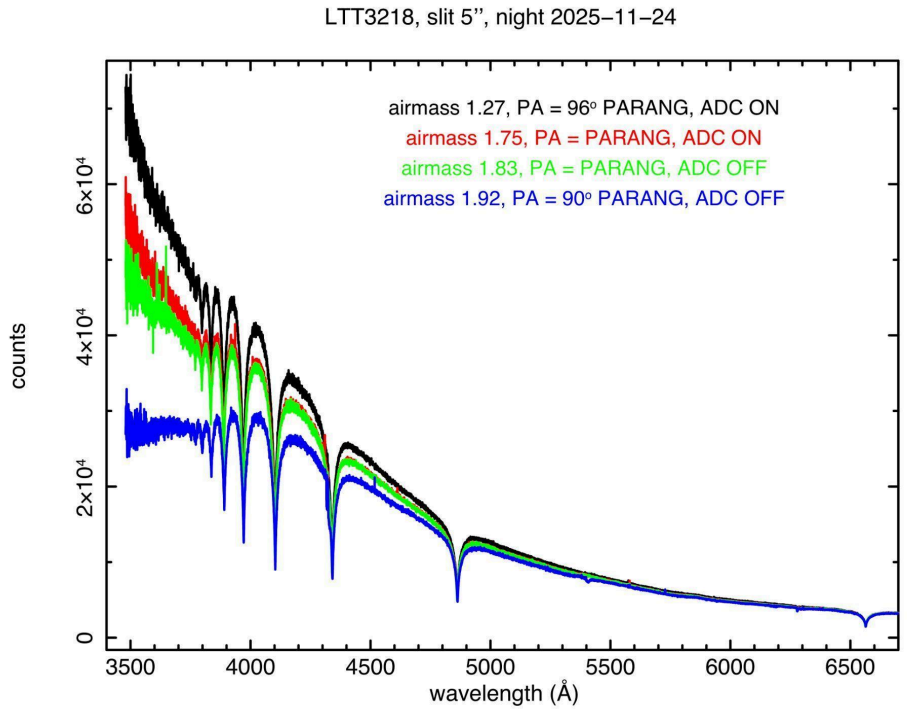

Figure 48: A series of UV-VIS spectra (detail on the bluer part) of the STD LTT3218 obtained on the night of 2025 Nov 24 at different airmasses with the 5" slit and an exposure time of 300s.

We then corrected the four spectra for the atmospheric extinction and computed the ratio of the extinction corrected counts. As shown in Fig. 49, when the ADC is ON, even in the worst possible case any drop of flux in the bluest part of the spectrum is lower than 5% - 10%. The same result can be achieved without the ADC by observing with the slit PA oriented along the parallactic angle. Without ADC and observing with the slit PA oriented perpendicular to the parallactic angle (worst possible case), flux losses of less than 10% can be achieved only at wavelengths redder than ~ 4200 AA for an airmass ~ 2.

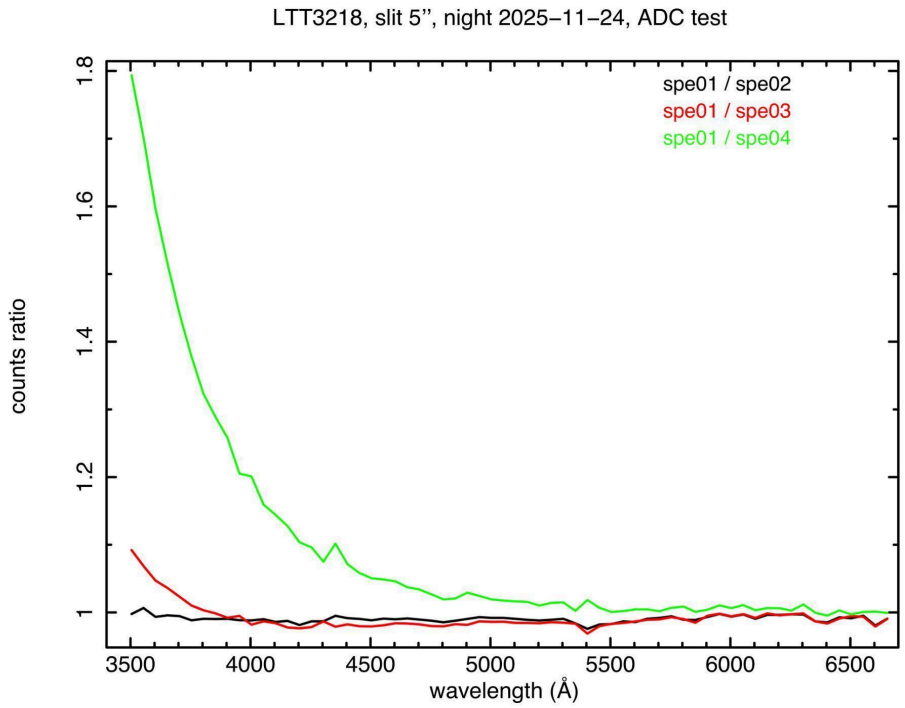

Figure 49: Ratio of the spectra shown in Fig. 41 after having applied the correction for the atmospheric extinction.

Further (similar) tests on the ADC performances have been carried out during the November - December 2025 and January 2026 run, all showing consistent results and evidence for a satisfactory functionality of the ADC.

To do. Done, no more activities planned.

4.10 Scale along the slit

Description. Take a spectrum by putting two stars with known angular separation along the slit and measure the distance in pixels of the two stars at different wavelengths, along with the orders in the raw 2D spectra.
Take a series of nodding observations with different nodding lengths and verify that the separation between the two spectra is as expected (one A-B pair for each separation value is enough).
With the two stars on the slit, check that the slit orientation command correctly positions the slit angle on the sky. Further check that the values recorded in the FITS header can be used to correctly and easily determine the on-sky slit angle.

Status. Done. UV-VIS CCD plate scale measured: 0.28”/pixel (1x1 binning; Fig. 50). NIR detector plate scale measured: 0.32”/pixel (Fig. 51)

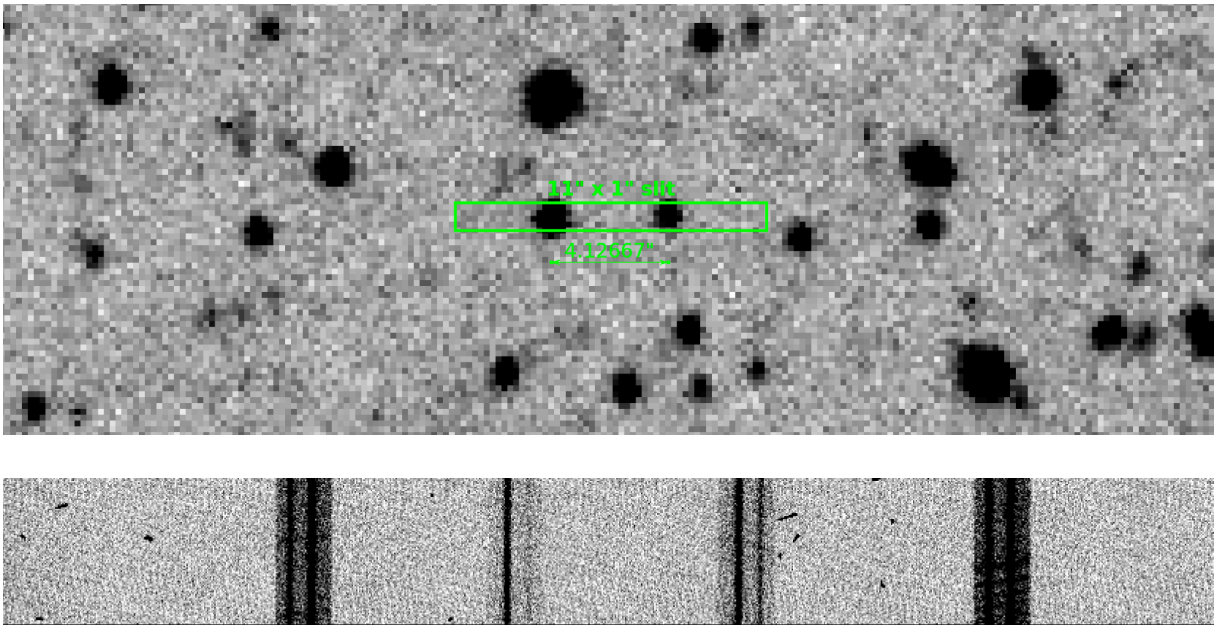

Figure 50: Acquisition image (SOXS.2025-10-22T04:50:55.102.fits) and UV-VIS spectrum (SOXS.2025-10-22T04:51:52.337.fits) of two stars with an angular separation of 4.1", both placed along the 1" slit (position angle = -86.3 deg). The measured separation between the two spectral traces in each order is 14.9 pixels, resulting in a plate scale of 0.28"/pixel.

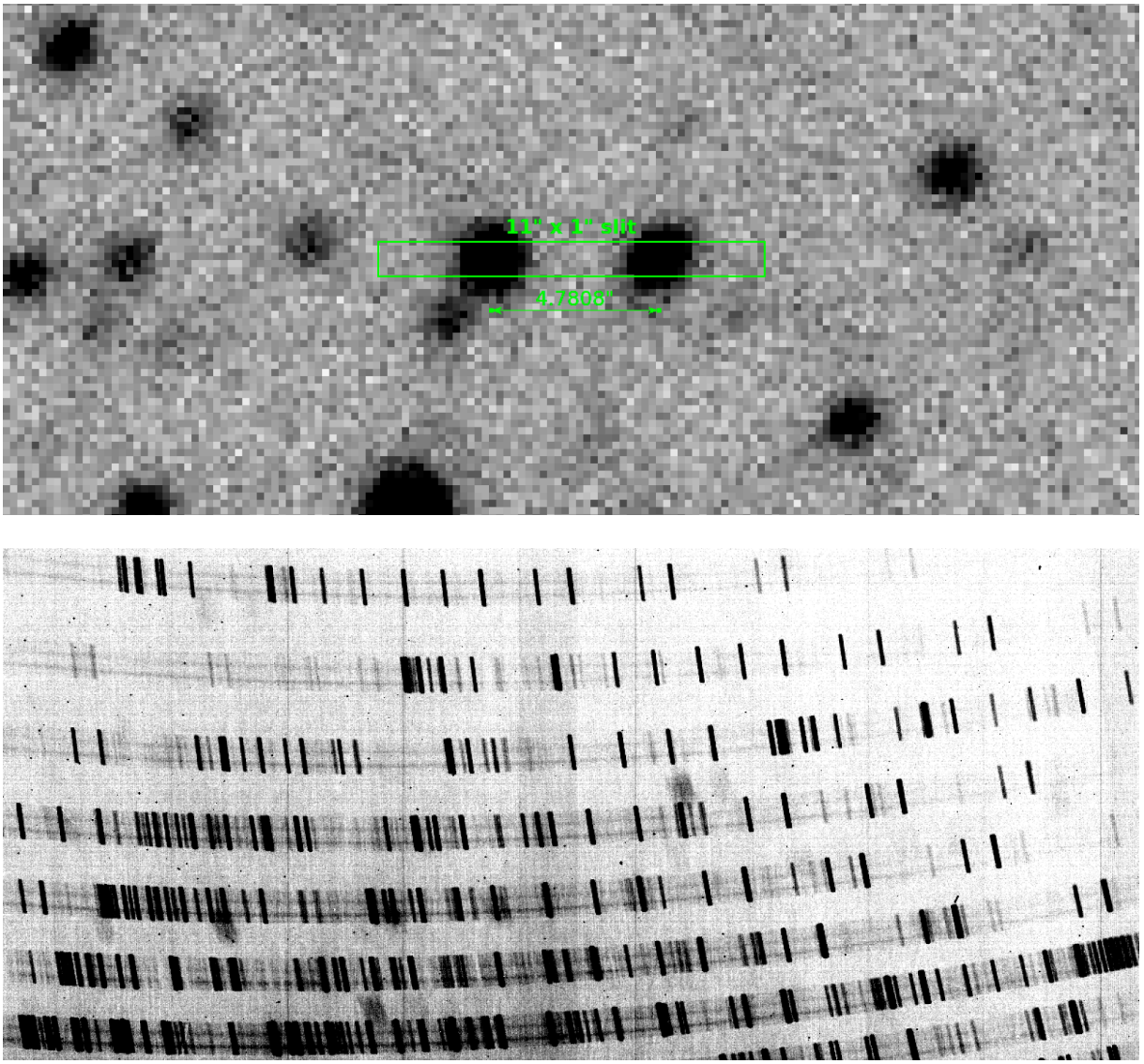

Figure 51: Acquisition image (SOXS.2025-11-28T05:58:09.834.fits) and NIR spectrum (SOXS.2025-11-28T05:58:41.467.fits) of two stars with an angular separation of 4.8", both placed along the 1" slit . The measured separation between the two spectral traces in each order is 15.1 pixels, resulting in a plate scale of 0.32"/pixel.

To do. Done (no more activities planned).

4.11 Overall sensitivity

Description. For each spectrograph arm and for the AC camera, observe a set of standard stars and of stellar and galaxy fields to check the (i) spectral response, (ii) limiting magnitude for point sources, and (iii) limiting surface brightness for extended sources.

Status. Done. The efficiency curve has been derived and compared with the ETC expectations. For the UV-VIS, a first test has been carried out by observing the same STD star with EFOSC2 and SOXS over the same night (June run). The SOXS UV-VIS efficiency has been manually computed, resulting in a factor of 1.2 - 2.0 below the ETC prediction (Fig. 52). The EFOSC2 efficiency curve resulted to be below the EFOSC2 ETC expectations too. Such a mismatch, measured for both instruments, could be explained by a reduced overall reflectivity of the NTT (from 85% for each of the three mirrors, as originally assumed by the ETC, to 73%). In general, extensive observations of spectrophotometric standard stars have been carried out during the SOXS commissioning using different slit apertures and observing at different airmasses with both the UV-VIS and NIR arms in both stare and nodding modes. For all these observations, the efficiency has been derived through the dedicated pipeline recipe. The efficiency is measured to be rather stable over time for observations carried out with the 5" slit. However, significant changes are observed when using narrower slits, even over short (night to night) time scales (Fig. 53). Such an odd behaviour, present in both UV-VIS and NIR data, can be due to slit misalignment, inaccurate target centroid or telescope guiding problems. Being the effect present over short timescales (night to night or even over the same night), the slit misalignment (although happened during the commissioning) is probably not the main cause. A test carried out in May by observing the same star with short AC exposures showed that the star centroid moves by less than 0.35" over a time scale of more than one hour (Fig. 54). As the exact cause is still uncertain, more tests should be planned.
The UV-VIS and NIR efficiency curves (5" slit) are shown in Fig. 55**.** The comparison with the ETC predictions are shown and discussed in Sect. 4.1.14. Finally, the results obtained from the observations of photometric standard fields show that the AC efficiency is within the expectations (Table 5).

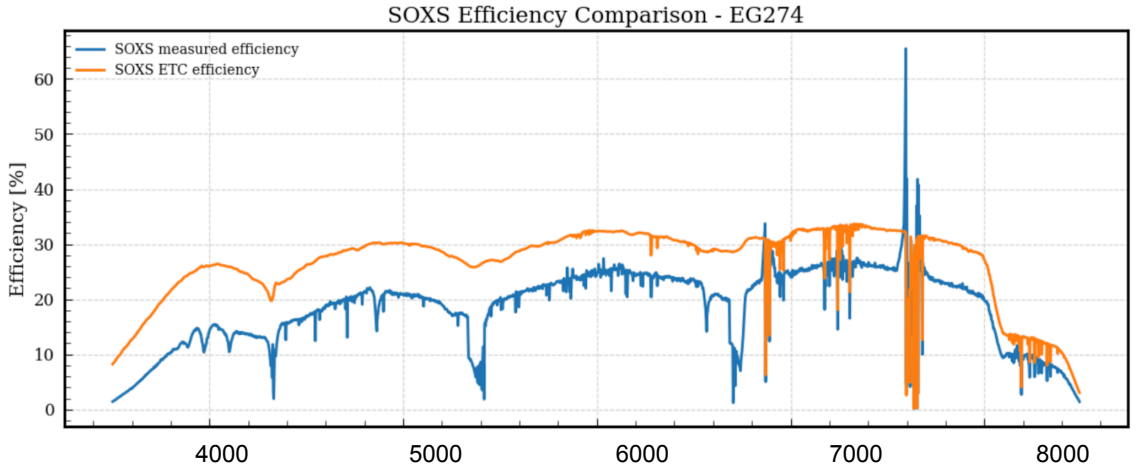

Figure 52: SOXS UV-VIS efficiency as measured from the observations of the spectrophotometric STD star EG274 (blue), compared to the expected efficiency from the ETC (orange, using 85% NTT mirror reflectivity).

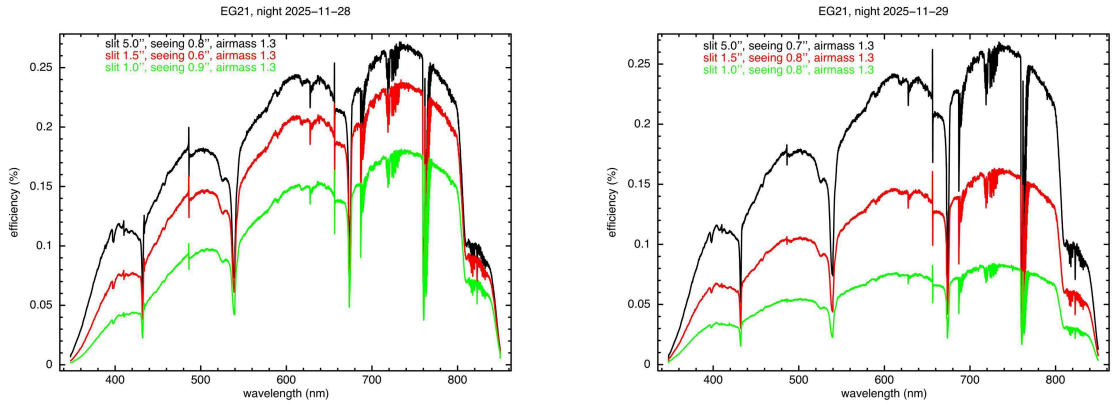

Figure 53: UV-VIS efficiency curves obtained from the observation of the spectrophotometric standard star LTT3218 over the nights of 2025, Nov 28 (left panel) and 29 (right panel) carried out with different slit apertures (SOXS.2026-01-29T03:21:54.024.fits). From the comparison of the two panels, it is evident that a significant drop in efficiency can be observed when using the narrower slits. Such an effect is observed in observations carried out with the NIR too.

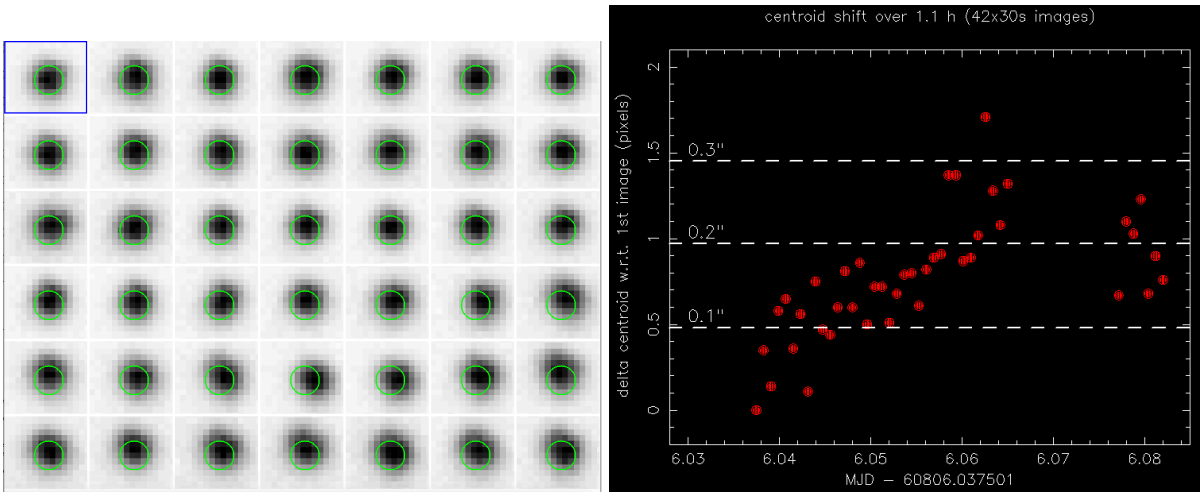

Figure 54: (Left panel) A sequence of 42 images (30s exposure time each) obtained with the SOXS AC on 2025, May 5 between 00:54 UT and 01:58 UT. During the image acquisition the NTT was guiding. The green circle marks the centroid of the star in the first image, with a radius of 0.5" (therefore mimicking the 1" slit). (Right panel) The relative shift of the star centroid over time (resulting to be always < 0.35").

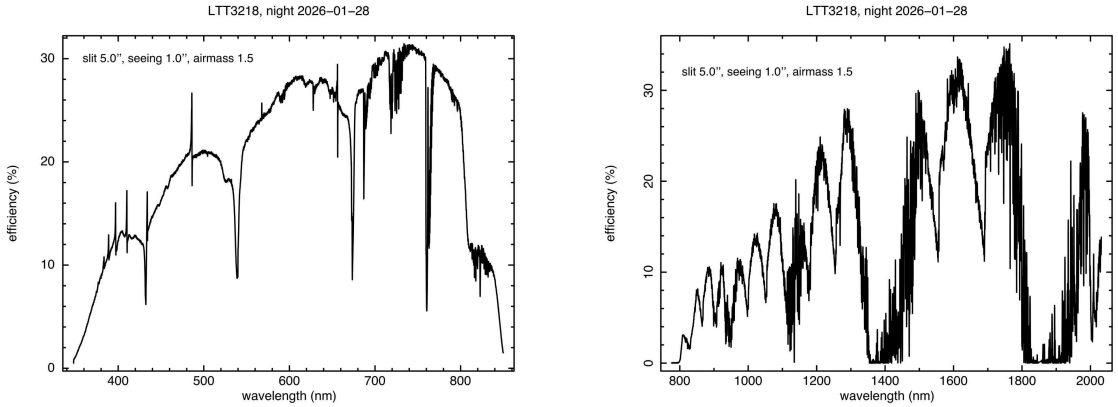

Figure 55: SOXS UV-VIS and NIR efficiency computed from spectrophotometric standard star observations using the 5'' slit.

Exposure time	seeing "	Saturation mag	5sigma limit mag	3sigma limit mag	Filename
1 sec	1.05	10.2	17.9	18.5	SOXS.2025-09-10T08:11:33.509.fits
5 sec	0.92	12.2	19.8	20.4	SOXS.2025-09-10T01:37:36.900.fits
5 sec	1.00	11.9	19.7	20.2	SOXS.2025-09-10T01:34:36.481.fits
20 sec	1.06	13.2	20.1	20.6	SOXS.2025-10-11T06:05:20.115.fits
30 sec	1.20	13.5	20.7	21.3	SOXS.2025-09-09T23:59:42.532.fits
60 sec	1.35	13.9	20.0	20.6	SOXS.2025-10-11T06:08:30.167.fits
120 sec	1.10	14.9	21.4	21.9	SOXS.2025-09-10T00:11:00.233.fits

Table 5: Limiting magnitudes for point-like sources in AC images. All values are for the Sloan-r band.

To do. Done. The SOXS efficiency has been extensively measured through the commissioning. Dedicated tests to unveil the cause of the efficiency drop present in some observations carried out with narrow slits are recommended.

4.12 Verification of the observing templates

Description. Check all the observing templates.

Status. Done. All templates (listed in the appendix) have been successfully tested with the whole instrument.

To do. Done. No more activities planned.

4.13 Parasitic light - ghosts

Description. Take a whole daytime calibration sequence with dome lights turned on in order to check for the presence of parasitic light.
Take spectra of calibration lamps and of bright stars (e.g. spectro-photometric standards) to check for the presence of ghosts.

Status. Test on parasitic light to be done. Test on ghosts in progress, preliminary results show no evidence for ghosts when observing bright stars.

To do. To be done.

4.14 ETC verification

Description. Compare the results of on-sky observations (in both spectroscopic and imaging mode) with the ETC predictions. The observation of standard stars is recommended for this purpose. Use the results of the on-sky observations to adjust the ETC parameters in case of mismatches.

Status. Done. From the analysis of spectrophotometric standard stars spectra, we compared the ETC predictions in terms of efficiency, photo-electrons detected from the target (not taking into account the flat field correction) and SNR with respect to the corresponding pipeline measurements. The results are shown in Fig. 56 and 57 for the UV-VIS and NIR arm, respectively. For both arms, a wavelength dependent scaling factor has to be applied to match the ETC predictions for the efficiency and detected photo-electrons. Such a factor is in the range 1.1 - 2.4 for the UV-VIS and 0.9 - 1.6 for the NIR. The current publicly available version of the ETC (https://soxs-etc.brera.inaf.it/) assumes a flat transmission of 60% total for the NTT (60% comes from assuming 85% reflectivity for each of the three mirrors). As discussed in Sect. 4.11, a reduced reflectivity of the NTT mirrors (from 85% to 73%) can broadly provide a scaling factor that would lead to a broad agreement between the observed values and the ETC predictions. However, as the mismatch is wavelength dependent, some atmosphere effect could be among the causes of what is observed. On the other hand, the tests carried out on the ADC performances (Sect. 4.9) show that atmospheric dispersion is satisfactorily corrected. Also, at NIR wavelengths any atmospheric extinction / dispersion is expected to be negligible. This suggests a wavelength-dependent degradation of the NTT mirrors, and the efficiency will be measured again after re-aluminising occurs.
Concerning the SNR, again a correction factor is needed to match the ETC predictions (0.7 - 1.1 and 1.8 - 3.6 for the UV-VIS and NIR, respectively). However, such a factor significantly differs from the one needed for efficiency and photo-electrons. A first investigation highlighted differences in the procedure used to determine the SNR with the ETC and the pipeline. Activity is in progress to ensure a uniform measurement procedure.

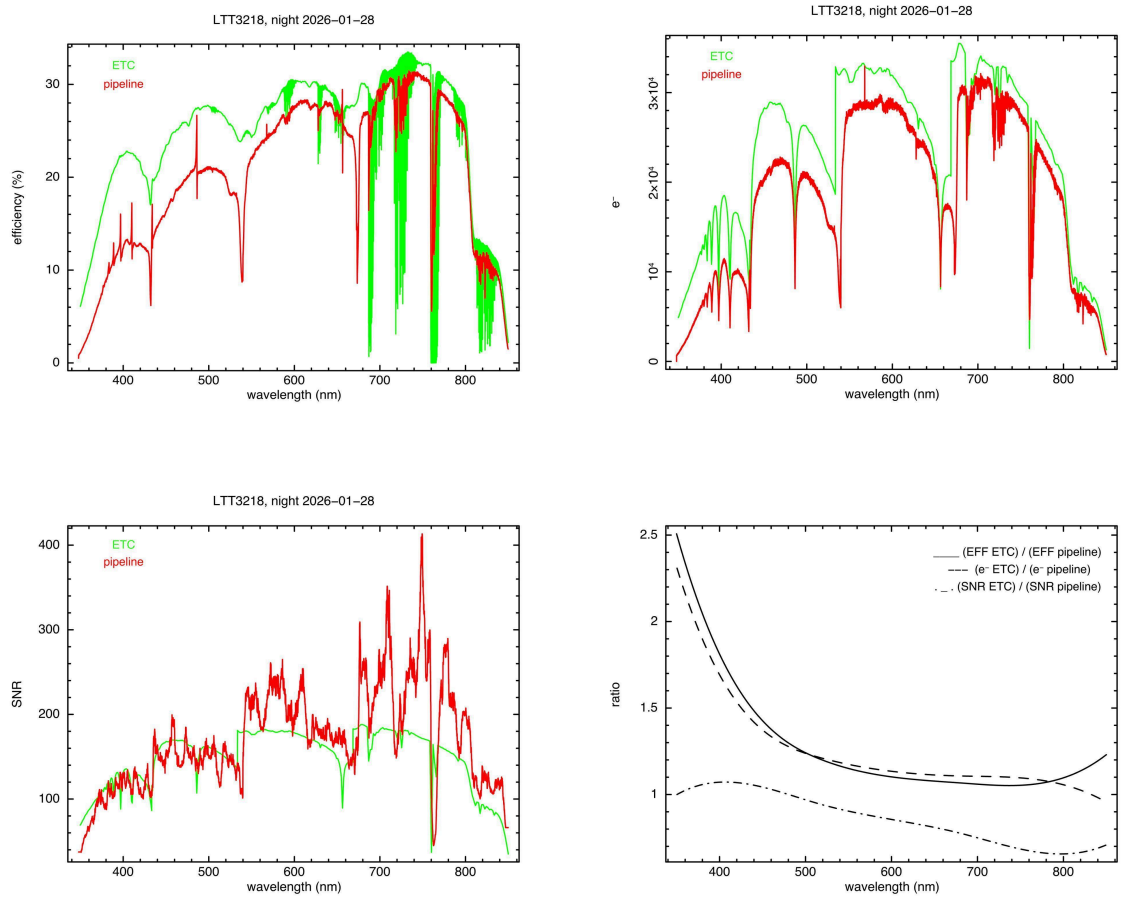

Figure 56: UV-VIS observations of the spectrophotometric standard LTT3218 carried out on 2026, Jan 28 (SOXS.2026-01-29T03:21:54.024.fits) compared to the ETC expectations in terms of efficiency, photo e- and SNR detected from the target source. The bottom right plot shows the scaling factor needed to match the ETC predictions.

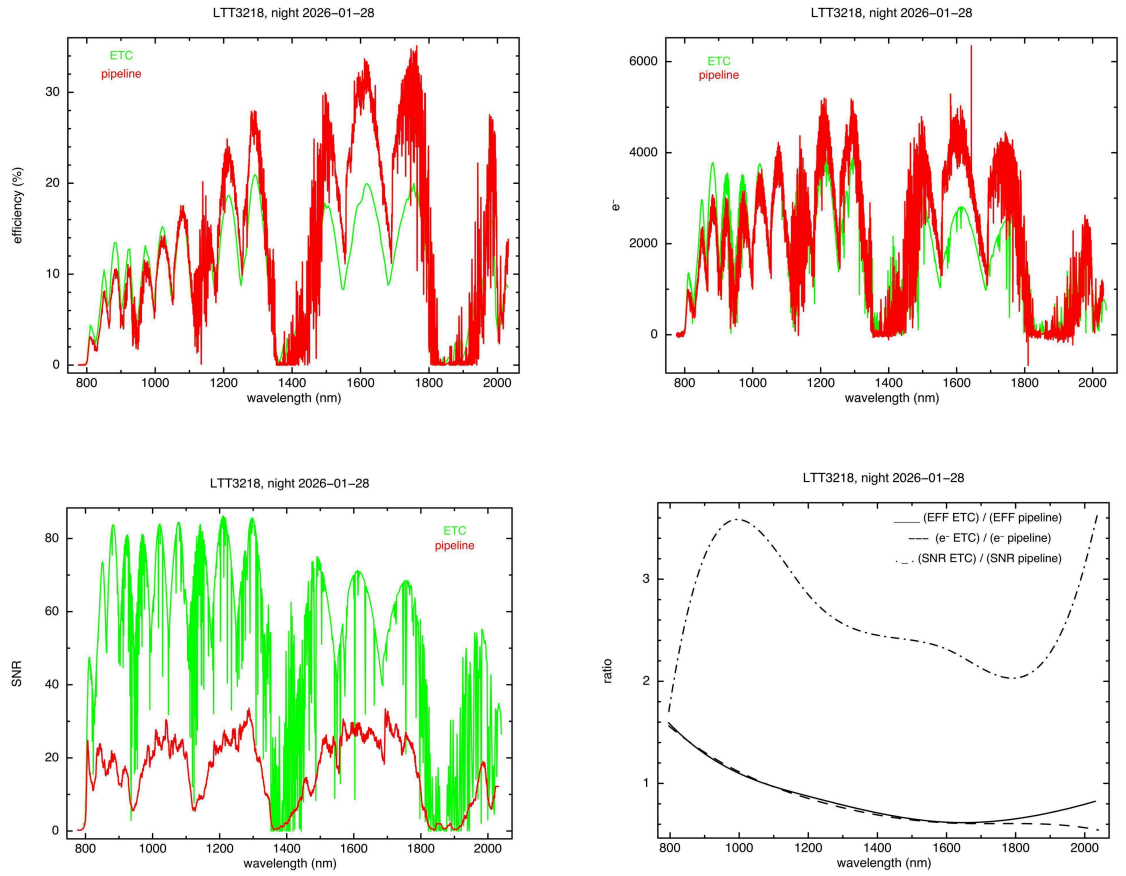

Figure 57: NIR observations of the spectrophotometric standard LTT3218 carried out on 2026, Jan 28 (SOXS.2026-01-29T03:21:54.024.fits) compared to the ETC expectations in terms of efficiency, photo e- and SNR detected from the target source. The bottom right plot shows the scaling factor needed to match the ETC predictions.

To do. Done. Further investigations on the procedure / recipes of the ETC and of the pipeline are recommended. Also, observations of spectrophotometric standard stars at different airmasses are recommended to be carried out after the re-coating of the NTT mirrors. This is considered a continuous activity to be carried out during the commissioning and normal operations, to keep monitoring the instrument efficiency.

4.15 Pipeline verification

Description. Check all the pipeline recipes, both in real-time nighttime data analysis and in off-line daytime data analysis.

Status. We have had twelve pipeline releases since the beginning of AIV / Commissioning activities. The pipeline latest version (0.17.1) has been installed and is working on the La Silla machines. The testing of the pipeline is intended as an activity to be carried out continuously during the commissioning. A systematic re-analysis of the commissioning data

obtained so far with the last pipeline version has been carried out. The results obtained so far indicate that the pipeline can carry out the whole reduction cascade for the UV-VIS spectra until the reduced and extracted 1D (wavelength and flux calibrated). Also, it stores into the fits headers of the products' QC data values, such as:

- Master bias value
- RON
- Efficiency

The order stitching, the stability of the wavelength calibration and the spectroscopic flat-field correction significantly improved w.r.t. previous versions.
We refer to the pipeline public web page and documentation (https://soxspipe.readthedocs.io/en/master/) and to the forthcoming pipeline report for a more detailed description of the pipeline products, performances and status.

To do. Done. Verify the compliance of pipeline reduced data with the phase 3 ESO standard.

4.16 Scheduler verification

Description. Operate an entire observing night ingesting the OBs in the NTT/SOXS queue using the scheduler only.

Status. The observations carried out during the 2026 January run have been almost completely managed by the scheduler, with the on-site presence of people from the consortium to carry out monitoring and debugging. Furthermore, “special cases” (e.g. observation of moving targets) have been successfully tested too. TiOs could manage the observations by simply refreshing the VOT workstation and fetching them in the BOB. More details can be found in [RD4].

To do. Done. The web graphical user interface of the scheduler has still to be finalised, but this will be used by the consortium. More extensive tests of the scheduler, simulating routine operations is highly recommended.

4.17 Data flow compatibility verification

Description. Check the compatibility with the ESO data flow system, including the submission of raw and reduced data to the ESO archive.

Status. Activity in progress. OBs can be prepared and scheduled through the p2ls. In Table 6 and Table 7 the instrument overheads for the UV-VIS and AC are reported. The NIR readout time is 4 seconds. These values will have to be updated to the p2ls. Since the beginning of the commissioning, the SOXS data flow is being tested on the ESO’s Special Access Science Archive Facility (https://archive.eso.org/wdb/forms/cas/eso_archive_main.html). The raw SOXS data are properly uploaded to the archive (see Fig. 58).

Readout Time (s)	Mode	BINX	BINY
25	1	1	1
10	1	2	2
19	1	2	1
17	2	1	1
14	2	2	1
25	3	1	1
10	3	2	2
19	3	2	1
17	4	1	1
8	4	2	2
14	4	2	1

Table 6: Readout time for the UV-VIS arm for different reading modes and binning combinations.

Readout Time (s)	Mode	BINX	BINY
21	50 kHz	1	1
9	50 kHz	1	2
10	50 kHz	2	1
4	50 kHz	2	2
1	1 MHz	1	1
0	1 MHz	1	2
0	1 MHz	2	1
0	1 MHz	2	2
0	3 MHz	1	1
0	3 MHz	1	2
0	3 MHz	2	1
0	3 MHz	2	2
0	5 MHz	1	1
0	5 MHz	1	2
0	5 MHz	2	1
0	5 MHz	2	2

Table 7: Readout time for the AC for different reading modes and binning combinations.

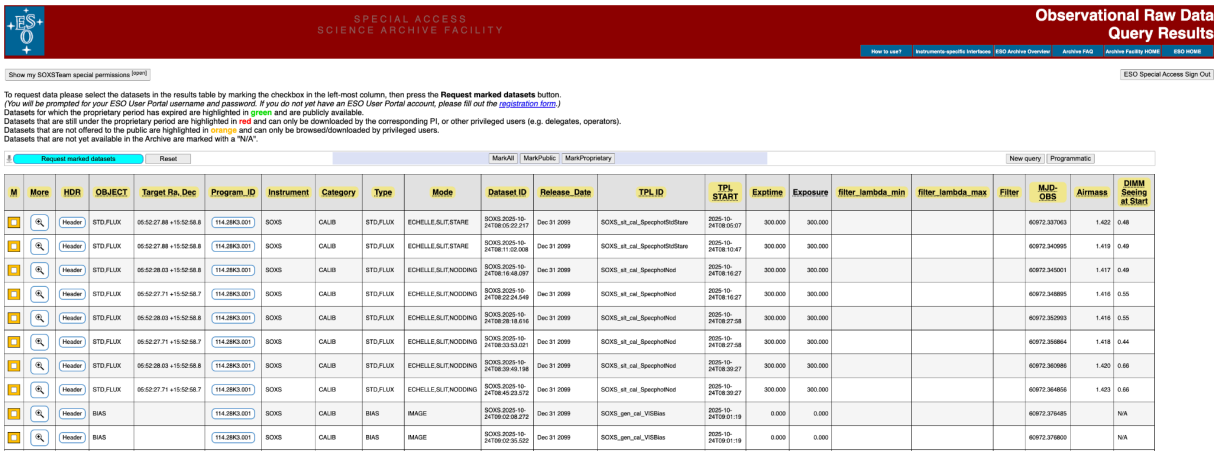

Figure 58: Screenshot showing how the SOXS raw data appear on the Special Access Service Archive facility of ESO.

To do. Verify compliance of all fits keywords with the ESO archive (contacts are in progress with ESO staff). Verify compliance of pipeline reduced data with the phase 3 ESO standard.

4.18 Quality Control procedures verification

Description. Verification of the quality control monitoring of the instrument by testing the correct transmission of the SOXS data log, the correct (user-friendly) visualisation with proper tools (e.g. *Grafana*), and the correct functionality of alerts.

Status. Activity in progress. Most QC parameters are already included among the standard pipeline products (Fig. 59). We received from ESO examples of data formats compliant with the ESO QC system (ascii tables).

To do. Set up a procedure to convert pipeline QC products into the ESO needed data format. A first QC webpage is now available, reporting all the QC parameters derived from the systematic pipeline reduction of the commissioning data:
https://molab.marimo.io/notebooks/nb_gG9uv5z7EgWLnfpF3iqip8/app

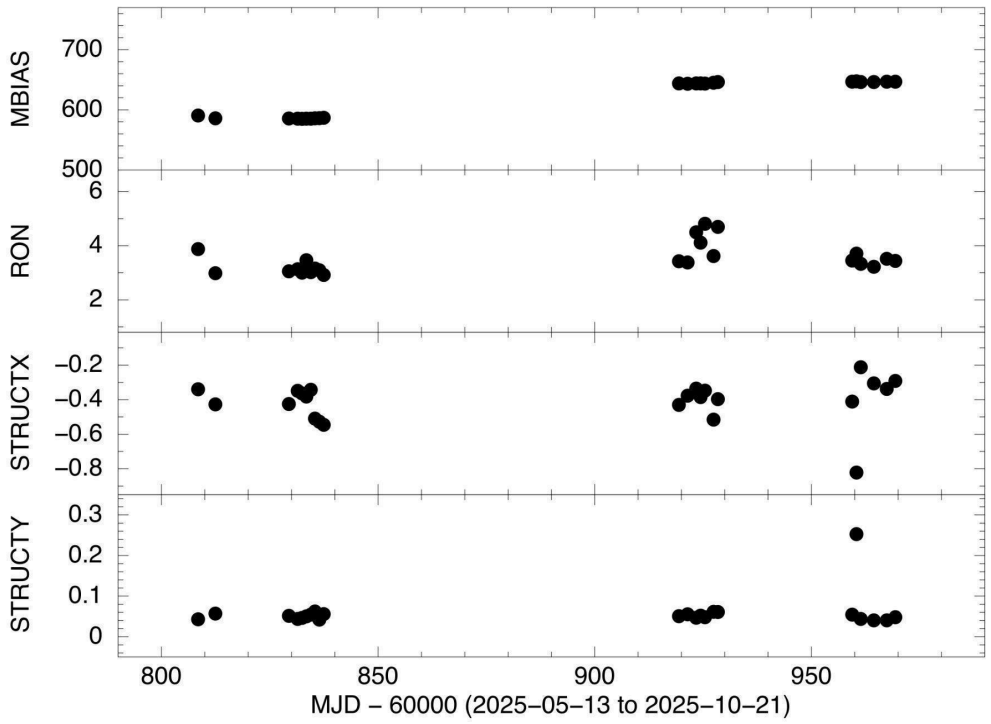

Figure 59: Evolution of the QC parameters related to UV-VIS master bias (Master Bias, Read Out Noise, structure along the x and y directions) over the 2025 May - October period.

4.19 Showcase observations

Description. Observation of at least one prototypical celestial source for each of the main science cases of SOXS (e.g., a gamma-ray burst, a supernova, a Tidal Disruption Event, an X-ray binary). Even if the typical science targets of SOXS consist of transient sources, examples should not be lacking during the commissioning runs. During these observations, the template for telluric standard stars should be tested too, to estimate the best number of counts to be reached for a proper correction in the science spectra.

Status. Observations of a number of targets have been made. Few telluric standards were observed (mainly due to the poor availability of the NIR). Data analysis in progress.

To do. Done.

5 Summary and next steps

The whole instrument has been extensively tested and characterised. All the observing modes and templates have successfully been tested.
The bias, dark, flat, the wavelength range, spectral format, spectral resolution are stable and within the specifications. The acquisition procedures have been set. The ADC is properly working.
A calibration OB has been prepared, optimised for all three sub-systems and is successfully run (with a duration of ~ 3.5 hours) on a daily basis since June.

A more detailed investigation and further tests/activities are needed on the following aspects:

- Both spectrographs seem to be less efficient (from a full atmosphere to detected electrons calculation) than expected in their bluer orders. A likely explanation is a reduced reflectivity of the NTT mirrors. This may be wavelength dependent and a similar degradation has been observed with EFOSC2 zeropoints over time. We also observed that the EFOSC2 throughput is lower than the ESO ETC, and we suggest the cause is the same. This is still to be fully explained and the acquisition of further data is recommended, particularly after the planned aluminising of the NTT mirrors.

- Some spectral observations carried out with narrow (1.5'', 1.0'' and 0.5'') slits show a drop in efficiency with respect to the expectations. Further on-site tests where the accuracy of target centroid and NTT guiding are carefully checked are needed to unveil the origin of this effect.

- The dispersion solution is typically stable within 1 Angstrom, although deviations up to 2 - 3 Angstrom are observed. A pipeline recipe to improve the derivation of the dispersion through a 2nd order correction that takes into account the sky lines positions will be soon tested and is expected to significantly reduce any deviation.

- Check for the full compliance of the SOXS raw data FITS Keywords and of the pipeline reduced data with the ESO data flow standards

- Implement procedures for the QC parameters starting from the already available QC notebook

- Plan TiOs and La Silla technical staff training

- Plan extensive testing of the scheduler, simulating routine operations

- Update the User Manual

The first three points of the above list may be accounted for during the 2026 June - July planned observing run.

6 Gallery of selected SOXS data

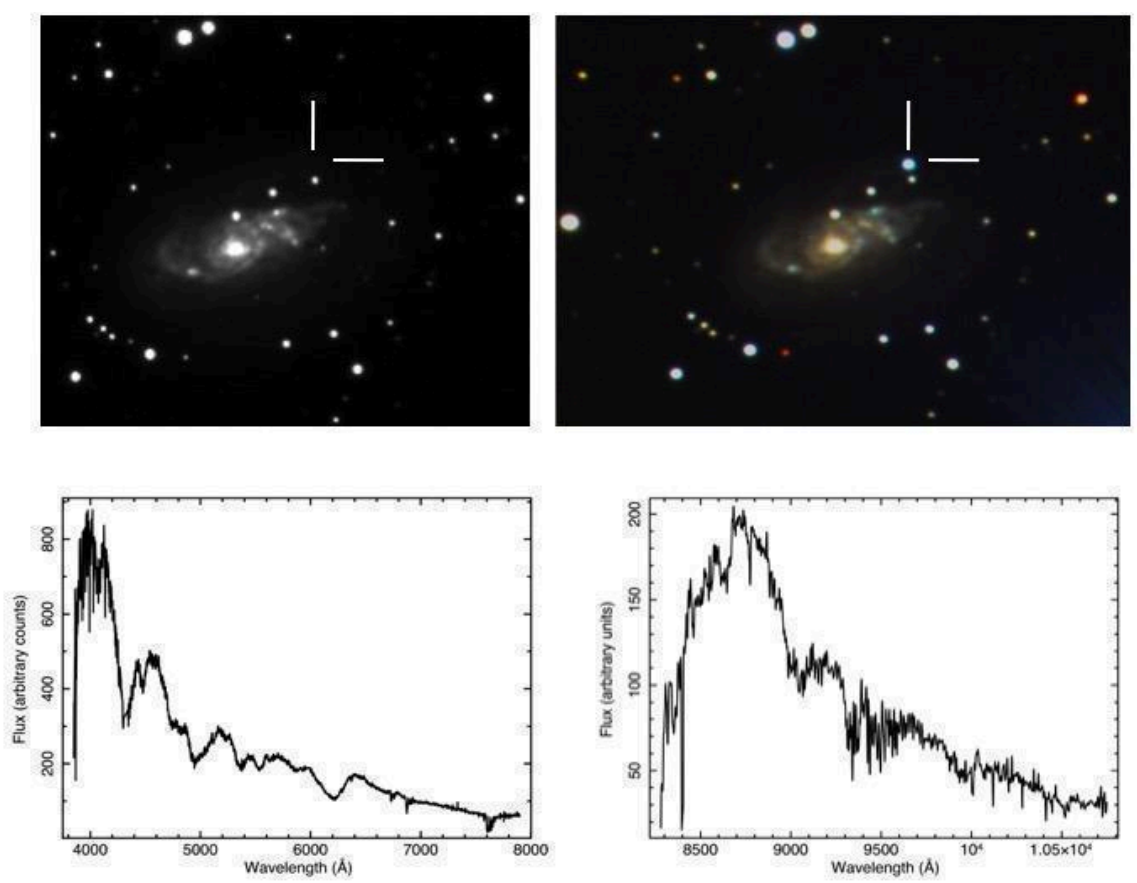

Figure 60: The SN 2025jsh and its host galaxy ESO 263-G 014 (75 Mpc) observed with the whole SOXS in May 2025.

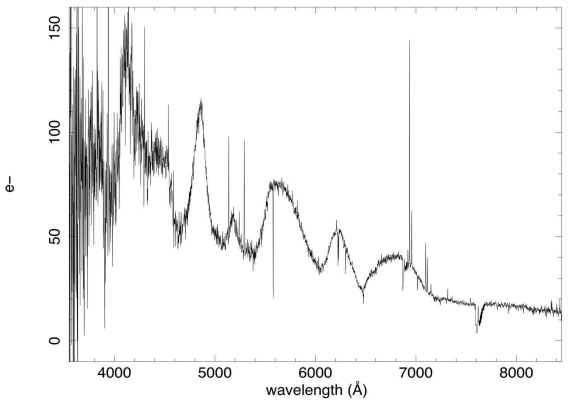

Figure 61: The SN 2025ygp observed with the UV-VIS spectrograph during the night of 2025 October 23, when the target brightness was at the level of ~ 19 mag. Narrow emission lines from the host galaxy at z = 0.057 are superposed to the SN spectrum. A Gaussian smooth has been applied for visualisation purposes.

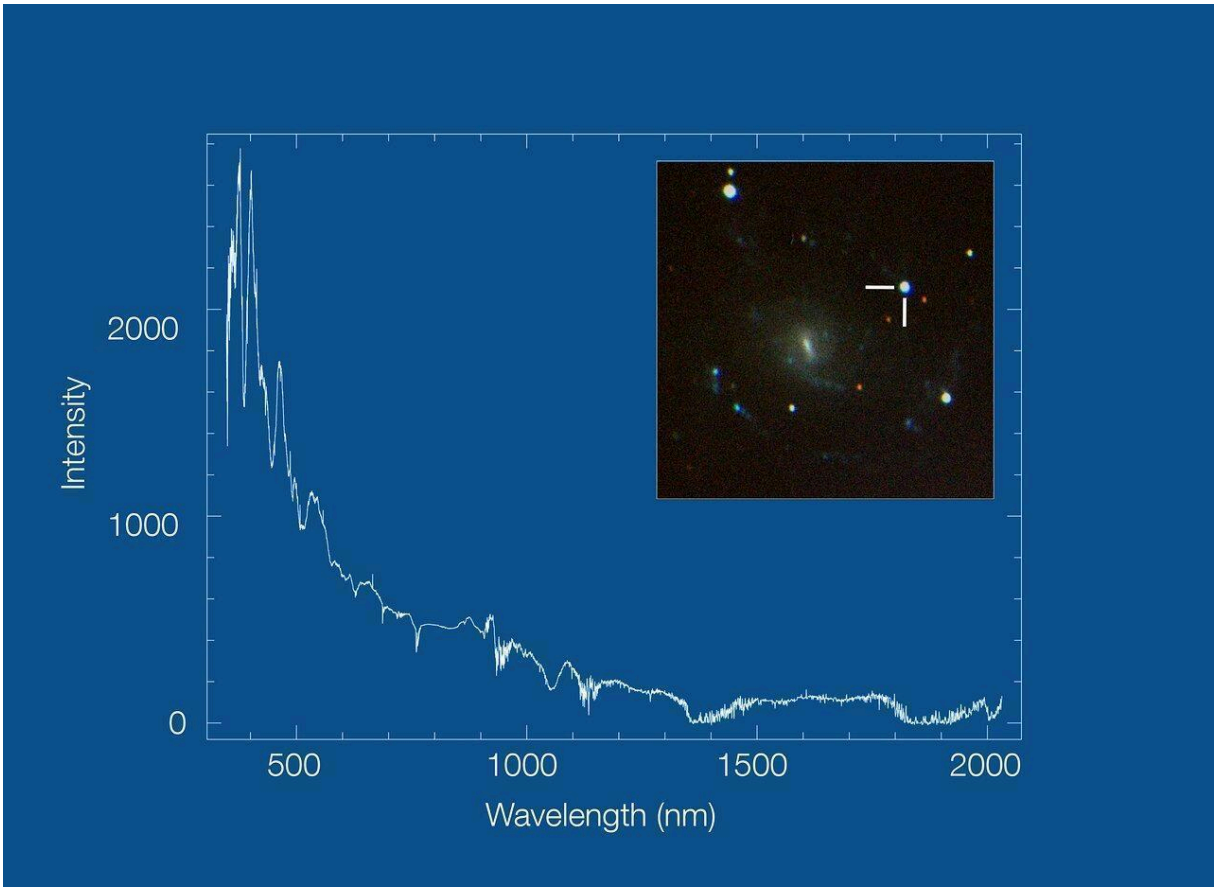

Figure 62: The SOXS first light. Full instrument observations of SN 2025advo (https://www.eso.org/public/images/ann25011d/)

6.1 Example of pipeline performances (v0.14.1): full reduction of the data obtained on the night 2025-05-16 (NIR) and on the night 2025-10-20 (UV-VIS)

Night 2025-05-16 (NIR)

Pipeline products available here:
https://drive.google.com/drive/folders/1N6jhDBKYLDpetpkNvZWVyMYAZHphAYWQ?usp=sharing

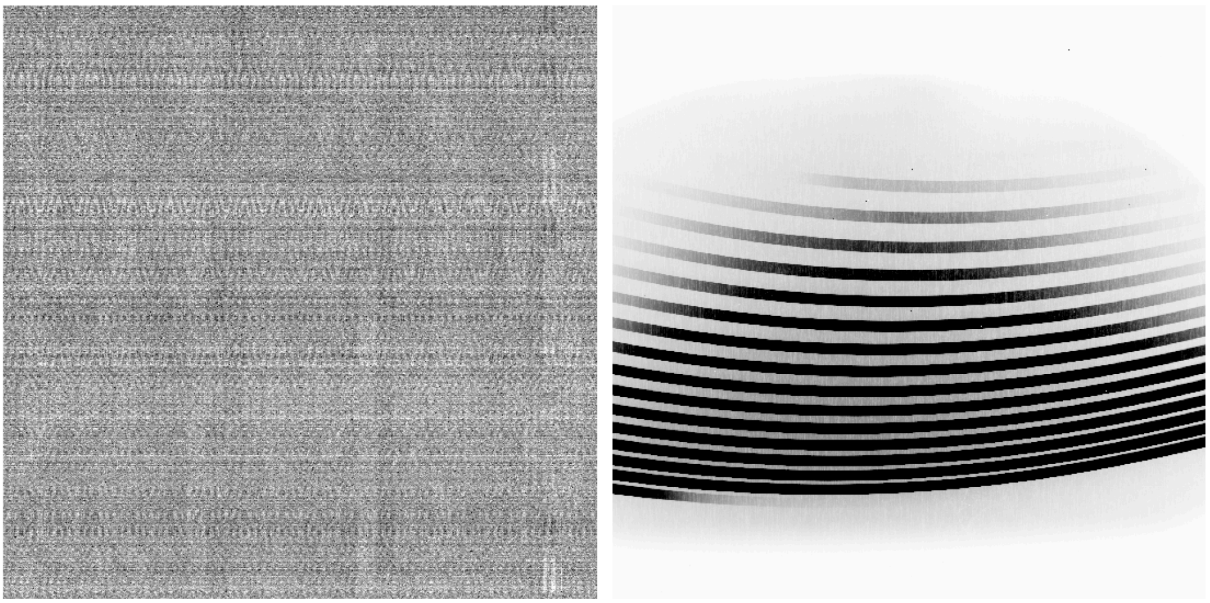

Figure 63: NIR master dark (20250517T114747_NIR_3_MDARK_BLANK_15.0S_SOXS.fits) and QTH 1" slit master flat (20250517T110527_NIR_3_MFLAT_QTH_SLIT1.0_3.75S_SOXS.fits).

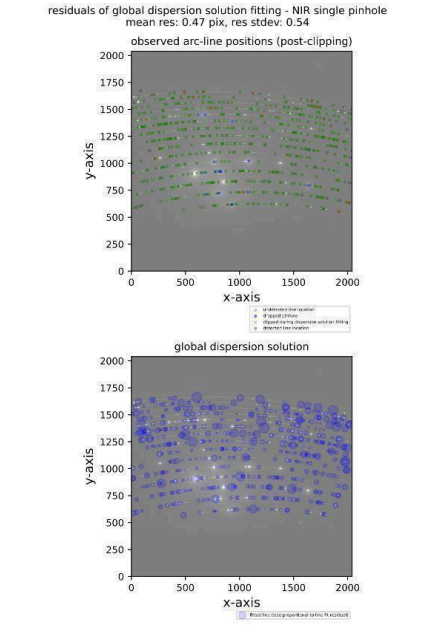

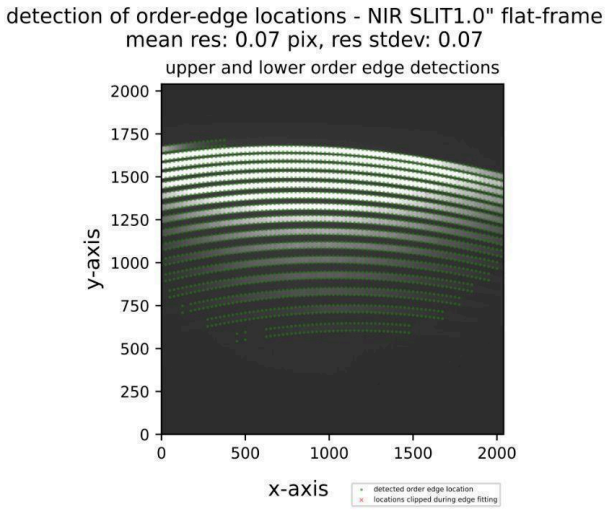

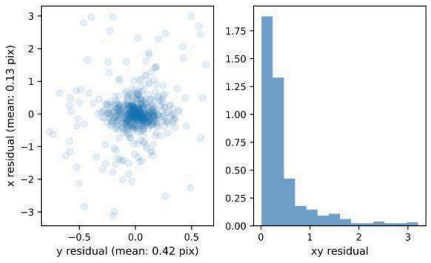

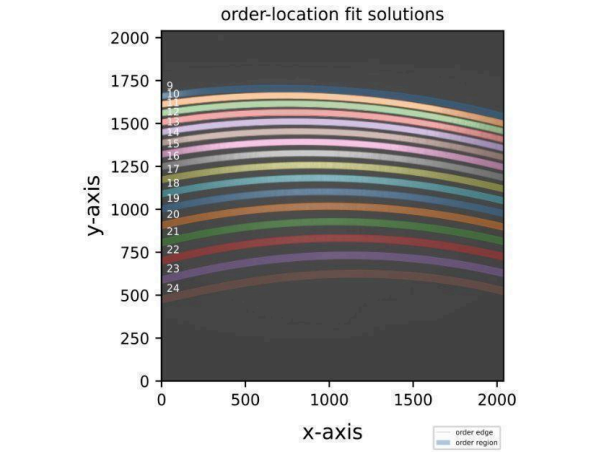

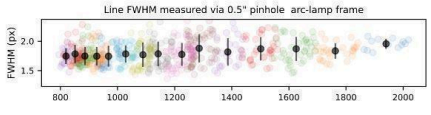

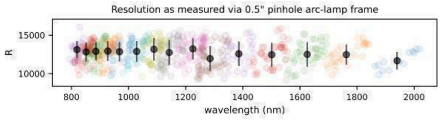

	value	qc_comment
ORDEXP10	209.50 electrons	[e-] 10th percentile inter-order flux
ORDEXP50	2709.09 electrons	[e-] 50th percentile inter-order flux
ORDEXP90	12888.52 electrons	[e-] 90th percentile inter-order flux
XRESMIN	1.49E-05 pixels	[px] Minimum residual in order edge fit along x-axis
XRESMAX	7.35E-01 pixels	[px] Maximum residual in order edge fit along x-axis
XRESRMS	7.25E-02 pixels	[px] Std-dev of residual order edge fit along x-axis

	value
subtract_background	True
stacked-clipping-sigma	3
stacked-clipping-iterations	3
centre-order-window	20
slice-length-for-edge-detection	70
slice-width-for-edge-detection	5
min-percentage-threshold-for-edge-detection	20
max-percentage-threshold-for-edge-detection	50
disp-axis-deg	5
order-deg	6
poly-fitting-residual-clipping-sigma	10
poly-clipping-iteration-limit	2
low-sensitivity-clipping-sigma	2
exptime	3.75

Figure 64: NIR reductions QC products (from left to right): dispersion solution (20250517T115316_NIR_3_DSOL_PINHOLE_15.0S_SOXS_RESIDUALS_534500.pdf), order location (20250517T110527_NIR_3_MFLAT_QTH_SLIT1.0_3.75S_SOXS_ORD_LOC.pdf).

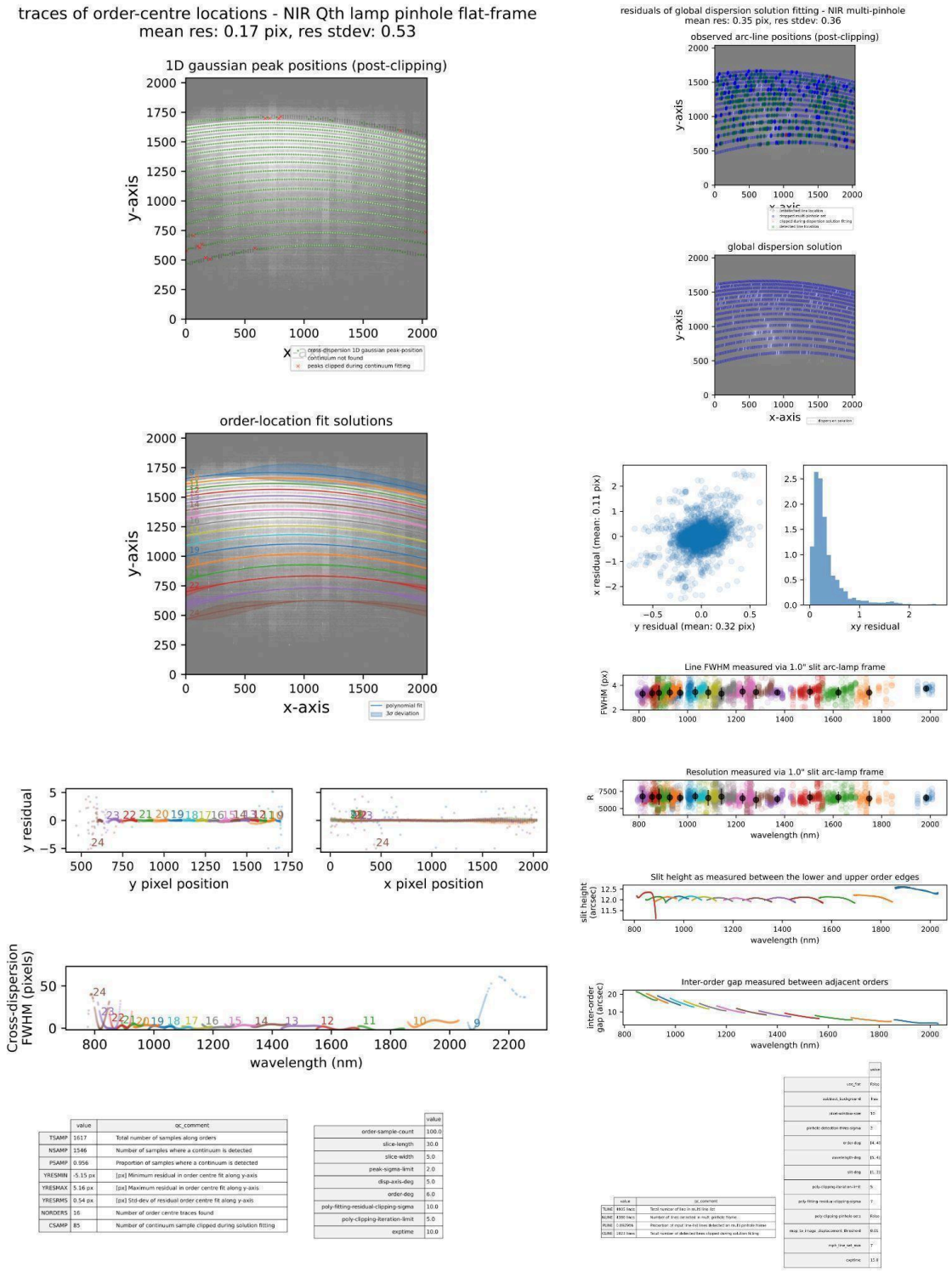

	value	qc_comment
TSAMP	1617	Total number of samples along orders
NSAMP	1546	Number of samples where a continuum is detected
PSAMP	0.956	Proportion of samples where a continuum is detected
YRESMIN	-5.15 px	[px] Minimum residual in order centre fit along y-axis
YRESMAX	5.16 px	[px] Maximum residual in order centre fit along y-axis
YRESRMS	0.54 px	[px] Std-dev of residual order centre fit along y-axis
NORDERS	16	Number of order centre traces found
CSAMP	85	Number of continuum sample clipped during solution fitting

	value
order-sample-count	100.0
slice-length	30.0
slice-width	5.0
peak-sigma-limit	2.0
disp-axis-deg	5.0
order-deg	6.0
poly-fitting-residual-clipping-sigma	10.0
poly-clipping-iteration-limit	5.0
exptime	10.0

Figure 65: NIR reductions QC products (from left to right): order FWHM (20250517T111933_NIR_3_OLOC_QTH_PINHOLE_10.0S_SOXS_residuals_65.pdf), spatial solution (20250517T115347_NIR_3_SSOL_MULTPIN_15.0S_SOXS_RESIDUALS_445412.pdf).

Night 2025-10-20 (UV-VIS)

Pipeline products available here:
https://drive.google.com/drive/folders/1cWf8SkT4o7JFdTELvCsmyQKJ0JTfrv6x?usp=sharing

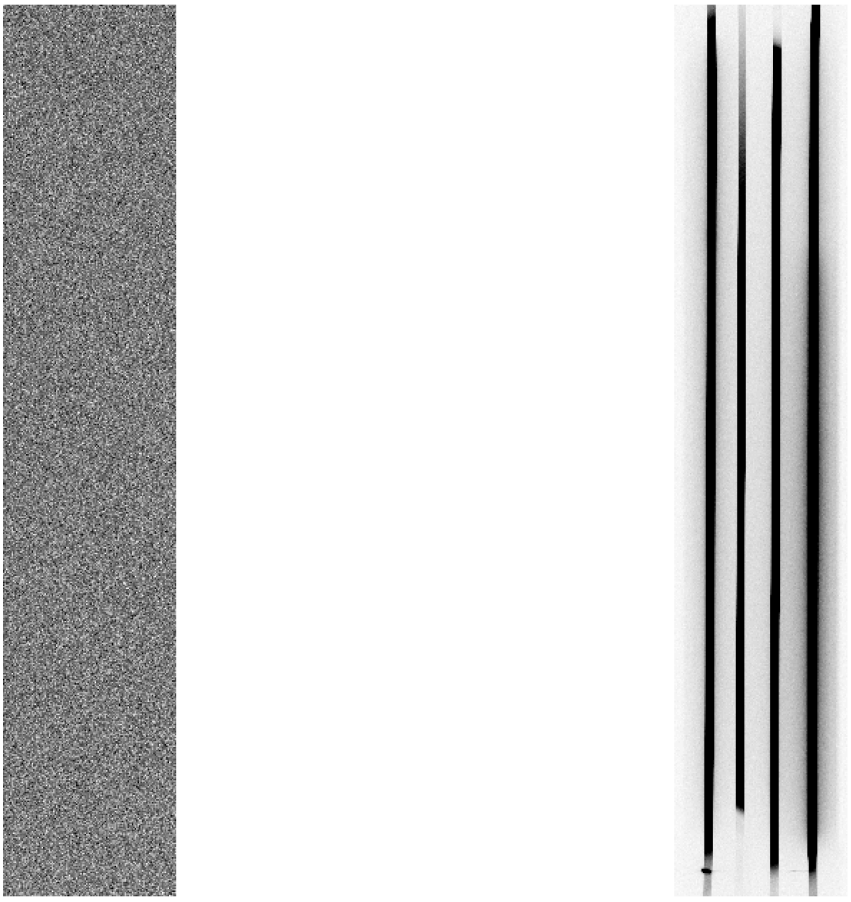

Figure 66: UV-VIS master bias (20251021T091028_VIS_1X1_1_MBIAS_SLIT0.5_SOXS.fits) and QTH 1" slit master flat (20251021T093133_VIS_1X1_1_MFLAT_QTH_SLIT1.0_10.0S_SOXS.fits).

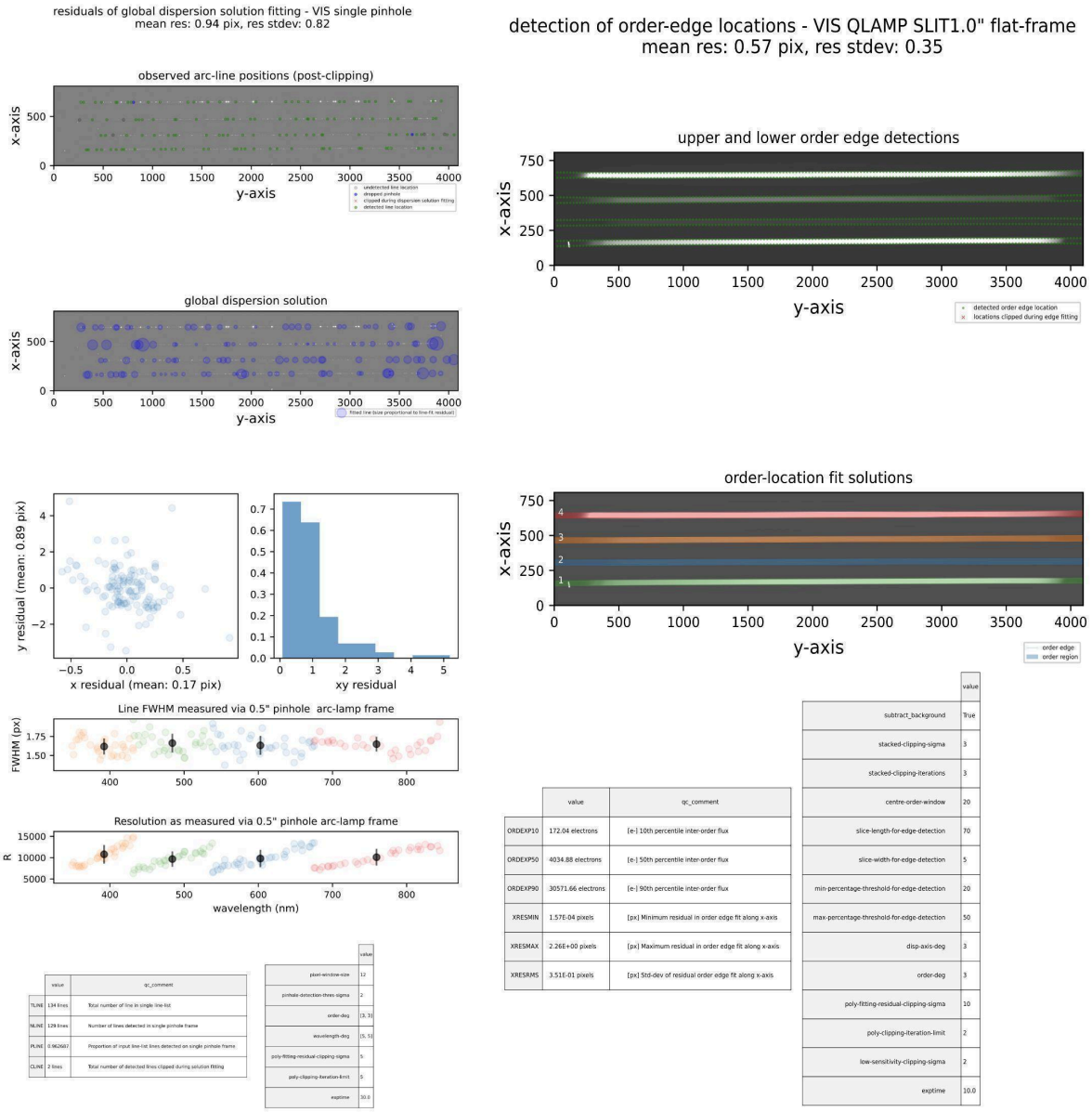

	value	qc_comment
ORDEXP10	172.04 electrons	[e-] 10th percentile inter-order flux
ORDEXP50	4034.88 electrons	[e-] 50th percentile inter-order flux
ORDEXP90	30571.66 electrons	[e-] 90th percentile inter-order flux
XRESMIN	1.57E-04 pixels	[px] Minimum residual in order edge fit along x-axis
XRESMAX	2.26E+00 pixels	[px] Maximum residual in order edge fit along x-axis
XRESRMS	3.51E-01 pixels	[px] Std-dev of residual order edge fit along x-axis

	value
subtract_background	True
stacked-clipping-sigma	3
stacked-clipping-iterations	3
centre-order-window	20
slice-length-for-edge-detection	70
slice-width-for-edge-detection	5
min-percentage-threshold-for-edge-detection	20
max-percentage-threshold-for-edge-detection	50
disp-axis-deg	3
order-deg	3
poly-fitting-residual-clipping-sigma	10
poly-clipping-iteration-limit	2
low-sensitivity-clipping-sigma	2
exptime	10.0

	value	qc_comment
TLINE	134 lines	Total number of line in single line-list
NLINE	129 lines	Number of lines detected in single pinhole frame
PLINE	0.962687	Proportion of input line-list lines detected on single pinhole frame
CLINE	2 lines	Total number of detected lines clipped during solution fitting

	value
pixel-window-size	12
pinhole-detection-thres-sigma	2
order-deg	[3, 3]
wavelength-deg	[5, 5]
poly-fitting-residual-clipping-sigma	5
poly-clipping-iteration-limit	5
exptime	30.0

Figure 67: UV-VIS reductions QC products (from left to right): dispersion solution (20251021T100323_VIS_1X1_1_DSOL_PINHOLE_30.0S_SOXS_RESIDUALS_335500.pdf), order location (20251021T093133_VIS_1X1_1_MFLAT_QTH_SLIT1.0_10.0S_SOXS_ORD_LOC.pdf).

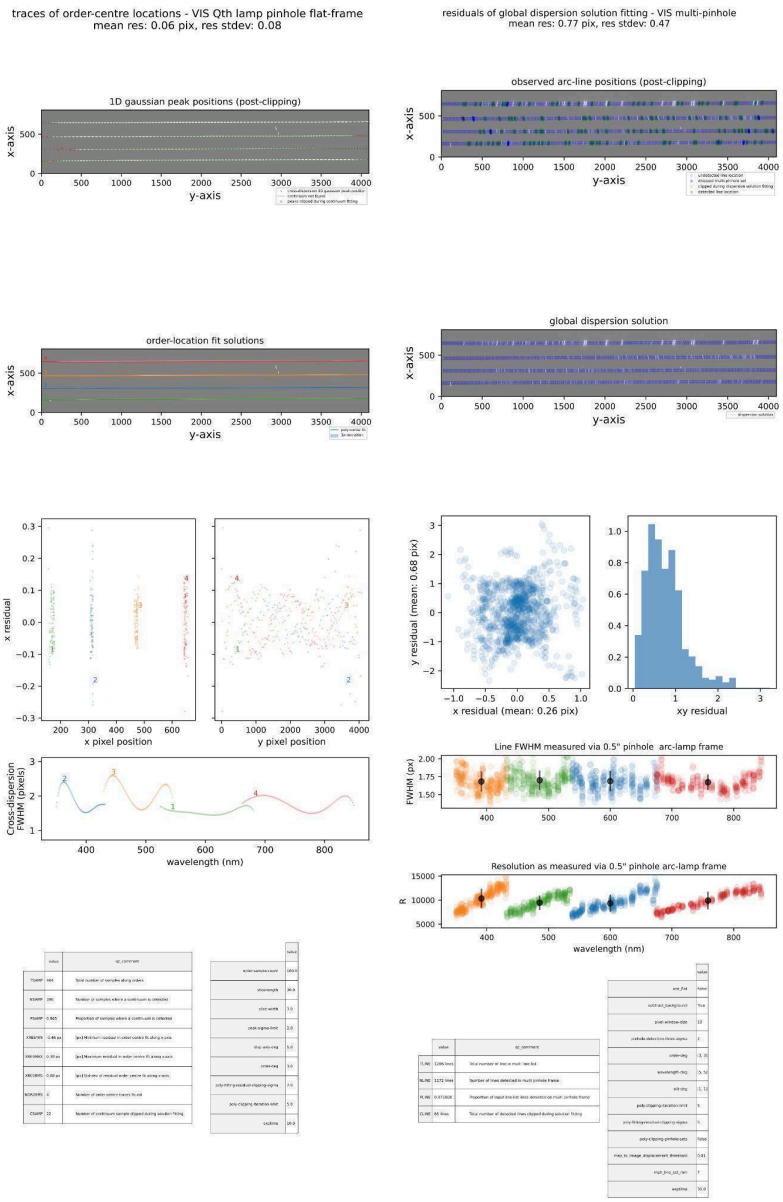

Figure 68: UV-VIS reductions QC products (from left to right): order FWHM (20251021T094041_VIS_1X1_1_OLOC_QTH_PINHOLE_10.0S_SOXS_residuals_35.pdf), spatial solution (20251011T101011_VIS_1X1_1_SSOL_MULTPIN_30.0S_SOXS_RESIDUALS_335511.pdf).

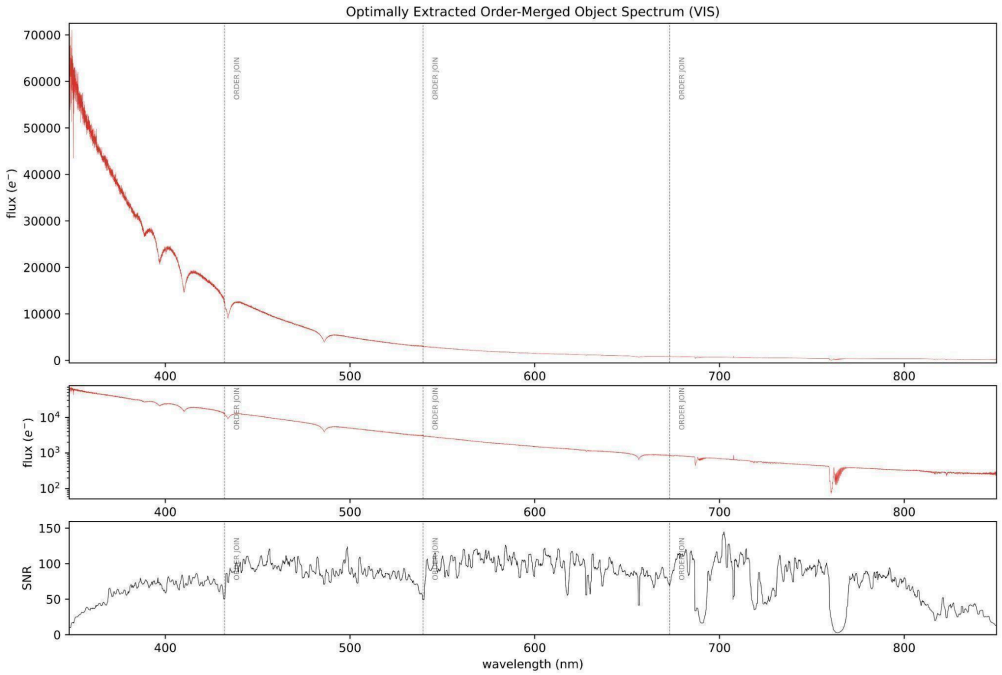

Figure 69: UV-VIS extracted 1D spectrum of the spectrophotometric STD GD71 (5" slit, texp = 300s, nodding mode; 20251021T072618_VIS_1X1_1_NOD_SLIT5.0_300.0S_SOXS_STD_FLUX_EXTRACTED_MERGED_QC_PLOT.pdf).

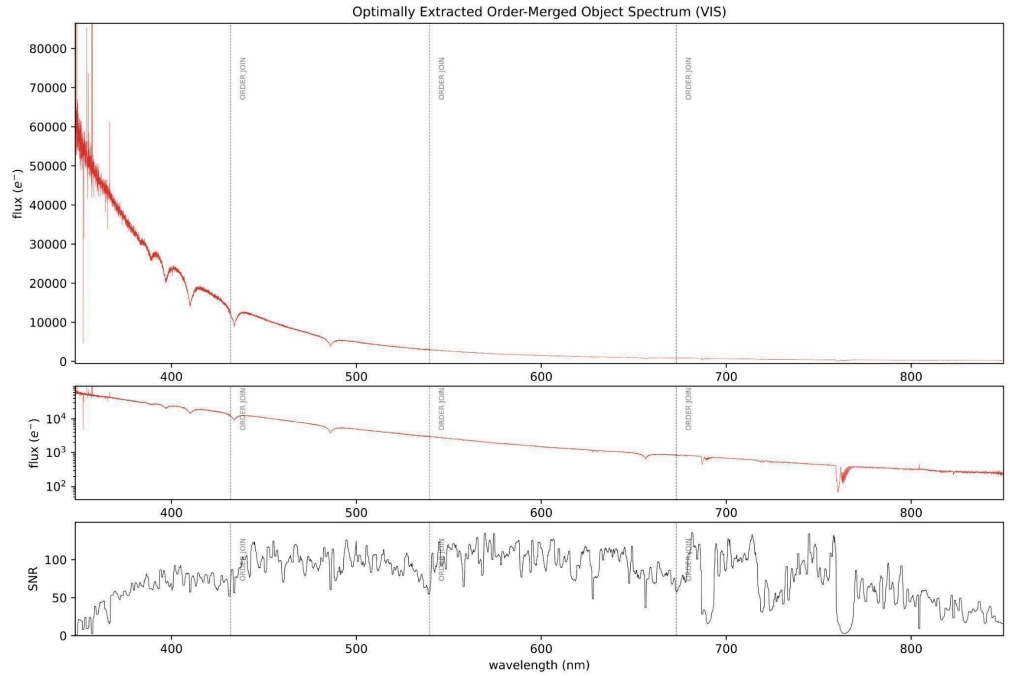

Figure 70: UV-VIS extracted 1D spectrum of the spectrophotometric STD GD71 (5" slit, texp = 300s, stare mode; 20251021T070906_VIS_1X1_1_STARE_SLIT5.0_300.0S_SOXS_STD_FLUX_EXTRACTED_MERGED_QC_PLOT.pdf).

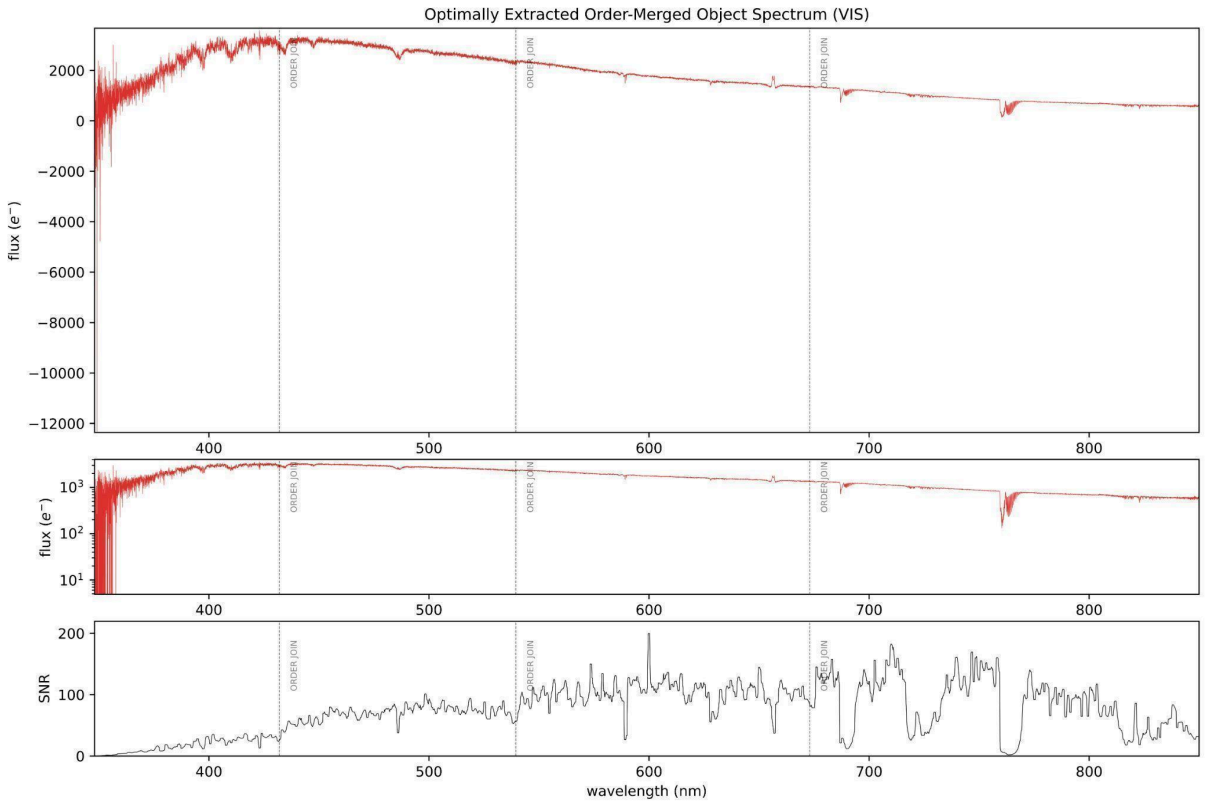

Figure 71: UV-VIS extracted 1D spectrum of the candidate nova STD PNV J072 (1" slit, texp = 240s, stare mode; 20251021T065737_VIS_1X1_1_STARE_SLIT1.0_240.0S_SOXS_PNV_J072_EXTRACTED_MERGED_QC_PLOT.pdf).

Appendix - Templates tested

SOXS_img_acq
SOXS_slt_acq
SOXS_gen_cal_NIRDark
SOXS_gen_cal_VISBias
SOXS_gen_cal_VISDark
SOXS_gen_tec_NIRDetLin
SOXS_gen_tec_VISDetLin
SOXS_img_tec_Focus
SOXS_slt_tec_NIRFocus
SOXS_slt_tec_VISFocus
SOXS_img_cal_Bias
SOXS_img_cal_Dark
SOXS_img_cal_dist
SOXS_img_obs_GenericOffset
SOXS_gen_cal_Astrometry
SOXS_img_cal_DomeFlat
SOXS_img_cal_phot
SOXS_img_obs
SOXS_slt_cal_DomeLampFlat
SOXS_slt_cal_LampFlatDeut
SOXS_slt_cal_NIRArcs
SOXS_slt_cal_NIRArcsAtt
SOXS_slt_cal_NIRArcsMultiplePinhole
SOXS_slt_cal_NIRArcsPinhole
SOXS_slt_cal_VISArcs
SOXS_slt_cal_VISArcsAtt
SOXS_slt_cal_VISArcsMultiplePinhole
SOXS_slt_cal_VISArcsPinhole
SOXS_slt_cal_SpecphotNod
SOXS_slt_cal_SpecphotStdOffset
SOXS_slt_cal_TelluricStdNod
SOXS_slt_obs_AutoNodOnSlit
SOXS_slt_obs_FixedSkyOffset
SOXS_slt_cal_LampFlat
SOXS_slt_cal_LampFlatAtt
SOXS_slt_cal_LampFlatMultiplePinhole

SOXS_slt_cal_LampFlatPinhole
SOXS_slt_cal_SpecphotStdStare
SOXS_slt_cal_TelluricStdStare
SOXS_slt_obs_Stare
SOXS_slt_tec_Stare
SOXS_gen_tec_SynchroCheck
SOXS_gen_tec_flexure
SOXS_slt_tec_AlignmentFocus
SOXS_img_cal_SkyFlat
SOXS_gen_tec_Lookup
SOXS_slt_tec_BackReflectionAuto
SOXS_slt_tec_BackReflection
SOXS_gen_tec_SlitLookVIS
SOXS_gen_tec_SlitLookNIR
SOXS_gen_tec_PipelineFlexures
SOXS_slt_obs_GenericOffset
SOXS_slt_obs_Mapping
SOXS_slt_obs_StareSynchro
SOXS_gen_tec_ADC
SOXS_gen_tec_ADC_steps
SOXS_gen_tec_FreeSetup
SOXS_gen_tec_LampCheck
SOXS_gen_tec_LampOff
SOXS_gen_tec_ObsFree
SOXS_gen_tec_ParkInstrument
SOXS_gen_tec_standby
SOXS_gen_tec_refacqCheck